ABSTRACT

Title of Document:	A Study of Aerosol Indirect Effects for Cumulus Clouds on a Global Scale
	Tianle Yuan, Doctor of Philosophy, 2008
Directed By:	Professor Zhanqing Li, advisor Department of Atmospheric and Oceanic Science/ Earth System Science Interdisciplinary Center

Using case study approach my investigation on aerosol's effects on fair weather cumulus clouds shows that not only can aerosol reduce cloud droplet sizes like in the case of stratiform clouds, but also they can increase droplet sizes. Atmospheric water vapor loading explains nearly 70% of variations in the dependence of droplet size on aerosol loading for cases over Eastern United States. This finding withstands serious scrutinizing under different scenarios of artificial correlations. A further study on a global scale indicates that only two areas, Eastern US and coastal region of Southeast China, show increasing trend of droplet size with aerosol loading. Results from other regions agree well with findings from past studies further ruling out artificial correlation. Relationship between aerosol loading and cloud liquid water path differs significantly for marine stratocumulus clouds and continental cumuli. Two possible explanations for our findings are confirmed by state-of-the-art cloud resolving model simulations.

Deep convective clouds properties are shown to obey a few universally observable relationships. Their cloud top ice particle sizes are positively correlated with their vertical height and they are significantly affected by topography; their optical depth distributions have signature shapes associated with individual regions; their brightness temperature distributions show agreement with the fixed anvil temperature hypothesis. A conceptual model is proposed to understand cloud hydrometeor evolution and is used to study aerosol's influence. Anthropogenic pollution and smoke are shown to decrease ice particle sizes by delaying coalescence process and prolonging condensational growth. As a result cloud glaciation height is increased that possibly leads to invigoration of cloud development. Dust particles are demonstrated to increase ice particle sizes probably by acting as giant condensation nuclei or ice nuclei. Ice particle size vertical structure is shown to have a significant latitudinal variation. Far reaching implications of our results are envisioned for climate studies.

A STUDY OF AEROSOL INDIRECT EFFECT FOR CUMULUS CLOUDS ON A GLOBAL SCALE

By

Tianle Yuan

Dissertation submitted to the Faculty of the Graduate School of the
University of Maryland, College Park, in partial fulfillment
of the requirements for the degree of
Doctor of Philosophy
2008

Advisory Committee:
Professor Zhanqing Li, Chair/Advisor
Professor Russell Dickerson
Professor Rachel T. Pinker
Dr. Lorraine A. Remer

Dedication

To my always loving and encouraging mom and dad

Statement of Originality

The original scientific contributions made in my study include:

(1) We developed a 'semi-collocated and synchronized' method, utilizing unique combination of products and high resolution data from MODIS, specifically for studying small, patchy fair weather cumulus and closed cell stratocumulus clouds. The method ensures that measured aerosols and clouds are truly interacting with each other, an advantage over many past studies that studied correlation between satellite measurements of aerosols and clouds far apart either spatially or temporally.

(2) A set of potential scenarios that may cause artificial correlations between aerosol optical depth (AOD) and droplet effective radius (DER) measurements is comprehensively investigated in our study. Cautions shall be paid to these scenarios and checks for these scenarios are a necessary step to rule out artificial relations for future studies.

(3) A possible positive correlation between AOD and DER for fair weather cumulus clouds is reported and possible physical mechanisms are discussed to explain the results.

(4) AIE on shallow cumulus clouds, including fair weather cumulus and stratocumulus, is discovered to vary systematically with aerosol types, cloud types and environmental conditions from investigations over the globe.

(5) A physically sound relationship between cloud top brightness temperature (BT) and crystal effective radius (CER) is constructed for deep convective clouds

(DCC) based on satellite ensemble measurements for the first time. The relationship is universally observed and provides a solid foundation to study AIE on DCC in a new way.

(6) A new method of studying AIE on DCC based on a physical conceptual model is developed with proper constraint of environmental conditions. Proper constraining and solid physical relationship are shown to be vital in avoiding pitfalls of previously simple but problematic methods.

(7) CER of DCC systems are shown to be reduced by both anthropogenic and smoke aerosols with the support of a large ensemble of data. These two aerosol types consistently show their ability to decrease ice particle sizes for different regions. This is an important step from a few case studies of individual storms. The important implications of our results based on large statistics are discussed.

(8) From CER-BT profiles homogeneous freezing level can be estimated for the first time based on satellite measurements. This information provides more insights into cloud development and serves as an important tool for future studies.

(9) Based on our estimation of freezing level smoke aerosols are shown to increase the freezing level height and thus probably invigorate convective cloud development for an ensemble of clouds. This discovery is among the first observational evidences that support the hypothesis of aerosol invigorating effect in an ensemble sense.

(10) Cloud optical depth (COD) of deep convective clouds (DCC) is shown to have stable, signature distributions for specific regions. The signature distribution

shapes vary systematically over the globe. Its implications for cloud structure and organization and model parameterization are discussed.

(11) The slope of CER-BT curve is shown to have significant geographical variations. A possible explanation is provided and its important implications for model parameterization are discussed.

Chapter 2 of the dissertation is published as a journal article:

Yuan, T., Z. Li, J. Fan, and R. Zhang (2008), Increase of Cloud Droplet Size with Aerosol Optical Depth: An Observation and Modeling Study, *J. Geophys. Res.*.

The author of this dissertation contributed the idea, the method, the data analysis and the wording of this document. His advisor, Professor Zhanqing Li, guided the study and provided important editing effort for the published paper. The modeling effort in Chapter 2 of this dissertation was carried out by Dr. Jiwen Fan of University of Texas, A&M who is now at Pacific Northwest National Laboratory, under the guidance of Professor Renyi Zhang. Some materials were produced by Dr. Brian Vant-Hull regarding comparisons between two methodologies in Chapter 2.

Acknowledgements

First of all I would express my deep appreciation and sincere thanks to my advisor, Professor Zhanqing Li, for his excellent guidance, insightful scientific discussion, encouragement and patience throughout my study that benefit tremendously to my progress in scientific research and beyond.

Many thanks go to my advisory committee members, professors Russell R. Dickerson, Robert Hudson and Rachael T. Pinker and Dr. Lorraine A. Remer, for their effort and help in refining my research ideas and improving my general research skills. I especially appreciate the encouragement and helpful scientific discussions from Dr. Remer.

I am very grateful and happy to have spent several precious years with my two former officemates, now Drs. Brian Vant-Hull and Myeong Jae Jeong, with whom numerous jokes, ideas and fun were exchanged during my study.

I would like to thank also Ms. Maureen Cribb and other group members for the help they provided.

Knowledgeable and nice faculty members of the department also benefit me a lot during my study and research.

I am also very thankful to Ms. Bingjie Hu for her support and love during my study.

Table of Contents

List of Acronyms

AIE – aerosol indirect effect

AOD – aerosol optical depth

BT – brightness temperature

CAPE – convective available potential energy

CCN – cloud condensation nuclei

CER – crystal effective radius

COT – cloud optical depth

CRM – cloud resolving model

CTP – cloud top pressure

CTT – cloud top temperature

DCC – deep convective cloud

DER – droplet effective radius

DNC – droplet number concentration

GCCN – giant cloud condensation nuclei

GCM – global circulation model

CER – crystal effective radius

IGB – Indo-Gangetic Basin

IN – ice nuclei

IWC – ice water content

LWP – liquid water path

PW – precipitable water

SSO – slightly soluble organics

Chapter 1: Introduction

1.1 General Overview

Aerosols are an important component of the atmosphere. Atmospheric aerosols are largely of natural source and they are highly variable due to their short lifetime in the atmosphere. Aerosols exert significant radiative forcing on the climate system by absorbing and/or reflecting solar radiation directly, referred as aerosol direct effect. Aerosol direct effects are not subject of this study, but are investigated in details in previous studies [Ramanathan et al., 2001; Haywood and Boucher, 2000; Penner et al., 1992]. Quantifying the aerosol direct effects has made significant progress with more available data from ground, in-situ and satellite measurements and with improved methods although remain largely uncertain compared to understanding of greenhouse effects [Schwartz et al., 2007]. Aerosols can also act as cloud condensation nuclei (CCN) and ice nuclei and modify cloud properties through many possible pathways, also known as aerosol indirect effects (AIE). We refer AIE more loosely as any aerosol induced modifications of cloud microphysics, cloud duration, cloud fraction, and precipitation etc. The experimental observations and theoretical explanations of AIE remain uncertain and unresolved although significant amount of efforts and some progress have been made [Lohmann and Feichter, 2004; Stephens, 2005]. AIE will be the focus of this study and specifically we concentrate on AIE on cumulus clouds.

In this chapter introductory comments and review of current knowledge on AIE are provided as a broad context for my investigation.

1.2 Background of Aerosol and Cloud

Aerosols can be categorized into different types depending on their chemical composition and origin. There are two categories of aerosols based on origin: anthropogenic and natural aerosols. Aerosols are better categorized into roughly five types: dust, largely natural and with sources in major deserts; smoke, from biomass burning due to both natural and anthropogenic causes; maritime aerosols, generated by wave breaking over ocean water; background continental aerosols, mainly originated from vegetation emission; and anthropogenic aerosols, man-made with complex compositions [Kaufman et al., 2002]. Due to different chemical compositions these aerosol types have starkly different composition and properties as well as abilities to act as CCN or IN. For example smokes and oceanic sulfate or sea salt are active CCNs while dust is less active and hydrophobic anthropogenic aerosols with non-soluble compositions are not active at all. The variability can be represented based on their compositions in a modified Kohler curve [Khvorostyanov and Curry, 2007]. Aerosol sizes also have important implications for CCN activity. One study by *Dusek et al.* [2006] shows that with their measurements mainly of pollution and oceanic aerosols size is the most important factor. CCN active aerosol particles with diameter larger than a micrometer can be considered as giant CCN (GCCN) that may speed up rain formation process [Hindman et al., 1977; Lu and Seinfeld, 2006]. Aerosol number concentration affects cloud droplet number concentration together

with maximum achievable supersaturation inside a cloud. It also has a dispersion effect on the cloud droplet size spectrum as suggested by *Liu and Daum* [2002]. All aspects of information on aerosols are needed when studying aerosol-cloud interaction.

Detailed measurements of aerosols are demanding and challenging due to their high variability, relatively low concentration and their sizes. Complete measurements of important aerosol properties are usually only available from a few comprehensive campaigns and thus are scarce. Scientists often opt to use aerosol optical depth (AOD) as a proxy for aerosol amount. AOD is measurable with different techniques and can be related to other quantities like number concentration with proper assumptions. Point measurements of AOD are usually made by ground based instruments that directly point to the Sun when the sky is clear. AOD is derived from the extinction of the direct solar beam when other influences are removed [King and Byrne, 1976]. Newly available multi-spectral sun photometers and innovative methods have made it possible to derive not only AOD, but an estimation of size distribution [Dubovik et al., 2002]. Although ground measurements now have expanded to cover many parts of the world they are still very limited. Global maps of AOD were available only when appropriate channels were available on satellite sensors. The first sensor with designated channels to observe aerosols is the Moderate Resolution Imaging Spectroradiometer (MODIS). Its resolution and variety of channels make it powerful tool to study aerosols (and clouds). AOD can be retrieved from MODIS measurements over both land and ocean for the first time and the latest algorithm offers excellent products that compare well with the de facto 'ground truth'

by aerosol robotic network (AERONET) [Levy et al., 2007]. Combined with source information and a priori knowledge aerosol types can also be derived from satellite measurements [Jeong et al., 2005]. In addition critical information on vertical distribution of aerosols is needed to study aerosol-cloud interaction. The vertical distribution of aerosols can be measured in-situ by aircraft, ground lidar and satellite lidar. Most of the aerosols are confined in boundary layer because of the stratification of the atmosphere. Long range transport of aerosols is possible through two major pathways: frontal lifting and convective vertical transport.

Clouds are one of the most important components of climate system. Depending on their phase clouds can be roughly categorized into three types: liquid water clouds, ice clouds and mixed phase clouds. Liquid-phase clouds are made up of cloud droplets and they exist only in lower troposphere. Common liquid phase clouds include fair weather cumulus clouds over land, shallow stratocumulus clouds over cool ocean water and shallow trade cumulus over the tropical ocean. Pure ice clouds types include cold stratus clouds and high cirrus clouds. Mixed phase clouds are found over cold surfaces like the polar region and inside deep cumulus clouds.

A variety of in-situ and remote sensing techniques have been developed to measure cloud macro and microphysical properties. In this study data are mainly from remote sensing technique. The cloud remote sensing of cloud microphysics from satellite is pioneered by the study by *Nakajima and King* [1990] where a size sensitive infrared channel was used in combination with a size insensitive channel in the visible. Simultaneous retrievals of cloud top droplet effective size (DER) and cloud optical depth (COD) can be made based on radiative simulation of prescribed

configuration of cloud properties. This technique can be extended to use for ice phase clouds to get crystal effective radius (CER) [King et al., 2004]. Cloud height can be sensed by using either a cloud emission channel within atmospheric region to get cloud top brightness temperature (BT), or a 'CO_2 slicing' technique to get cloud top pressure [Platnick et al., 2003].

1.3 AIE on Liquid Phase Clouds

Aerosols are necessary for cloud formation by thermodynamic considerations of droplet nucleation. The idea of aerosols changing cloud shortwave albedo through modifying the cloud droplet number concentration by acting as CCNs was not noticed until 1950's by *Twomey* [1954]. He proposed that more but smaller cloud droplets due to increased concentration of aerosol particles will result in a more reflective cloud if cloud liquid water amount remains unchanged [Twomey, 1977]. This ignited interest in looking at aerosol-cloud interactions and series of in-situ measurements probing aerosol-cloud interactions were carried out following this idea [Hobbs et al., 1970; Fitzgerald et al., 1973; Eagan et al., 1974; Hindman et al., 1977].

The best example of aerosol-cloud interactions was not found until 'ship tracks' were noticed from the first generation of satellite imageries [Conover, 1966]. The ship tracks are generated by ships at sea where concentration of natural aerosols are too scarce to form clouds. Pollution particles emitted from ships perturb marine stratocumulus clouds and change cloud albedo [Coakley et al., 1987; Ferek et al., 1998]. More efforts focused on investigations of aerosol-stratocumulus interactions were made after *Albrecht et al.* [1989] proposed that due to aerosol induced cloud

microphysical changes cloud duration can be altered and cloud cover may thus change. Statistics of satellite cloud retrieval data over the globe also supports Twomey's hypothesis [Han et al., 1995; Breon et al., 2002]. Most of these studies followed the paradigm outlined by the assumption in Twomey's hypothesis where cloud liquid water amount is fixed.

Aerosols can not only directly affect cloud formation by acting as CCN or IN, but they can also modify the atmospheric stratification through interacting with solar radiation [Hansen et al., 1997]. *Koren et al.* [2004] found evidence of cloud fraction reduction for fair weather cumulus clouds by absorbing smokes over the Amazon.

Radiative forcing due to AIE is estimated from general circulation models (GCM) by carrying out simulations with present-day and pre-industrial configurations of aerosol concentrations. The difference in the top-of-atmosphere radiation budget is taken as the AIE radiative forcing. The model consensus is that radiative forcing due to AIE is negative although significant variations exist depending on how models parameterize AIE [Lohmann and Feichter, 2005; Anderson et al., 2003].

1.4 AIE on Mixed-Phase Clouds

Cloud droplets can exist at temperatures colder than $0\ ^{o}C$, so called supercooled water, where the temperature is too warm for homogeneous freezing. To freeze the supercooled droplets IN are required. Aerosols like soot, mineral dust and some biological materials are active ice nuclei [Diehl et al., 2001]. Since most precipitation originates from the ice phase, so called cold rain process, the possibility

of aerosol-cloud-precipitation interactions is explored. *Rosenfeld* [1999] used satellite measurements of cloud top microphysics and inferred an aerosol precipitation suppression effect based on a few cases, which was later successfully simulated by a cloud resolving model [Khain et al., 2001]. The ice process is complicated and so far poorly understood [Pruppacher and Klett, 1997]. The difficulty of mimicking real cloud environment in the lab and lack of in-situ measurements contribute to our poor understanding. Most recent studies have focused on modeling to test different possibilities.

Aerosols can also potentially affect ice particle sizes and other cloud properties and even affect the circulation of atmosphere. *Sherwood* [2002] made an attempt to study possible relationship between ice particle sizes at the top of deep convective clouds and aerosol index. His results suggested that smokes could potentially reduce ice particles size. *Kaufman et al.* [2006] proposed an intriguing possibility of aerosol invigorating cloud effect by analyzing MODIS data. *Lau et al.* [2007] postulated the possible thermodynamic effect of absorbing dust particles on DCC formation over both the Indian Monsoon region and on cyclone genesis over the Atlantic Ocean off the West Africa coast.

1.5 Objectives of Current Investigation

It has been noted that most past studies of aerosol-cloud-microphysics interactions within liquid-phase clouds have focused on stratiform clouds while cumulus clouds have their roots in the boundary layer where most aerosols stay. Interactions between cloud and aerosol are expected to be more direct for cumuliform

clouds. We also note the framework outlined by Twomey has its limitations in that it considers a cloud as a static system, while in reality clouds are dynamic and constantly evolving. Important questions remain to be answered. For example, do aerosol-induced microphysical changes of clouds feedback to cloud development itself? When an ensemble of clouds under a similar environment are considered can we observe changes induced by aerosols in macro cloud properties like liquid water path and cloud vertical reach? Do aerosol types matter in terms of AIE? In Chapter 2 of this study a new method will be developed to investigate AIE on cumulus clouds in a different angle where we do not compare two clouds that have the same amount of water already to find signals of aerosol influence, rather we look at ensembles of clouds that have similar environmental conditions to begin with and study how the statistics of their properties responds to aerosol change. In other words we want to observe how clouds as a system react to aerosol changes by studying variations in their statistics. Fair weather cumulus clouds are the best candidate for this purpose because they are relatively small in scale and numerous in sampling opportunity.

Deep convective cloud formation and development are dominated by dynamical conditions. Complicated liquid phase and ice phase microphysical processes are involved in DCCs, which has hampered qualitatively assessing the AIE. We will answer several critical questions regarding AIE on DCCs with a new method constructed based on physically sound relationships using MODIS data:

1. Do DCC cloud microphysical properties respond to aerosols?
2. If so, can we observe the signal from satellite data?
3. How does aerosol signal vary?

4. Can aerosols modify cloud development?

As a first step basic distribution, occurring frequency, microphysical and other properties of DCC will be discussed in Chapter 3. From these examinations important measures will be constructed to probe the four listed questions.

Chapter 2: Global Study of AIE on Shallow Cumulus and Stratocumulus Clouds

2.1 Introduction

As noted in Chapter 1 aerosol indirect effects (AIE) can refer to any aerosol-induced alteration of cloud microphysics, cloud duration, precipitation, etc. It was pioneered by an analysis done by *Twomey* [1977] where it was hypothesized that cloud particle size is reduced by adding aerosols as cloud condensation nuclei (CCN) for a fixed liquid water amount, termed the first AIE or Twomey effect. The Twomey effect has been supported with ample evidence from satellite [*Han et al.*, 1994; *Wetzel and Stowe*, 1999; *Nakajima et al.*, 2001; *Liu et al.*, 2003] and ground and in-situ observations [*Leaitch et al.*, 1996; *Feingold et al.*, 2003; *Penner et al.*, 2004; *Kaufman and Fraser*, 1997]. In addition more and smaller cloud droplets suppress cloud precipitation and hence increase cloud duration [*Albrecht*, 1989], termed the second AIE or cloud lifetime effect. Both AIEs are rooted to the fundamental change in cloud droplet size by aerosol. Through aerosol direct radiative heating *Ackerman et al.* [1995] proposed that stabilizing effect of heating by elevated soot may suppress cloud formation and reduce cloud cover, which is demonstrated with clear observation evidence by *Koren et al.* [2004].

Although there is a consensus that aerosols reduce cloud droplet size a range of variation (by a factor of 3 or more) was found concerning the sensitivity of cloud microphysics to aerosol, as measured by the ratio of the change in cloud particle size

to aerosol parameters. While some of the differences are related to the use of different analysis methods and/or observational data [*Rosenfeld and Feingold*, 2003], natural variation is observed [*Feingold et al.*, 2003; *Kim et al.*, 2003]. It is uncertain yet what drives the variation. Note that all previous studies showed a negative dependence of cloud particle size on aerosol loading. Some studies showed the opposite but did not elaborate on the finding [*Sekiguchi et al.*, 2003; *Storelvmo et al.,* 2006].

The impact of AIE on climate is generally measured in terms of aerosol radiative forcing, which is the difference in the radiation budget with and without the consideration of AIE. There have been estimations of the global aerosol indirect forcing (AIF) with large disparities [*IPCC*, 2001; *Anderson et al.*, 2003]. Models following forward calculations and inverse calculations have shown different magnitude of the global AIF. The forward calculations using observation-based cloud-aerosol relations [e.g., *Boucher and Lohmann,* 1995] led to AIF estimates ranging from -1.1 to -4.4 Wm^{-2}, while the inversion methods constrained by global temperature records produced systematically lower values and narrower ranges in AIF (-1 to –1.9 Wm^{-2}). Which sets of calculations are more accurate is debatable [*Anderson et al.*, 2003], but it is indisputable that we must reconcile the two sets of estimations in order to better predict the climate change.

Overestimation of AIF by the forward approach was conjectured based on a General Circulation Model's (GCM) overestimation of the rate of decrease in cloud particle size with aerosol optical depth relative to that from satellite observations [*Lohmann and Lesins*, 2002]. One explanation for the overestimation was that aerosols could have a warming effect by increasing the relative dispersion of the

cloud droplet spectrum [*Liu and Daum*, 2002]. Incorporating this effect into a GCM reduces the magnitude of the AIF by 12 to 35% [*Rotstayn and Liu*, 2003], narrowing, but not bridging the big gap. Even if the gap is closed by a new mechanism, one cannot disregard the results obtained from forward calculations [*Anderson et al.*, 2003] unless past observations were proven erroneous or biased.

The majority of previous studies on AIE concentrated on stratiform clouds formed in relatively dry regions/seasons or decoupled from the water vapor source [*Miller et al.,* 1998], as the Twomey effect is founded on the competition for water by cloud droplets. The parameterizations developed thereafter were likely skewed towards such conditions. Cloud droplet size is an "output" of a complex system, which involves interactions and feedbacks among aerosols, clouds, dynamics and thermodynamics. Derivation of the "partial derivative" between clouds and aerosols is thus a very challenging task, but it is critical for improving AIE estimates by models. In general, the AIE is veiled by a large variation in dynamic and thermodynamic conditions. To isolate and quantify the AIE, we need to develop "conditional AIE functions" to take into account different processes, as was attempted by *Feingold et al.* [2003]. To this end, we postulate and test a hypothesis that AIE is contingent upon atmospheric dynamics which may be delineated by cloud types, to the first order of approximation, and upon the atmospheric environment for which available water vapor amount is a key factor. Convective clouds developed in the summer over moist regions and stratus/stratocumulus clouds over dry regions or decoupled situations have distinct dynamic and thermodynamic settings. We selected

both cumulus and marine stratiform scenes around the globe, with focused case-by-case analysis on the southeast United States (US) in the summer season.

The following section describes the data sets used and section 2.3 describes the methodology followed in this study. Section 2.4 presents major findings. Potential artifacts are discussed and physical explanations are examined by means of model simulation in section 5. The study is summarized in section 6.

2.2 Data Sets

The bulk of the data used in this chapter are from the Moderate Resolution Imaging Spectroradiometer (MODIS). MODIS provides an extensive remote sensing dataset of aerosol, cloud, and atmospheric and surface variables over both ocean and land around the globe. The aerosol product (MOD04) includes aerosol optical depth (AOD) at three wavelengths: 0.47, 0.56 and 0.65 μm at a spatial resolution of about 10 km [*Remer et al.*, 2005]. The resolution is degraded from the original 1 km or less following several cloud screening tests [*Remer et al.*, 2005]. In this chapter, AOD at 0.56 μm is used as proxy of aerosol loading, which has its limitations but for our focus region AOD has been demonstrated to be quite a good proxy [*Hegg and Kaufman,* 1998]. The MODIS cloud products (MOD06) provide retrievals on cloud optical depth (COD), droplet effective radius (DER), liquid water path (LWP, a product of COD and DER), and cloud top temperature (CTT) [*King et al.*, 1992; *Platnick et al.,* 2003]. MOD06 has a spatial resolution of 1 km. Total column water vapor or 'precipitable water' (PW) was retrieved from the 0.94 μm channel [*Gao and*

Kaufman, 2003] at 1 km. Level-2 granule data for aerosol, cloud and water vapor products are used. In addition, the Level-1 sub-sampled reflectance product (at 5 km resolution) helps in choosing a case as explained in the methodology section. Level-1b 1km resolution radiance data are used to calculate brightness temperature (BT) as a proxy for cloud vertical development [*Rosenfeld and Lensky,* 1998].

The multi-angle imaging spectroradiometer (MISR) onboard the Terra satellite measures in four spectral bands, at each of nine viewing angles spread out in the forward and aft directions along the flight path. AOD at 0.5 μm is retrieved over land and ocean using the radiances at these angles, and stored in the MISR level-2 aerosol product. It has a spatial resolution of approximately 16 km. The area coverage of MISR is smaller than MODIS because its swath width is 360 km compared to MODIS's 2330 km. The MISR AOD has been validated against AERONET ground observations [*Kahn et al.*, 2005] and proves to be of high quality over land.

Geo-potential height, precipitable water and wind data from the National Centers for Environmental Prediction (NCEP) Reanalysis are used to depict the atmospheric circulation pattern over the study region. These daily reanalysis data have a spatial resolution of 2.5° x 2.5°. Over the center of our focus study region (the eastern US), much observational data are assimilated into the reanalysis so the quality of the NCEP reanalysis data is relatively high.

2.3 Methodology and Study Regions

An ideal means of studying aerosol-cloud interactions would be to measure the properties of both quantities simultaneously. This is impossible for a passive remote sensing instrument like MODIS, as the cloud would block any signal from aerosols located beneath a cloud layer. This problem may be overcome/alleviated because aerosol properties are relatively homogeneous spatially compared to cloud properties, especially for cumulus clouds. We developed a 'semi-collocated and synchronized' technique to study the AIE for broken cumulus clouds. From the visible reflectance product (MOD02SSH), patches of broken cumulus clouds were first selected as our target scenes. The area of a target scene, a **case,** was chosen such that its coverage is large enough to include a statistically meaningful set of pixels and small enough to assure relatively homogenous dynamic and thermodynamic conditions. A case usually encompasses areas on the order of 10,000 km^2. Clear and cloudy pixels are collected for each 10-km by 10-km region over which one aerosol retrieval and up to 100 cloud retrievals are available. Mean cloud retrieval quantities are used here. It is worth noting that such cloudy scenes are not ideal from remote sensing point of view due to the three-dimensional (3-D) effects of clouds. We have taken various measures to minimize the effects, as explained later. On the other hand, use of cloud retrievals for large-scale more homogeneous cloud system would face a different challenge. Since no aerosol parameters can be obtained under cloudy conditions, previous AIE studies rely on cloud and aerosol data retrieved from cloudy and clear scenes that are far apart in time (e.g. a few days) and/or in space (e.g. hundreds of kilometers). As a result, the aerosol quantities used may not be representative of the cloudy scenes.

We applied a set of screening criteria to these cloudy pixels to ensure data quality: (1) only highly confident overcast cloudy pixels, which is indicated by MODIS cloud mask, were selected; (2) COD is greater than 5 so that the uncertainty of cloud particle size and optical depth retrievals is reduced [*Nakajima and King*, 1990]; (3) only water clouds are considered because ice particles have very different properties from water droplets and low clouds topped with cirrus are excluded by applying a criteria of cloud top pressure larger than 600hPa and cloud phase being water as indicated in cloud product; and (4) DER retrievals less than 4 and larger than 28 μm are considered problematic and discarded. With these criteria and the fact that precipitation associated with convective cumulus clouds occurs often in late afternoon, precipitating clouds, if any, are unlikely to distort our statistics. PW data were retrieved from nearby clear pixels to represent column-integrated water vapor. For each aerosol retrieval over a 100 km^2, retrieved cloud quantities (DER, COD and BT) were averaged for all cloudy pixels, and a mean PW was obtained by averaging the PW data from all clear pixels in a scene. Quasi-coincident aerosol and cloud data were thus created. These ensure that measurements for aerosol and cloud properties are close enough to each other. Over such a small scale, aerosols and clouds are more likely to interact. On the other hand, the retrievals could be contaminated, leading to a potential artifact that will be addressed later.

Over our focus region of eastern US, the AIE is studied case-by-case by correlating aerosol and cloud quantities, following the conventional method but applied over much smaller areas with simultaneous aerosol and cloud observations. Our basic assumption is that for each case, the general environmental conditions

remain identical across that area, effectively reducing the impact of large scale meteorology. The relationships retrieved thereafter would be a signal of AIE, which has certain superiority over those derived from clear and cloudy scenes far apart in time and/or space. Correlation analyses were done among multi-variables: AOD, COD, DER and PW.

To study the aerosol effect on cumulus clouds formed under conditions where water vapor amount is variable, we chose a transect from southeastern US to northeastern US as our focus region. Abundant convective clouds form over land surrounding the Gulf region during summer and the water vapor amount varies considerably from the coast to inland. Water vapor is blown inland from the ocean by the winds created by the prevailing Bermuda high-pressure system and the local ocean sea breeze in summer. Land surface heating generates sufficient convection to fuel cumulus cloud development. The interaction between cloud microphysics and aerosol for locally generated clouds is expected to differ considerably from that of clouds transported from elsewhere by a front or other large-scale weather systems.

Figure 1 shows the distribution of a convective cloud scene, which contains two cloud regimes: sea-breeze-induced small-scale convective clouds in the south and a frontal meso-scale cloud system driven by large-scale atmospheric circulation in the north. It is the former cloud type that is investigated in this study. We have browsed through a number of MODIS images taken during July of 2001.

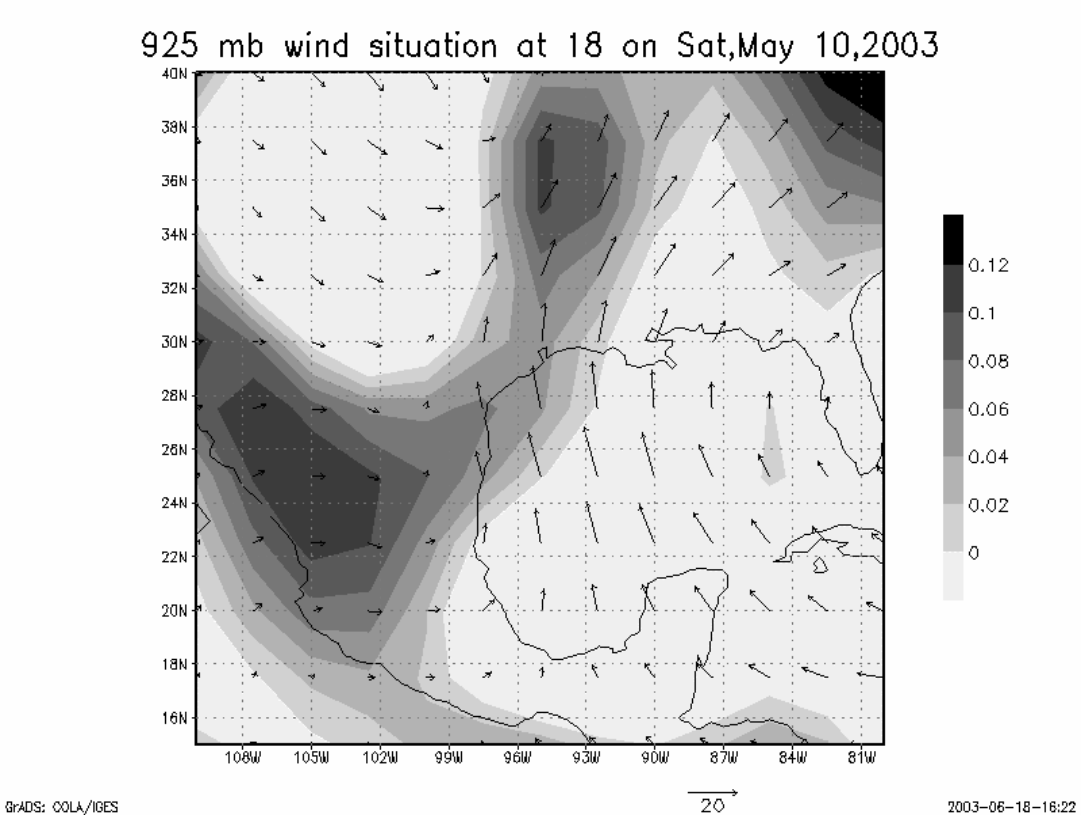

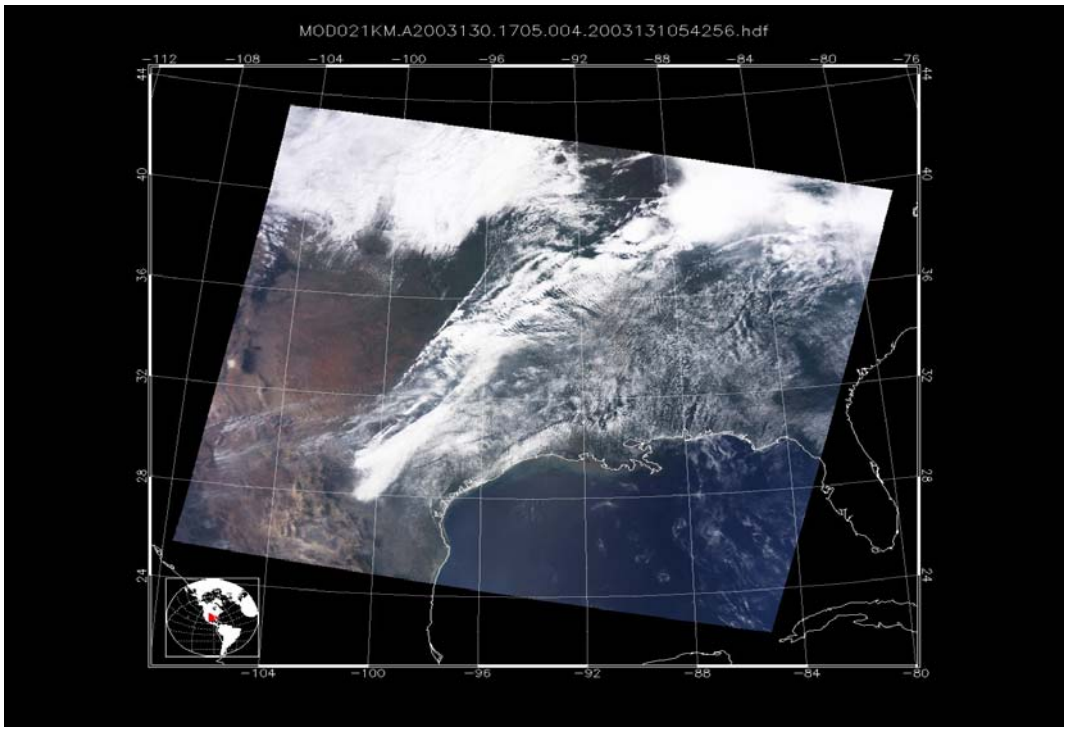

Fig. 1. Upper panel: NCEP/NCAR reanalysis of wind vector (m/s) and vertical velocity (shaded area for updraft) at 18 UTC, both on May 10, 2003; Lower panel: MODIS cloud image at 17:05 UTC

We extend our analysis to other regions over the globe like the Indian subcontinent, Eastern China, the Amazonia, Northern and Southern Atlantic, Southeastern Pacific, and Indian Ocean as summarized in Table 1. Cloud types over these regions encompass fair-weather cumulus, marine stratiform clouds and trade cumulus; aerosols are also diverse, including sulfate, dust, sea salt, smoke, organics and mixture of them. The wide spectrum of cloud and aerosol types covered in the analysis offer an opportunity to both investigate the variation of AIE and gauge our analysis against previously well-established results over regions like Brazil and Indian Ocean. Consistency/inconsistency is a further test of the validity of our analysis method, data and results. For each region we use the same technique to select and filter the data, and combine the filtered data points together to gain enough samples to get stable statistics. Data were stratified in each region in terms of environmental variables like water vapor amount, viewing geometry etc to suppress large scale influence. For each stratified sub-set, the data are binned into three equal-size groups based on their AOD values, for which BT-DER profiles [*Rosenfeld and Lensky,* 1998] are calculated and the AIE is examined as the difference among profiles that have distinct aerosol loadings. We use *student's t-test* to examine the significance of the difference.

Region	Latitude range	Longitude range	Dominant Aerosol/Cloud Types	Period	AIE efficiency	Sample size
North Atlantic	10-20N	20-40 W	Dust, Stratocumulus	June-August, 2002	Negative	99,978
South Atlantic	5-20S	5E-20W	Smoke, Stratocumulus	June-August,2002	Negative	100,377
Southern Pacific	5-25S	75-105W	Sea salt, sulfate and pollution, Stratocumulus	August-October,2002	Negative	74,216
Indian Ocean	12-20N	60-70E	Dust with pollution, Trade cumulus	June-August, 2002	Negative	94,023
India	13-24N	70-85E	Mixture of sulfate, dust, sea salt and smoke, cumulus	June-August,2002	Neutral	53,888
Amazonia	8S-12N	44-76W	Mainly smoke	August-October, 2002	Negative	672,421
Southeastern China	23-43N	100-120E	Mixture, cumulus	June-August,2002	Positive	179,533

Table 1. Regions analyzed. The location, dominant aerosol and cloud types, time span, the AIE efficiency and sample sizes are given. These regions are analyzed using 'ensemble approach' as discussed later in the text. The sample size in the table equals to the total number of qualified cloud-aerosol pairs.

2.4 Result from Focus Region (eastern US)

AOD-DER plots of four representative cases are presented in Fig. 2. The slope of the AOD-DER relationship can be interpreted as the change of DER for a unit change of AOD and here it is referred to as the AIE efficiency. Like previous findings, the AIE efficiency varies considerably, but they can be either negative or positive in our study, ranging from -7.7 μm to 12 μm. The majority of cases in our focus region (eastern US) have a positive AIE efficiency, which means that the cloud droplet size increases with increasing loading of aerosols. This is a different result from earlier studies and could imply a different physical process governing the AIE for cumulus clouds relative to stratiform clouds, barring the presence of retrieval artifacts inherent to remote sensing. Potential artifacts are investigated below.

PW was once hypothesized as a factor dictating the variation of AIE [*Kaufman and Fraser*, 1997], but it was later negated for smoke aerosols observed during the dry season in the Amazon [*Feingold et al.*, 2001]. This may imply that the different sensitivities have something to do with aerosol hygroscopic properties. Along the corridor from Texas to the Northeast US (our focus region), industrial emissions and sea salt (near the coast) are dominant. Other factors have also been hypothesized such as cloud type, dynamics, turbulence, and aerosol properties, or their combinations [*Feingold et al.*, 2001] but few have been confirmed with real observational data. Close correlation was found between the AIE and vertical turbulence measured by an aircraft (*Leaitch et al.*, 1996]. Using a cloud parcel model,

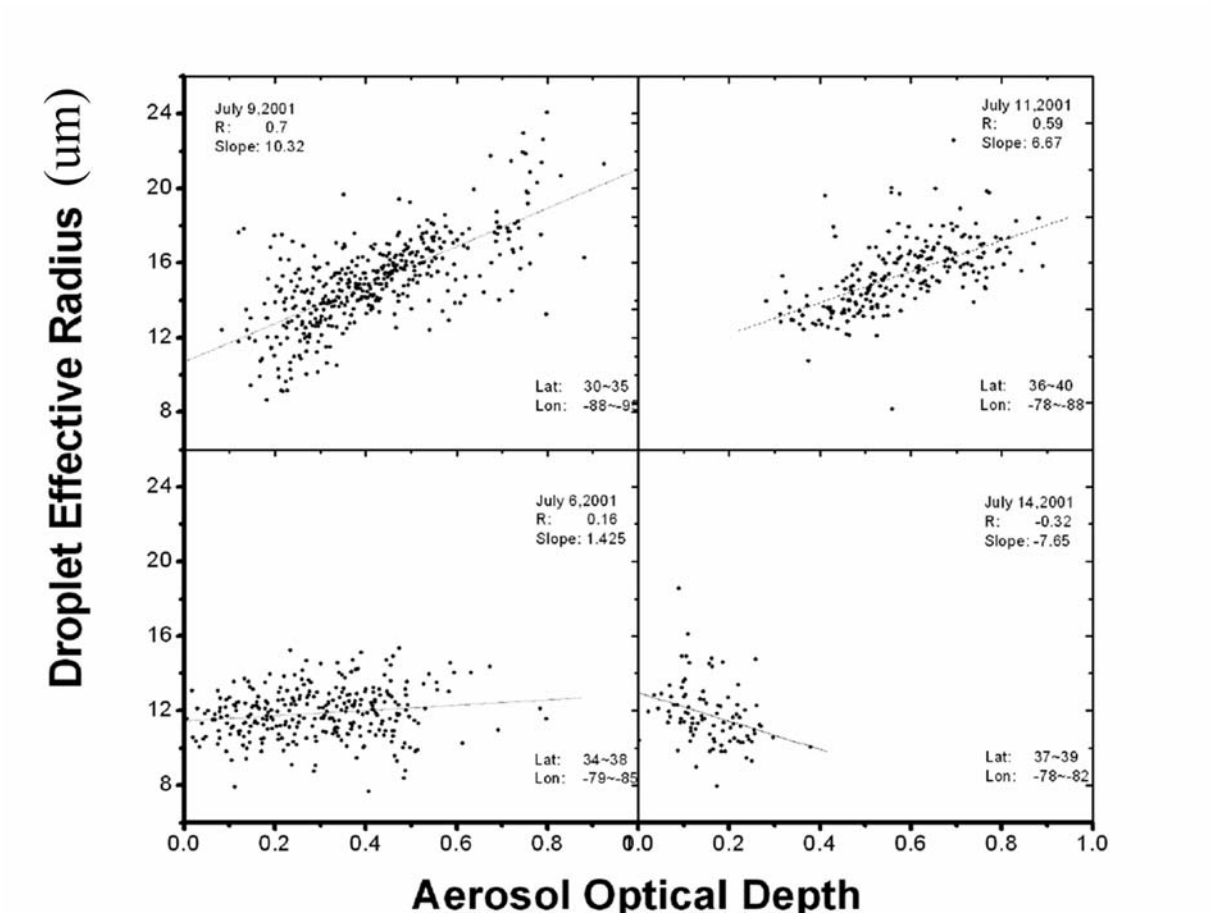

Fig 2. AIE efficiency for four cases. The time and location, correlation coefficient (R), and the slope of each case are provided in each panel.

Feingold et al. [2003] found that changes in DER with aerosol extinction have a strong dependence on updraft for high aerosol loading conditions.

To find factors that influence the AIE efficiency in our study, a set of statistical analyses were performed. PW turns out to be the most influential factor in driving the variation of AIE efficiency as demonstrated in Fig 3. Each point in Fig 3 represents a case corresponding to a cumulus cloud scene. The correlation coefficient between AIE efficiency and PW is as high as 0.84. In other words, about 70% of the variance of AIE efficiency is explained by changes in PW. The AIE efficiency is positive and large for moist regions and small, or negative, for dry regions. This relationship is also clearly seen from a map showing the spatial variation of the AIE efficiency and the distribution of mean PW averaged over July 2001 for our study region (Fig. 4).

2.5 Possible Explanations

2.5.1 Artificial Correlation Explanations

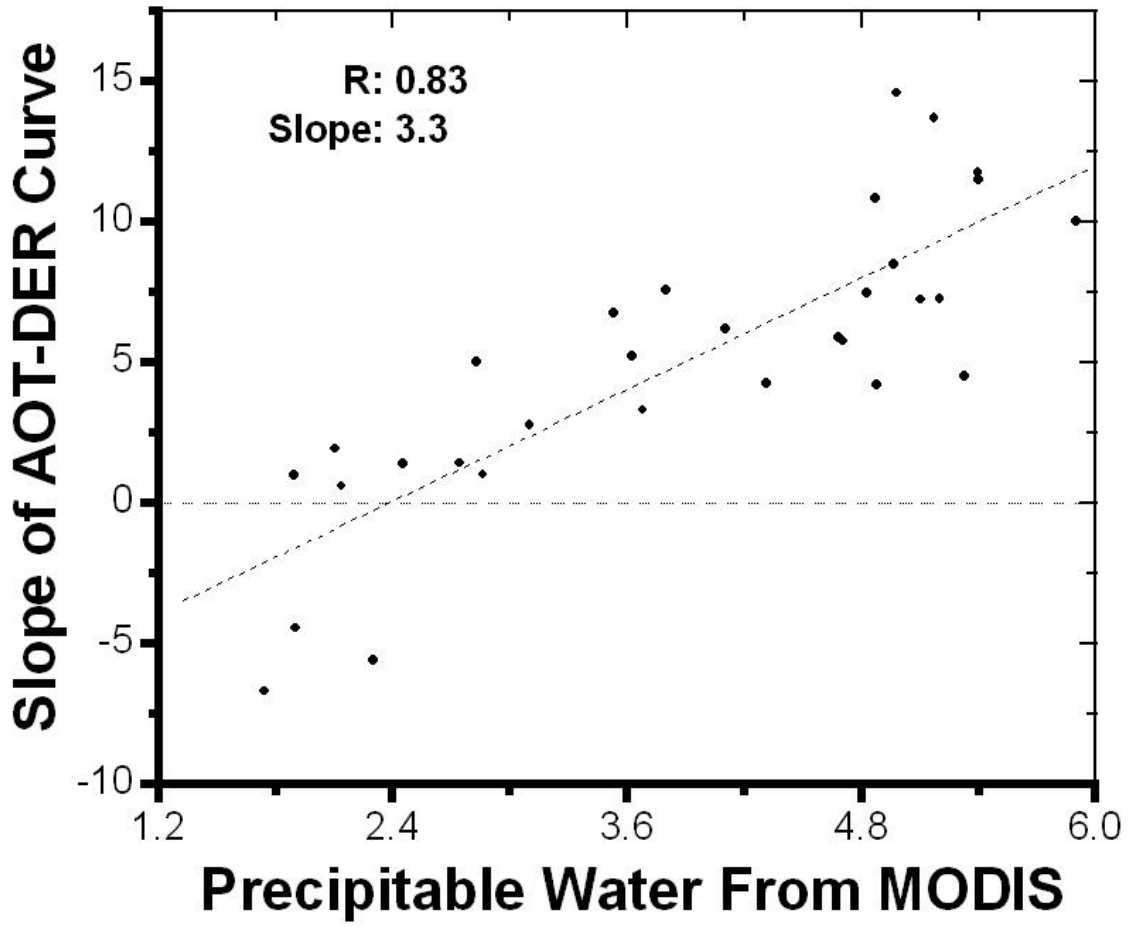

Fig 3 Dependence of the AIE efficiency on precipitable water (with unit cm/m^2, or simply cm) for all cases studied in southwest and interior US (see Fig. 4). The correlation coefficient (R) and slope between these two quantities are given.

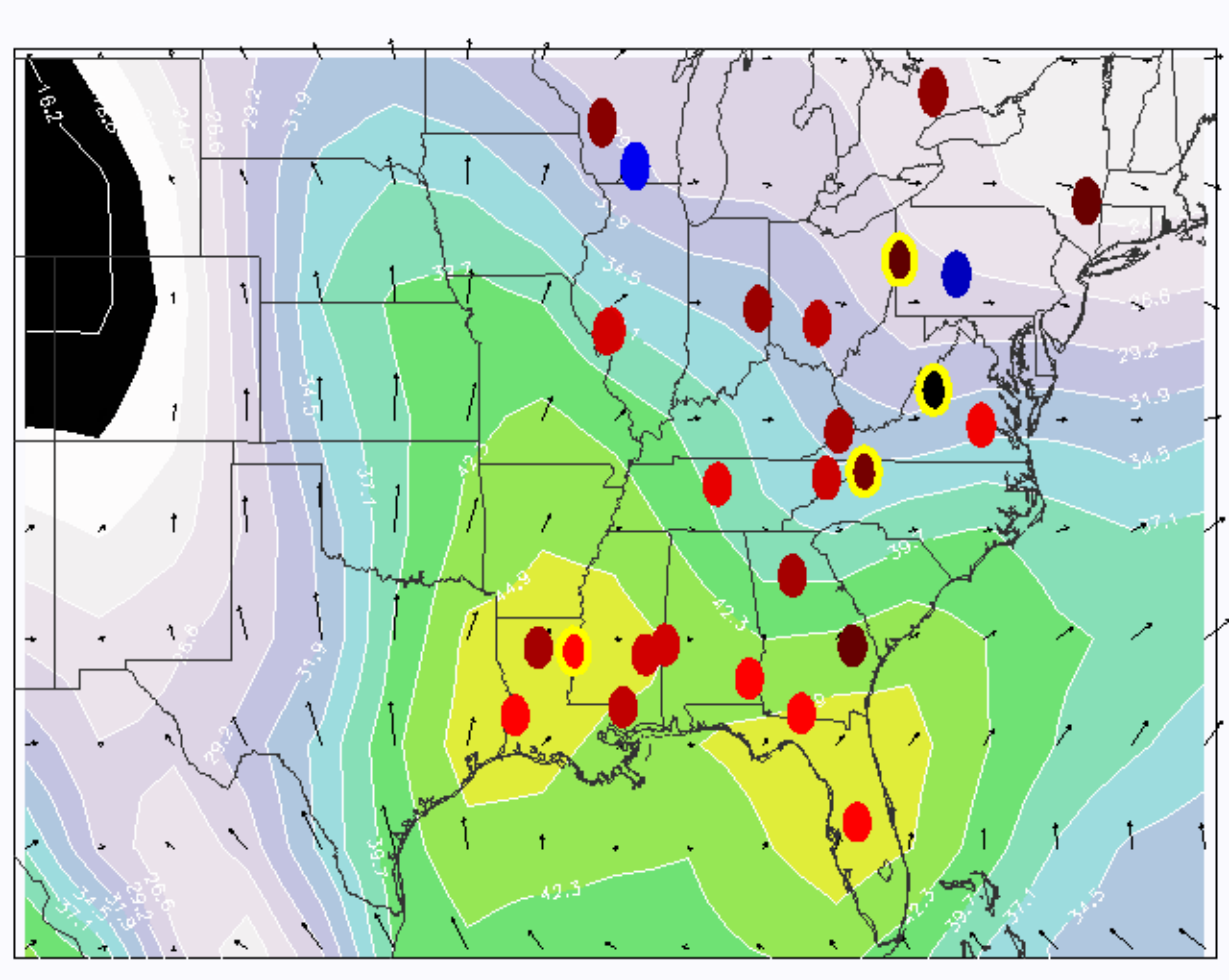

Fig. 4 Distribution of the locations for the scenes selected in the study. Bright red dots denote large slopes, darker red for smaller slopes and blue for negative slopes. Monthly mean precipitable water and wind vectors for July 2001 from the NCEP-NCAR reanalysis are superimposed. Precipitable water has unit of mm/m^2,or simply mm. The yellow circles are the four cases presented in Fig 2.

Caution is warranted in accepting the above finding in light of various data uncertainties. A critical question is whether the dependence of DER on AOD and their slope on PW result from observational artifacts. If an error in one variable is correlated with an error in another, a false correlation may occur between the two quantities. Even if the two quantities had no retrieval errors, they could be physically linked to a third factor, leading to an "apparent" or false correlation. We examined all potential third factors including cloud contamination, aerosol humidity effect, cloud dynamic effect and 3-D effects that could explain the observed correlation.

i) Partially Cloudy Effect

MODIS aerosol algorithm has a strict cloud masking procedure to ensure that only clear pixels are retrieved [*Remer et al.*, 2005]. It uses spatial variability to identify low clouds [*Martins et al.*, 2002] and 1.38 μm channel [*Gao et al.,* 2002] to detect high clouds in addition to standard cloud mask product. It also excludes the 50% brightest pixels and the 20% darkest pixels for possible cloud contaminations including both the scattering and shadowing effects of broken clouds. Nevertheless, some cloud-contaminated pixels might still be erroneously identified as clear. Meanwhile, reflected radiance from partially clear pixels may be accentuated due to cloud scattering and reflectance, leading to overestimation of AOD. Also a partial cloudy pixel can result in the overestimation of DER due to lowered reflectance at the 2.1 μm channel [*Nakajima and King*, 1990]. Thus the co-existence of partially cloudy

and partially clear scenes could incur a false correlation between DER and AOD.

Several tests were conducted to assess the potential effect of partially cloudy scenes. First, correlations between cloud fraction and AOD and DER are calculated to determine the impact of cloud fraction on both retrievals. No significant correlations were found between AOD-DER slopes and cloud fraction in our study. The correlation coefficients between cloud fraction and AOD for the four cases shown in Fig. 2 are 0, 0.05, 0.26, and 0.05. To further examine the effect of cloud fraction, the data were stratified by cloud fraction and the AOD-DER slopes were determined for high, greater than 20%, and low, less than 10%, cloud fractions. As plotted in Fig 5, the two slopes are almost identical to each other and the mean values of AOT and DER for these two sub-datasets are also identical. Secondly, clusters of cloudy pixels were identified that are connected to each other. Inside a 10km by 10km aerosol pixel, the number of clusters is an indicator of the 'brokenness' of clouds. The data were then stratified and the AOT-DER relationships were analyzed corresponding to different numbers of clusters. Nearly identical slopes were obtained for the data with a higher number of clusters, 3 to 5, and lower, 2 to 3 (Fig not shown here). Connectivity of a cloudy pixel is defined by the number of cloudy pixels that are directly connected to it. If a cloudy pixel is surrounded by all immediate neighboring cloudy pixels, the connectivity is equal to 8 and this pixel is less likely to be partially cloudy than those with a low number of connectivity. An AOD-DER analysis for the data with

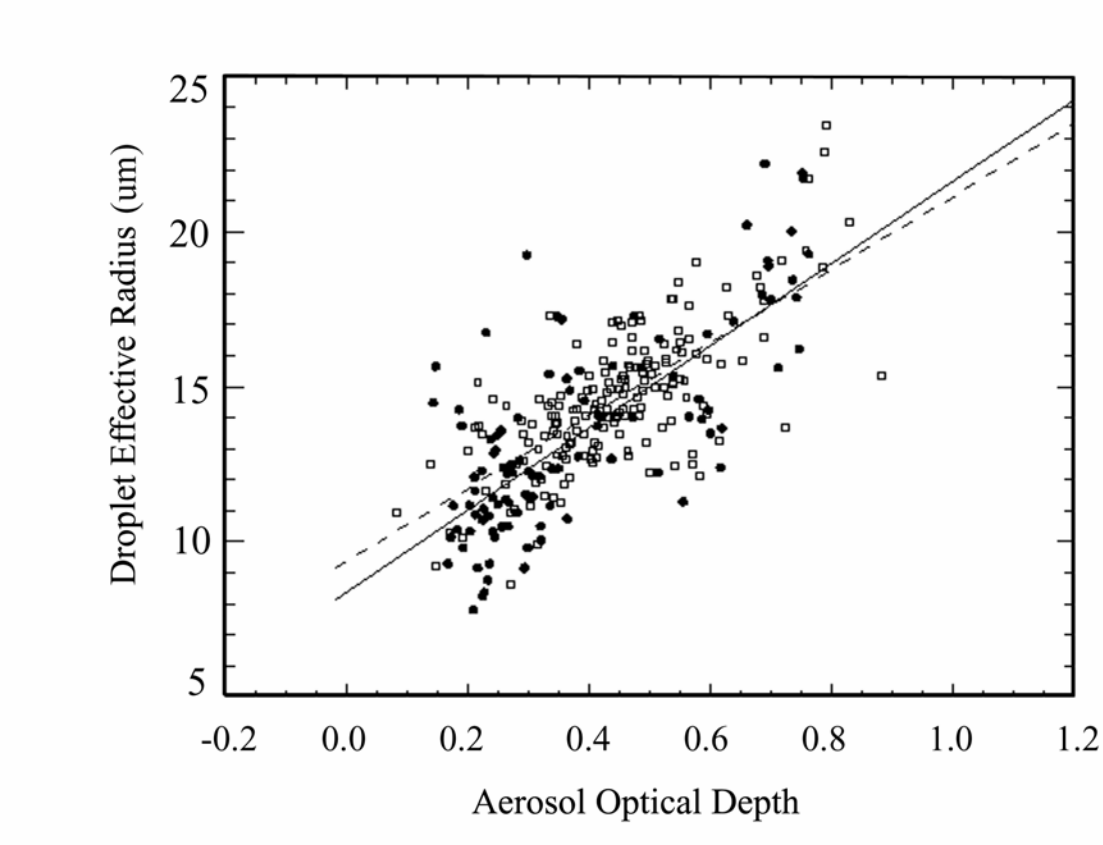

Fig 5a AOD-DER plots using pixels classified by cloud fraction. Solid line is for cloudy pixels at the lower end of cloud fraction distribution (solid dots) and the dashed line is for those at the higher end of cloud fraction distribution (open square).

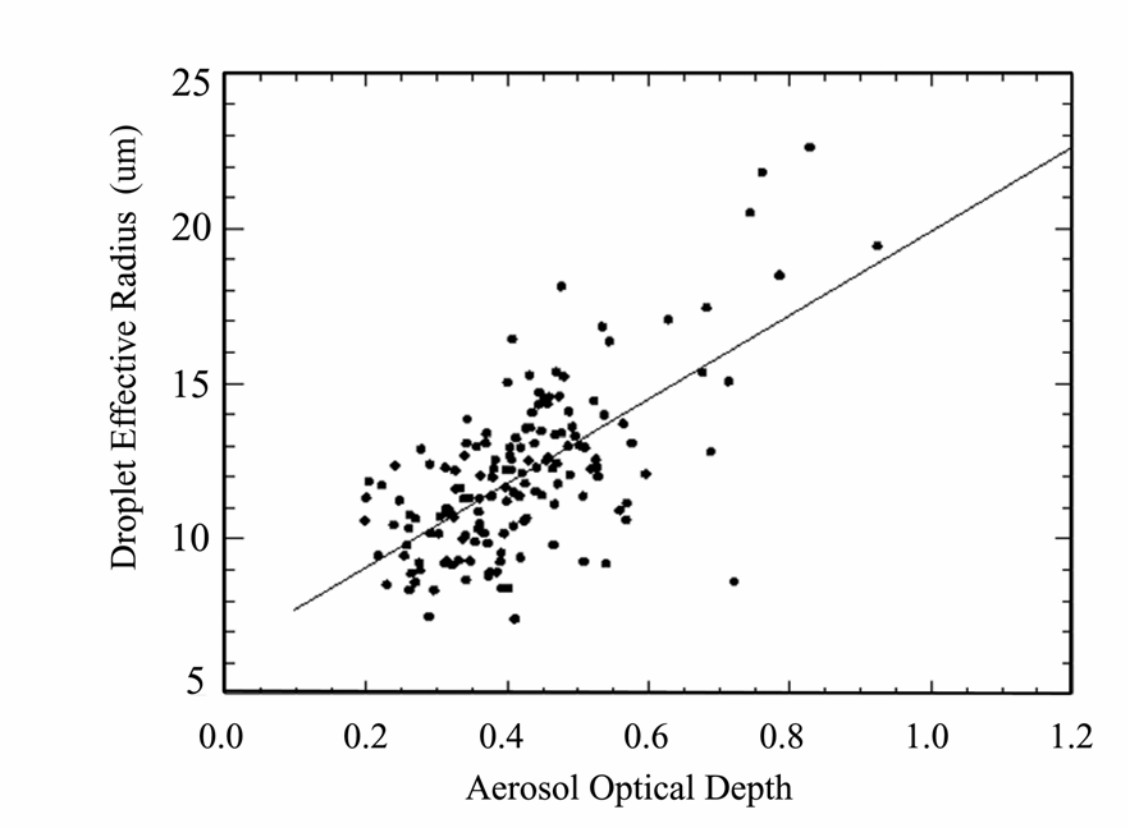

Fig. 5b The AOD-DER correlation using only cloudy pixels with connectivity equal 8

connectivity equal to 8 showed a similar slope to the plot in Fig 5b that includes all possible pixels. From the analyses, we may conclude that the partially cloudy effect is not likely the cause of the observed relationship, at least not a major one.

ii) Cloud 3-D Effect

The cloud retrieving algorithms that were used to produce the MODIS cloud products (MOD06) assume plane-parallel clouds [*Nakajima and King,* 1990]. For 3-D shaped clouds, variations in the satellite viewing geometry (relative to the Sun's position) can change satellite-measured signals and incur errors in the retrievals of both aerosol and cloud properties as discussed in depth by *Vant-hull, et al.* [to be submitted] and *Wen et al.* [2006]. If a satellite sensor and the sun are on the same side relative to the nadir, a portion of the incoming solar radiation is reflected by the cloud side and larger radiances are measured. Across a swath of a satellite image, the viewing geometry varies from backward to forward scattering directions, or vice-versa, depending on the spacecraft orbits, namely local morning or afternoon. *Vant-hull et al.* [2006] noted that the relative azimuth angle (RAA) between satellite and the sun is a key parameter determining the retrieval biases. To minimize the influence of this cloud 3-D effect, we selected narrow image slices in north-south directions so that the RAA remains virtually identical. For nearly all cases studied, the correlation slopes between AOD and DER for the sliced

scenes are in agreement with those derived using all pixels, while the magnitudes of the slopes may differ somewhat, as shown in Fig. 6. The slight deviation in the magnitude could result from sampling errors, as data samples are fewer for sliced scenes than for the overall scenes. The variations in the slope may also be a manifestation of the 3-D effect, but the persisting general agreements seem not to support the suggestion that the cloud 3-D effect is the major cause for a false correlation between AOD and DER. Further evidence against 3-D effect will be presented below.

iii) Swelling Effect of Water Vapor

Aerosols can be divided into two categories according to their hygroscopicity. Hygroscopic aerosols grow in size when soaking up water vapor and deliquesce when the humidity passes their 'deliquescence relative humidity' [*Hanel*, 1976]. Hydrophobic aerosols do not change much in size with humidity. It has been reported that AOD increases in response to both size and refractive index changes due to water vapor swelling [*Feingold et al.*, 2003]. Suppose aerosols around deeper clouds, for example, swell more because of higher relative humidity and thus have a larger optical depth. At

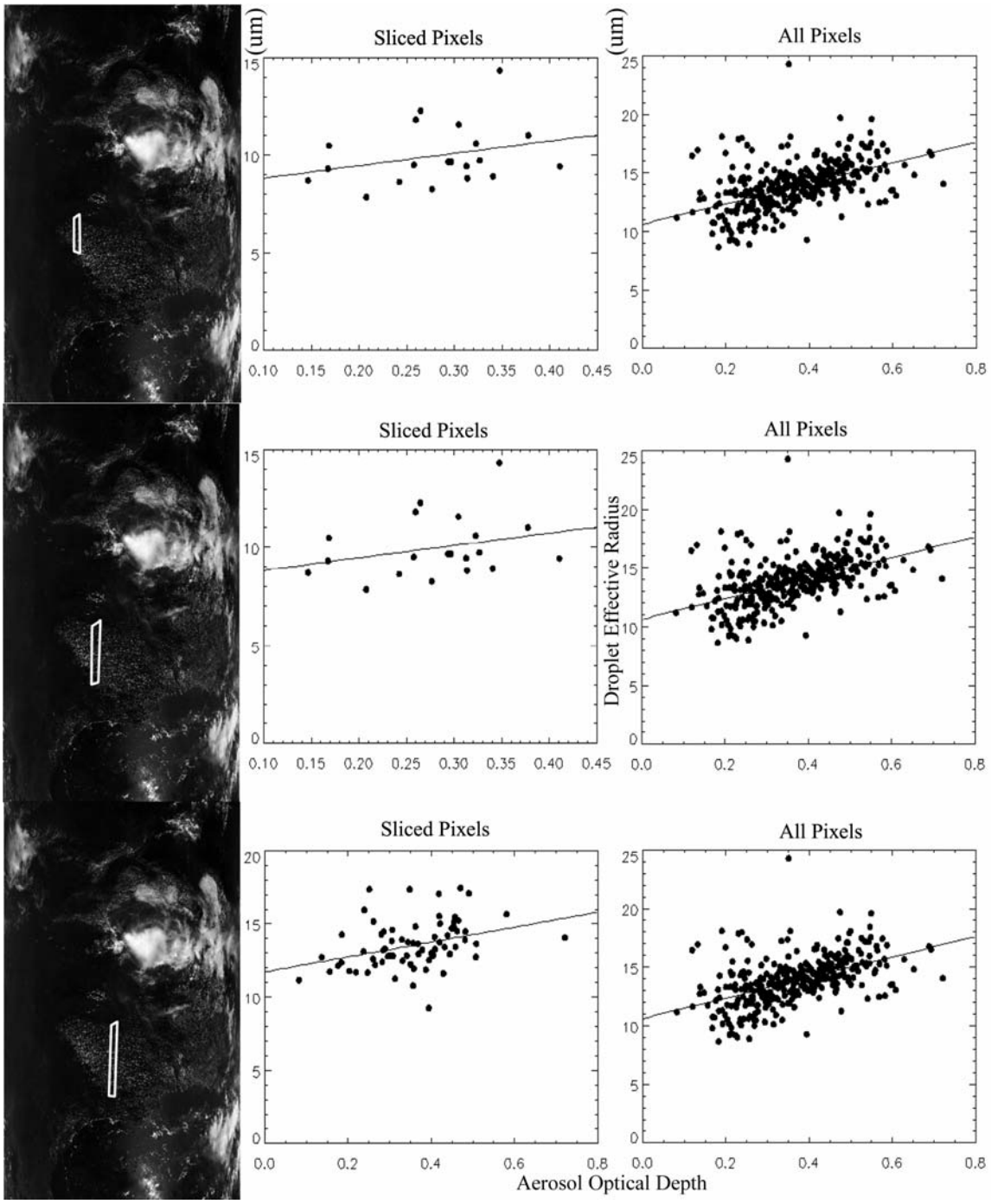

Fig 6 Three slices of a convective cloud scene (bright white polygons on left images) at 1900 UTC on July 9, 2001 and associated AOD-DER plots (middle panels), in comparison with the AOD-DER plots for the entire scene (right panels). X-axis is AOD and y-axis is DER (in μm) in each scatter plot.

the same time, deeper clouds tend to have larger droplets than shallower clouds. A positive correlation may thus be observed between aerosol loading and cloud droplet size even with perfect retrievals of the two quantities.

For aerosols over the Southern Great Plains, *Sheridan et al.* [2001] showed that hygroscopic growth is an important factor in determining the aerosol optical depth for sea salt aerosols. Using aircraft and lidar data from the Atmospheric Radiation Measurement program (ARM), a positive correlation between humidity and aerosol extinction was observed [*Jeong and Li*, 2006, to be submitted shortly]. Precipitable water is used here to check the swelling effect. In our analysis, we do observe some degree of correlations between DER and AOD and PW, as seen in Figs. 7. However, the correlations are too weak to explain the tight correlation between AOD and DER. The weak correlation between AOD and PW might have something to do with the fact that the variability of AOD itself often is large and hence can outweigh the effect of humidity. Therefore the humidity effect cannot explain the AIE.

iv) Dynamic Effect

There is another scenario under which higher aerosol loading may be anticipated, namely, the "pumping effect". Stronger convection produces deeper clouds. For convective clouds during the developing stage, deeper clouds tend to have larger droplets at cloud tops. In-situ aircraft

measurements in the Amazon showed a clear dependence of DER on the height above the cloud base (personal communication with V. Martins at

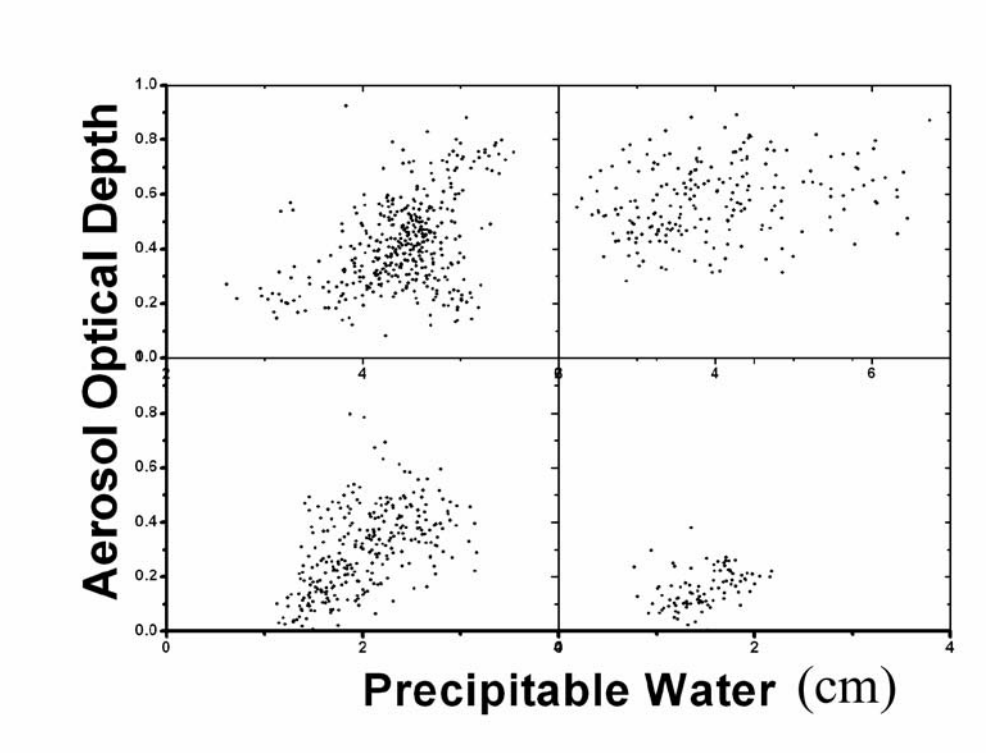

Fig 7a. Dependence of aerosol optical depth data on precipitable water (in *cm*) amount for the same four cases as in Fig 2.

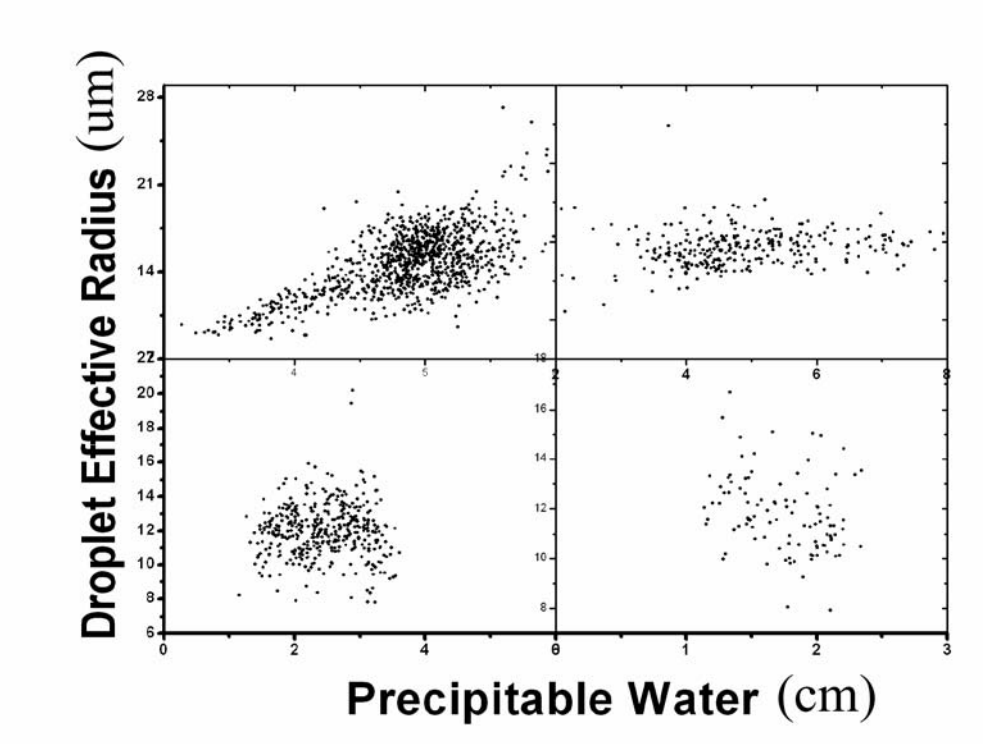

Fig 7b. Dependence of droplet effective radius on precipitable water (*cm*) for the four cases as in Fig 2.

NASA/GSFC). Meanwhile, convergence accompanying updrafts and detrainment of particles by clouds can 'pile' up aerosols around clouds. Both scenarios result in a false correlation between AOD and DER, which is referred to here as the 'dynamic effect'. On the other hand, as postulated in *Young* [1993], aerosols not only impact directly on cloud microphysics but also affect the dynamics through modification of radiative and thermodynamic heating. Locally generated cumulus clouds are formed from rising thermals containing aerosols that serve as CCNs. Interaction between aerosols and cloud development is thus likely to take place under these circumstances. Therefore the correlation can be a manifestation of the interaction between aerosol and cloud.

To get a first glance of the potential dynamic effect, we assume that clouds have a uniform cloud base height over the relatively small study region. CTT is then a proxy for cloud depth. In either scenario, a negative correlation would be expected between CTT and DER, and between CTT and AOD, which appeared to be true for some cases. To check if cloud dynamic effects are the cause for the correlation between AOD and DER, the two variables were analyzed with the condition that the CTT fall within very narrow intervals (1^{o}) (Fig 8). Suppose the dynamic effect is the sole cause for the correlation observed, we would observe no positive correlation. However, the same positive correlation between AOD and DER exists for the sliced sub-

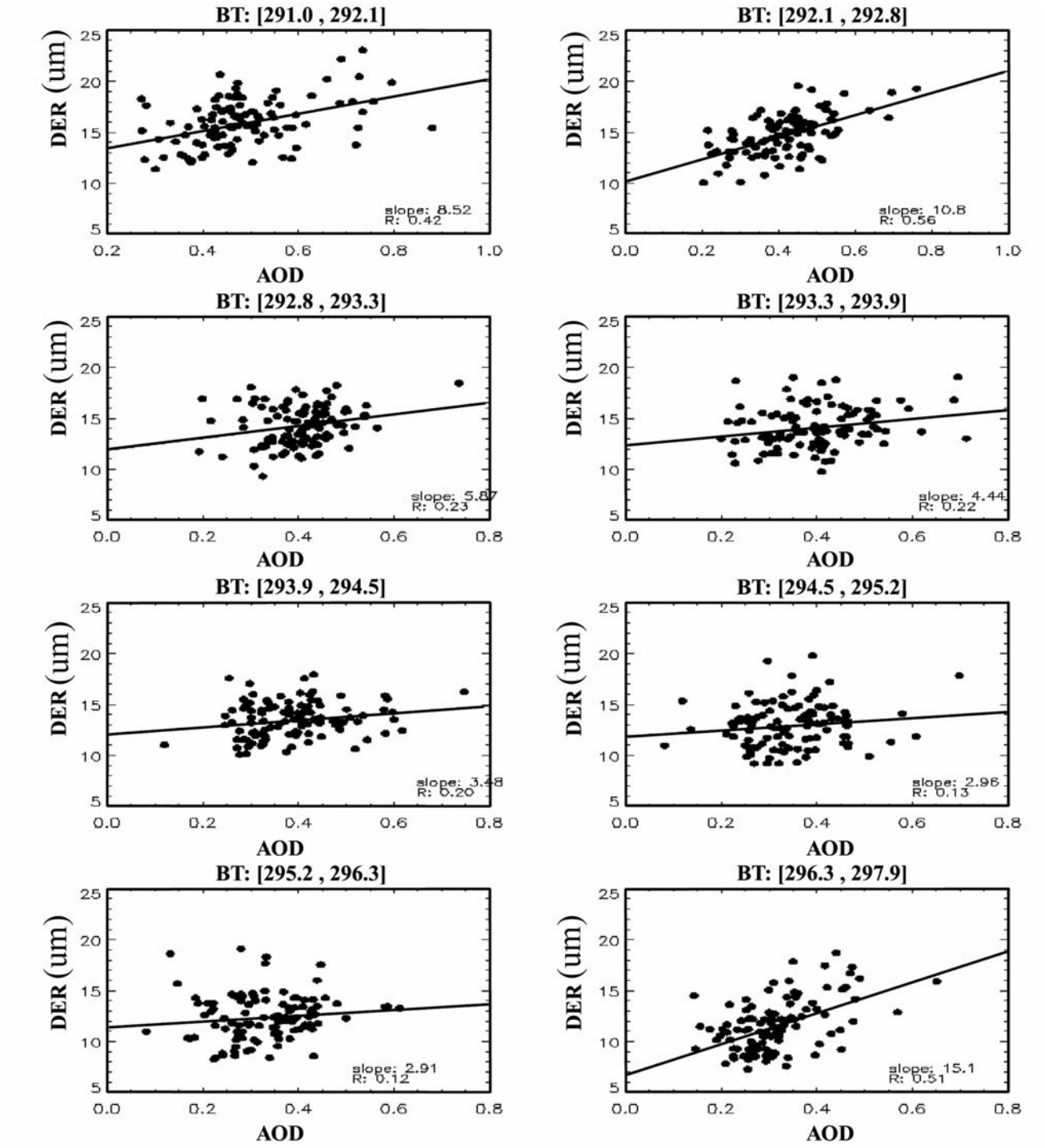

Fig. 8. AOT-DER plots for eight intervals of cloud top temperature for a case at 1900 UTC on July 9, 2001. The intervals of temperature are provided in the plot titles.

samples, which suggests that the dynamic effect is not the sole cause for AOD-DER correlation.

v) Surface Effect

Retrieval of AOD over land is much more challenging than over oceans, due to the influence of the surface. The retrieval uncertainty is significantly smaller over ocean than over land [*Remer et al.*, 2005]. Prior to MODIS, most global aerosol products were confined to oceans [*Nakajima and Higurashi*, 1998]. AOD-DER correlation analyses were performed using data collected over the ocean to check if the correlation is unique to land. Many cases of positive correlations were found and an ensemble analysis done over the Caribbean Sea also reveals positive AIE efficiency (not shown here). This may imply AIE's dependence on cloud regime and aerosol type, which is further explored in our global analysis below. It has also been shown in previous studies that different cloud types have different susceptibility to aerosols [*Platnick and Twomey*, 1994].

A fixed relation between surface albedo at 2.1 μm and visible channels is assumed for AOD retrievals over land [*Kaufman et al.*, 1997]. This method is sound in general [*Kaufman et al.*, 2002B] with a potential exception over wetland surfaces where the correlation established for global applications may have systematic errors. Since thermally induced cumulus clouds are more likely to occur over wetter than drier areas, a false correlation between AOD and DER might exist. Unfortunately, we cannot address the issue directly. An

indirect approach was pursued using MISR AOD data. The principle of AOD retrieval from MISR is very different from the MODIS AOD retrieval. The former is based on changes in atmospheric scattering from different viewing angles, which is much less sensitive to errors in surface albedo [*Kahn et al.*, 2005]. Within the narrower strips of MISR images, MODIS and MISR instruments deployed on the Terra platform observe the same aerosol field. There are much less coincident MISR AOD and MODIS DER data due to spatial coverage differences and more importantly, differences in the retrieval algorithms, especially the cloud masking procedure. Nevertheless, for all the cases we analyzed, similar trends and slopes, though much worse correlation, between MISR AOD and MODIS DER were found, as seen in Fig. 9. This implies that the surface effect is not a dominant factor.

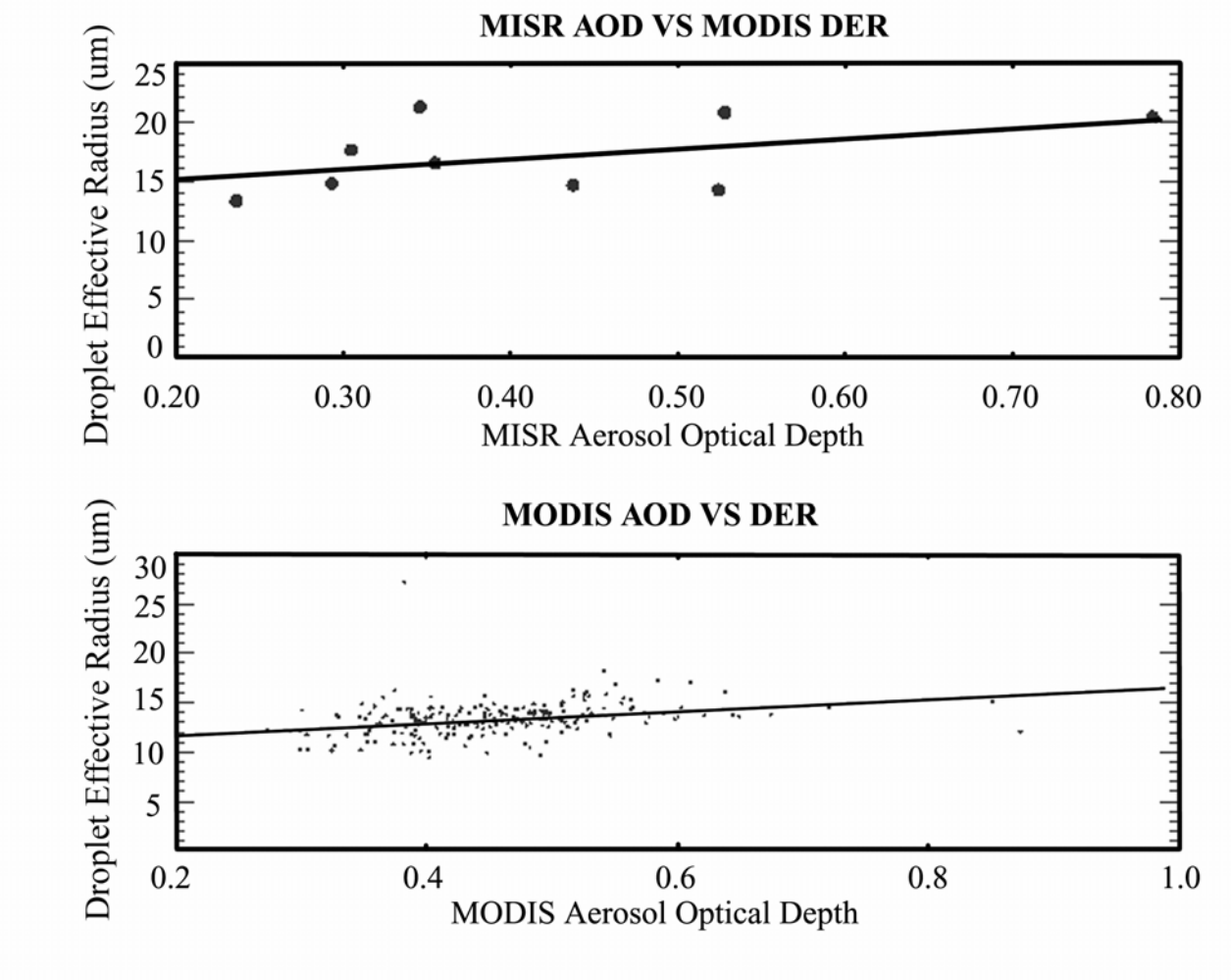

FIG. 9: Collocated MISR (upper, slope: 8.3 and R: 0.43) and MODIS (lower, slope: 5.9 and R: 0.5) AOT-DER plots for a case at 1835 UTC on July 6, 2001.

2.5.2 Possible Physical Mechanisms

The various analyses presented above lead to a sound argument that the observed positive relation between DER and AOD is likely a real phenomenon. This is further reinforced by analyzing more aerosol and cloud data over several other regions around the world as is presented below. We present two plausible mechanisms to explain the observed relationship, one regarding to aerosol composition, which is an important factor in determining the activation of droplets [*Facchini, et al.*, 1999], and the other to the existence of giant CCNs.

i) Intercomparison of Two Methods

Our investigations of the various potential artifacts are extensive while we note that there still could be other unrecognized and/or unverifiable possibilities. For example, a study by *Vant-Hull et al.* [2007], hereafter referred as VH07, investigating the same type of clouds over Amazon found cloud droplet size decreases with aerosol loading as expected and confirming with previous studies over that region [*Kaufman et al,* 1992 and 1998; *Andreae et al.*, 2004]. The sampling technique is different in their study from what is used here. One obvious explanation for this contradiction is that two investigations used different methods sampling the cloud field. The apparent

contradiction could also be attributed to regional differences in aerosol types and other conditions. How aerosol type may make a difference will be discussed in details later in this manuscript. We focus here on compare these two sampling techniques by applying both of them to both regions to check whether they qualitatively agree with each other.

The technique used in VH07, an automatic 'statistical ensemble' approach, first discards cloudy pixels that have brightness temperature colder than 270K, optical thickness less than 3, effective radius smaller than 4μm or larger than 29μm or that are located in coastal areas or regions with elevation higher than 500m to control the data quality before the deployment of an automated fair-weather cumulus selection algorithm. The selection algorithm is developed based on cloud fraction and local average number of cloud edges in an 11X11 pixel box centered on each cloudy pixel. It has been demonstrated in VH07 to perform well to correctly separate cumulus clouds from other cloud types. MODIS data from the Amazon basin during burning season of 2002, August to October, is processed to form a large sample. The ensemble data are then binned by using different constraints to select subsets that have similar environmental conditions. For each subset the BT-DER plots [*Rosenfeld and Lensky*, 1998] will be utilized with data evenly divided into three aerosol profiles, representing 'clean, normal, and dirty' conditions. With sufficient amount of data having similar environmental conditions the difference in DER among the profiles is a manifestation of AIE. The significance of the difference between two profiles is evaluated by applying

the student's t-test. The detailed discussion on this method can be found in VH07.

We apply the statistical, ensemble approach to our US study region for inter-comparison. Dependence of DER on aerosol loading was presented in Figure 10. To minimize potential artificial correlations data included in Fig 10 all have cloud optical depth larger than 8 and fall within backscattering region. The middle panel shows three aerosol loading profiles as a function of BT. Mean cloud BT-DER profiles for three aerosol profiles are shown in the left panel. In the right panel the $AIE \equiv -\frac{d(\ln r_e)}{d(\ln \tau_a)} \approx -\frac{(\Delta r_e / r_e)}{(\Delta \tau_a / \tau_a)}$ is displayed, where it is noted that *IE* has opposite sign to AIE efficiency. Polluted clouds with heavy aerosol loading have larger droplets than clean ones, meaning DER increases with AOD or positive AIE efficiency, qualitatively agreeing with our result using scene-by-scene technique. To get even higher quality data to remove surface contamination clouds with optical depth below 20 are filtered out [*Vant-Hull et al.*, 2007; *Rosenfeld et al.*, 2003]. Results are presented in Fig 11 where the AIE efficiency remains positive for this region after this filtering process. The AIE efficiency's dependence on PW is investigated in Fig 12, where two sets of clouds are separately analyzed: One with PW equal or lower than 2 cm and the other with PW greater than 2 cm. AIE efficiency changes from neutral or slightly negative for low PW conditioned clouds, to positive for high PW conditioned clouds, which

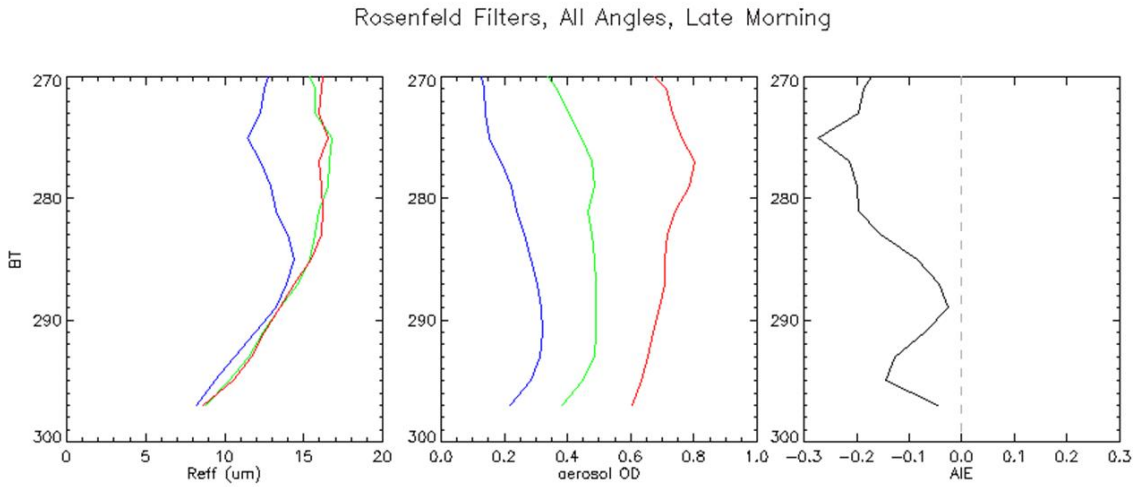

Fig 10 DER profiles using the ensemble approach for eastern US region. AIE is negative, positive AIE efficiency, agreeing with results from our study. Three lines in the middle panel represent clean (blue), normal (green), and polluted (red) conditions.

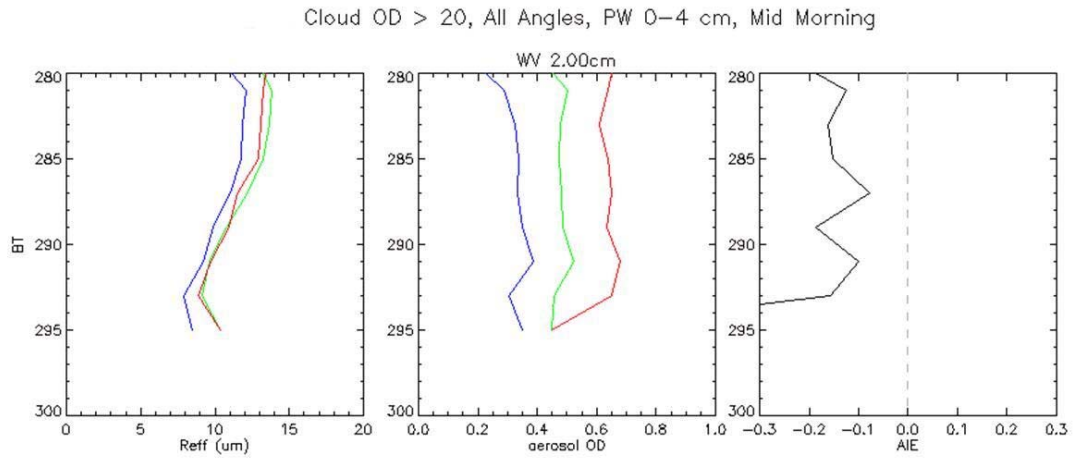

Fig 11 DER profiles for focus region with COD greater than 20 to minimize potential artifacts. AIE efficiency is still positive. The colors have the same meaning as in Fig 10.

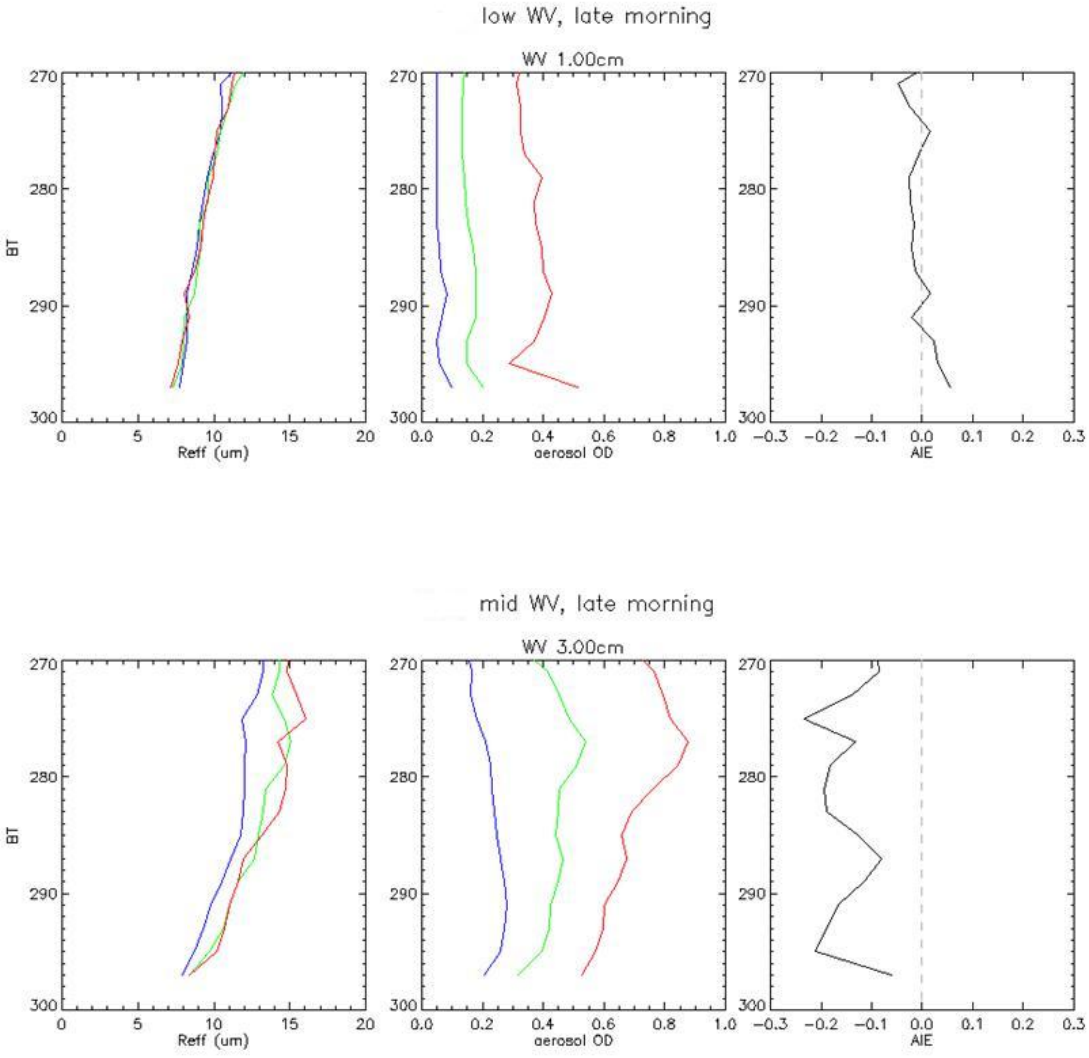

Fig 12 Upper panel: data with PW between 0 and 2cm; Lower panel: data with PW between 2 and 4cm. The AIE efficiency positively depends on PW.

qualitatively agrees with our results presented above. That is, AIE efficiency is positively correlated to PW.

For inter-comparison purpose we visually inspect numerous images over Amazonia to select large number of scenes and data from these scenes are collected to form an ensemble set to apply similar analysis by the ensemble approach. To avoid possible retrieval artifacts as discussed in details above and in VH07 we screened the data by constraining the viewing geometry in back-scattering regime and by filtering out clouds with COD below 10. Figure 13 shows results from Amazon with our scene by scene approach after proper data screening. DER increases nicely with decreasing BT as expected based on physical grounds. AIE efficiency is negative for this region agreeing with VH07 and past investigations.

Together by switching methodologies results from both methods agree with each other for both regions, which demonstrates that our new findings are not due to biased selection of individual scenes. As summarized in Table 1 and detailed discussion later, results from our analysis agree well with past studies, which further validates our results and negates the null hypothesis that our new findings simply results from an artificial correlation. We will proceed with further discussions on possible physical mechanisms and come back to show results from global analysis.

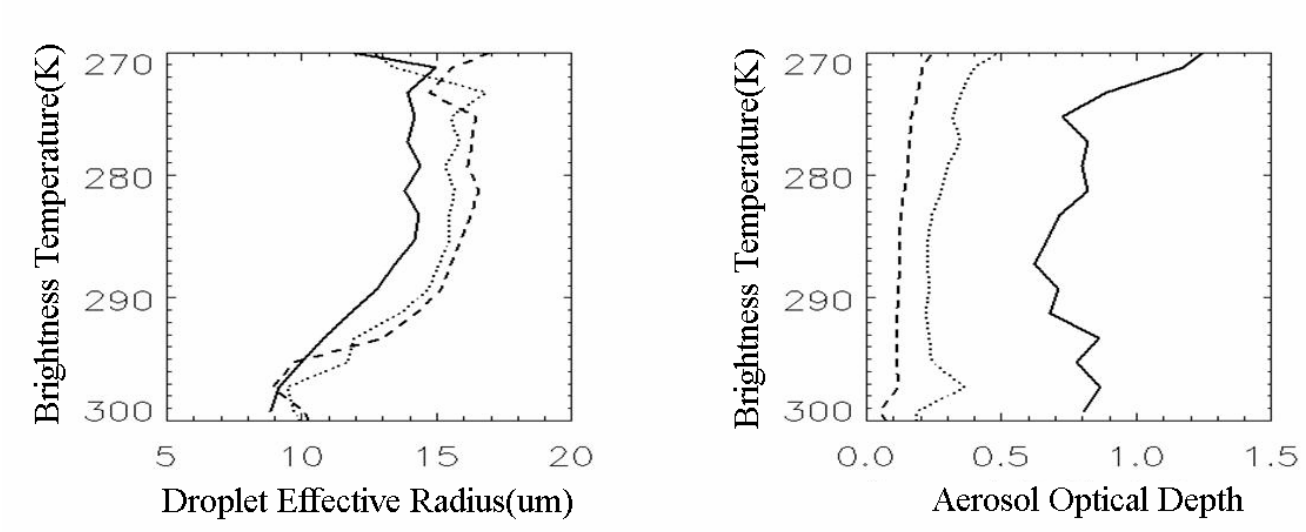

Fig 13 DER profiles with data from scene-by-scene approach over the Amazon region.

Negative AIE efficiency is observed as in VH07 and in past studies, confirming that the same conclusion is reached with either analysis approach.

ii) Aerosol Composition

In the southeast of Texas, oxidation of volatile organic compounds (VOCs) from industrial and transportation sources contributes significantly to formation and growth of aerosols [*Zhang et al.*, 2004; *Fan et al.*, 2006]. Aerosol composition is an important factor to affect the activation processes, especially for aerosols containing low solubility organics [*Laaksonen et al.*, 1998; *Shantz et al.,* 2003; *Fan et al.*, 2007]. The organics are the major aerosol components in Houston area as shown in the observational and modeling studies of *Russell et al.* [2004] and *Fan et al.* [2005]. Those organics are generally considered to be slightly soluble with very low solubility of about 0.001 kg/kg (of water) set in the simulations [*Fan et al.*, 2007], so called slightly soluble organics (SSO). With increasing content of SSO, the low solubility increases the critical supersaturation, resulting in less activated particles as noted by *Broekhuizen et al.* [2004] and *Shantz et al*. [2003]. In order to include the effect of slightly soluble substances, the Köhler theory has to be reformulated to calculate CCN activation, which has been described in detail in *Laaksonen et al.* [1998]. This reformulation of Köhler theory to include the effect of SSO has been incorporated in a 2-D Goddard Cumulus Ensemble model (GCE) with a spectral-bin microphysics [*Tao et al.*, 2003] and the results have been validated by the observed cloud properties in Houston [*Fan et al.*, 2007]. This revised cloud-resolving model is employed

here to investigate the impact of changing SSO on cloud microphysics over southeast of Texas and Galveston Bay near the Gulf of Mexico. Details of the model configurations are described in *Fan et al.* [2007]. Eight simulations were performed, in which total aerosol concentration was assumed to increase from 150 to 2200 cm^{-3} gradually. The content of SSO was also assumed to increase with total aerosol concentration.

Simulations were performed based on a sounding on August 24, 2000 at 7:00 am (local time) from Lake Charles (93.21° W, 30.11°N). The vertical temperature and dew point profiles revealed an unstable atmosphere with convective available potential energy (CAPE) of 1800 J kg^{-1}, integrated from the level of 500 m. The surface temperature was about 26°C and the surface relative humidity was high, up to 87%. The observed surface mass fluxes were imposed to initiate the convection. The horizontal resolution was 0.5 km (test runs with 250m do not change results). The stretched vertical resolution was used with 28 m for the lowest layer. Shallow cumulus clouds were generated at about 210 min. Figure 14 presents the relationship between the cloud DER and the aerosol number concentration (14a) and AOD at 0.55 μm (14b) for eight simulations. The different colors in Fig. 14a denote the different stages of cloud evolution with an interval of 5 min from the beginning of cloud formation. The clouds simulated are warm cumulus of no precipitation.

(a)

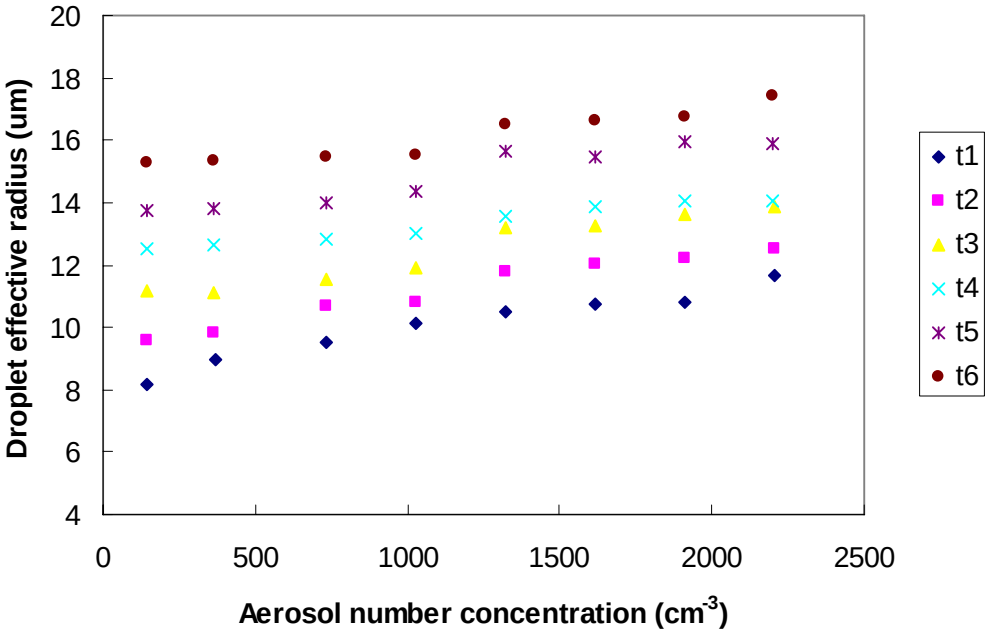

(b)

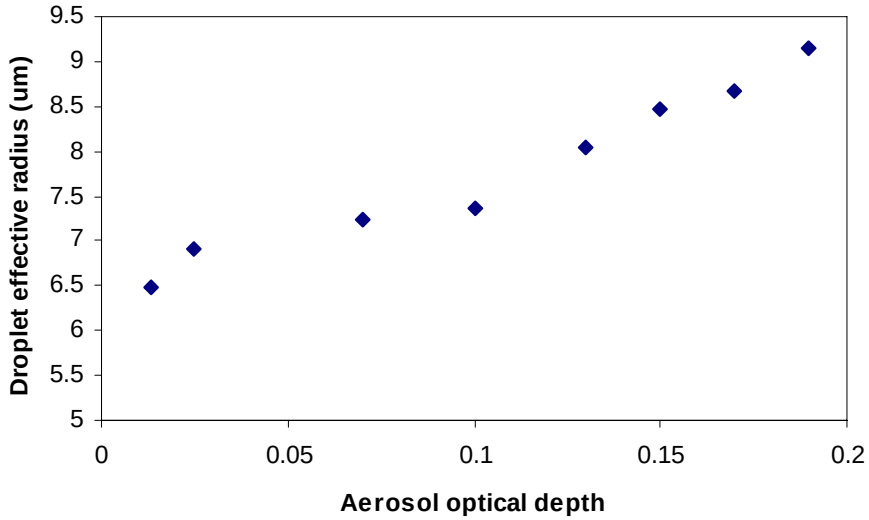

Figure 14 (a) Cloud droplet effective radius vs. aerosol number concentration at varying time intervals increasing from t1 to t6 with a 5 min step, (b) Cloud droplet effective radius vs. aerosol optical depth at t1 (integration time 210 min). All the values indicated in the figure were averaged over the selected domain.

DER increases with both aerosol concentration and AOD. It becomes less pronounced with the evolution of clouds. The increases originate from a decreasing number of activated aerosols with an increasing SSO content. The low solubility of SSO acts to the increase of the critical supersaturation for particles to be activated since the solution term is getting smaller, resulting in less activated particles and thus smaller droplet number concentration (DNC). In our simulation the positive AIE efficiency only exists in a warm and humid environment (with relative humidity of 87% at the surface). Simulations with a reduction of 15% in relative humidity show that the AIE efficiency is not positive anymore, supporting the correlation between AIE efficiency and water vapor amount.

To verify the modeling results, we estimated the DNC from COD and DER following the method of *Han et al.* [1998]. Figure 15 shows that DNC decrease with AOD when the AIE efficiency is positive and vice-versa. The slopes between AOD and DNC correlate well with the AIE efficiency and have a correlation coefficient of -0.8. The positive AIE efficiency and the negative slope between AOD and DNC suggest that the relationship between DNC and DER appears to be at odds with the Twomey's hypothesis. It is worth noting, however, that LWP increases with AOD in our case, while the Twomey's hypothesis assumes a constant LWP. The assumption is not always valid [*Twohy et al.,* 2005] and an increase of LWP with AOD has been reported [*Peng et al.*, 2002].

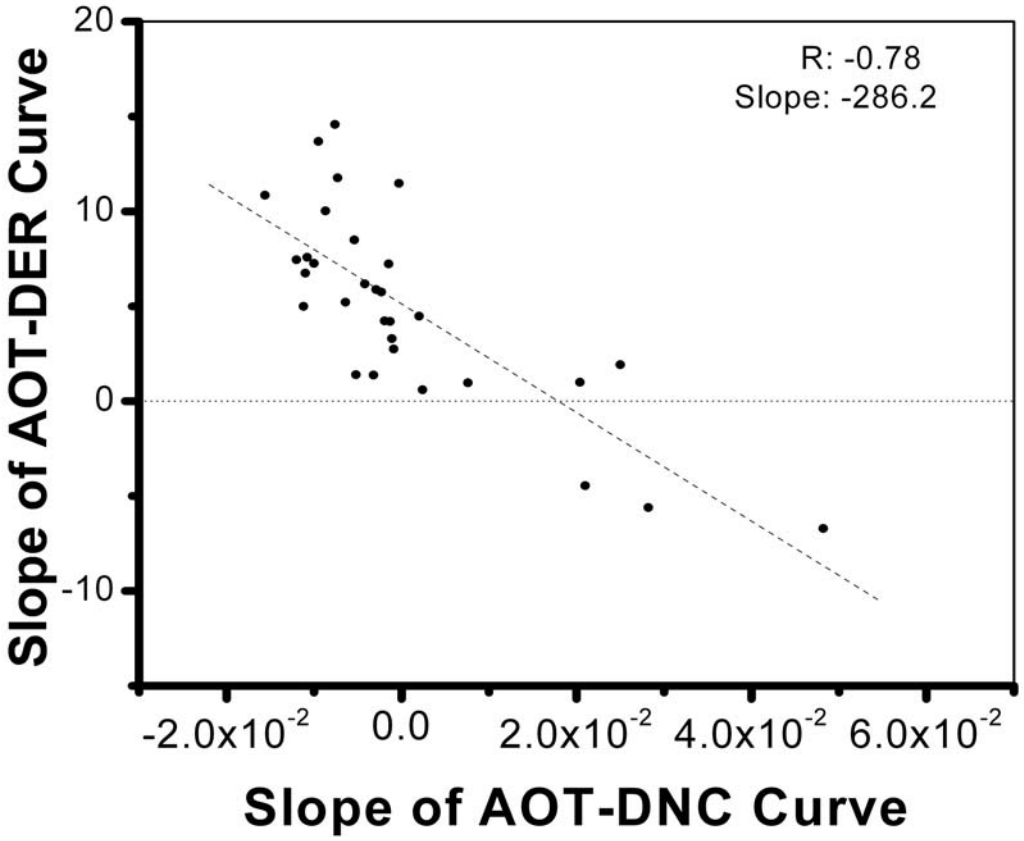

Fig.15 The relation between AIE coefficients and slopes of AOT-DNC for all cases; the correlation coefficient and the slope are provided with legend in the plot.

To constrain the variability caused by changes in LWP, we first apply strict filters to keep only high quality data (discussed in previous sections), limit LWP variation to three narrow ranges and re-plot DER against AOD as shown in Figure 16. The AIE still shows positive relationship. It should be pointed out that LWP is not an independent measurement in our analysis but retrieved from COD and DER. Direct and independent measurements of LWP are needed to verify the estimates of LWP as pointed out by *Brenguier et al.* [2003].

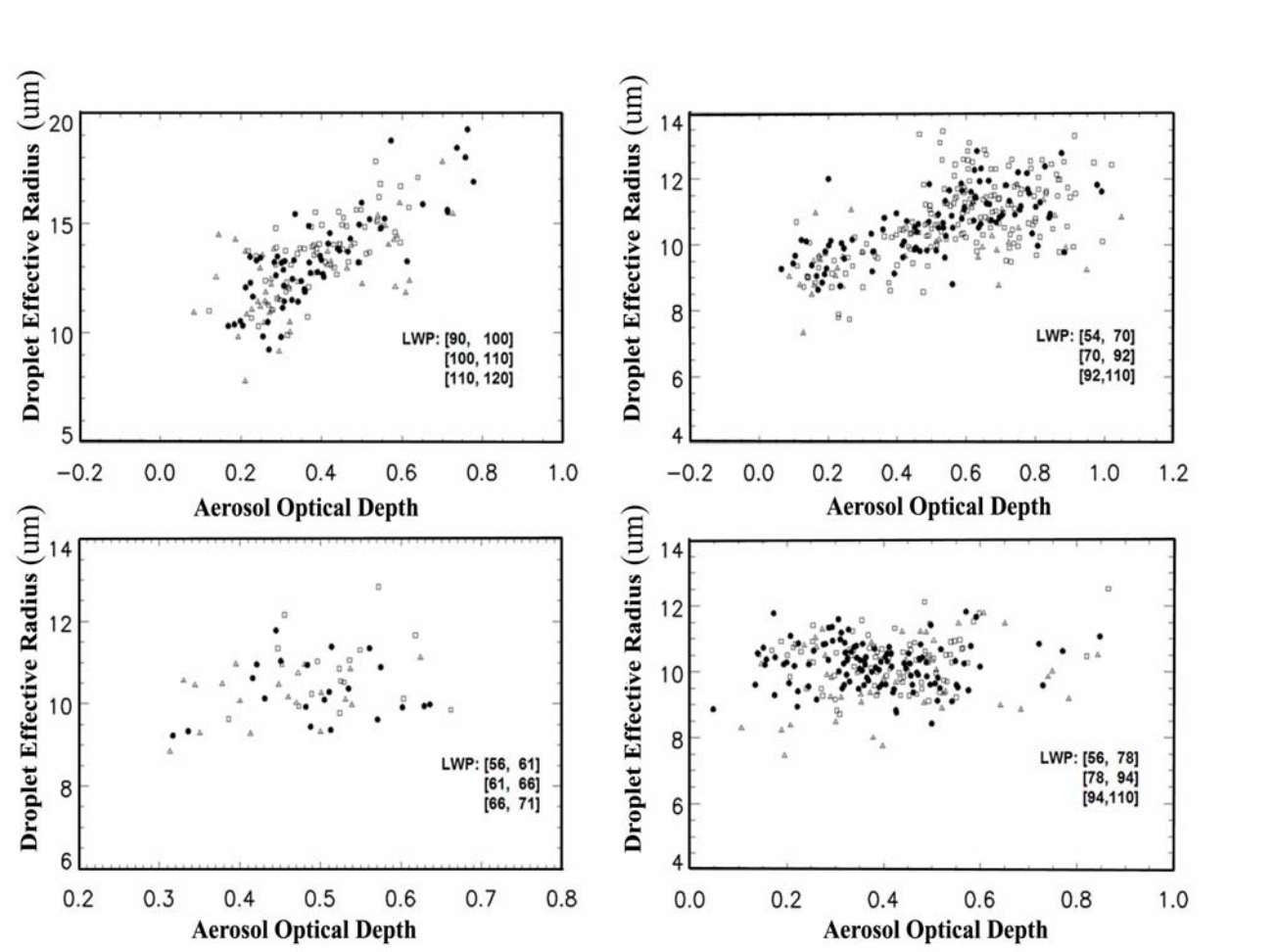

Fig. 16 Data for each case are stratified into 3 intervals (open circle, open triangle and solid dots in increasing LWP order) with narrow LWP range that is indicated in each panel. The stratifying intervals are so chosen based on LWP distributions that each interval contains maximum and similar number of data points. These four cases are not exactly the same four cases presented before, which is due to strict filtering.

iii) Giant CCN

O'Dowd et al. [1999] show that giant CCNs can reduce the number of cloud droplets under polluted conditions by suppressing the supersaturation reached in a cloud based on their in-situ observations and parcel model simulations. The reduced cloud droplet number concentration together with presence of giant CCNs could lead to increased droplet effective radius [*Lu and Seinfeld*, 2006]. Giant CCNs also have great potential to ignite the coalescence process in cloud development, as demonstrated by both model simulation [*Feingold, et al.*, 1999] and observation [*Hindman et al.*, 1977]. To simulate the impact of giant CCN, we employ the same cloud resolving model to perform additional sensitivity studies by increasing the aerosol concentration to about 1910 cm^{-3} from controlled simulation of 1610 cm^{-3} with inclusion of giant aerosol particles at the concentration of 0.02 cm^{-3} to the bins with radii from 0.5 to 2.0 μm.

The giant CCN was assumed to have the same compositions with the rest of aerosols (i.e., ammonium sulfate with SSO) in our model simulations because of the model limits. In reality, sea salt is the most likely giant CCN in this region because sea salt particles can be transported inland as giant CCNs in the summer season along the coast of the Gulf [*Verma et al.*, 2006]. A discernible increase in DER was found due to the addition of giant CCN as in Figure 17.

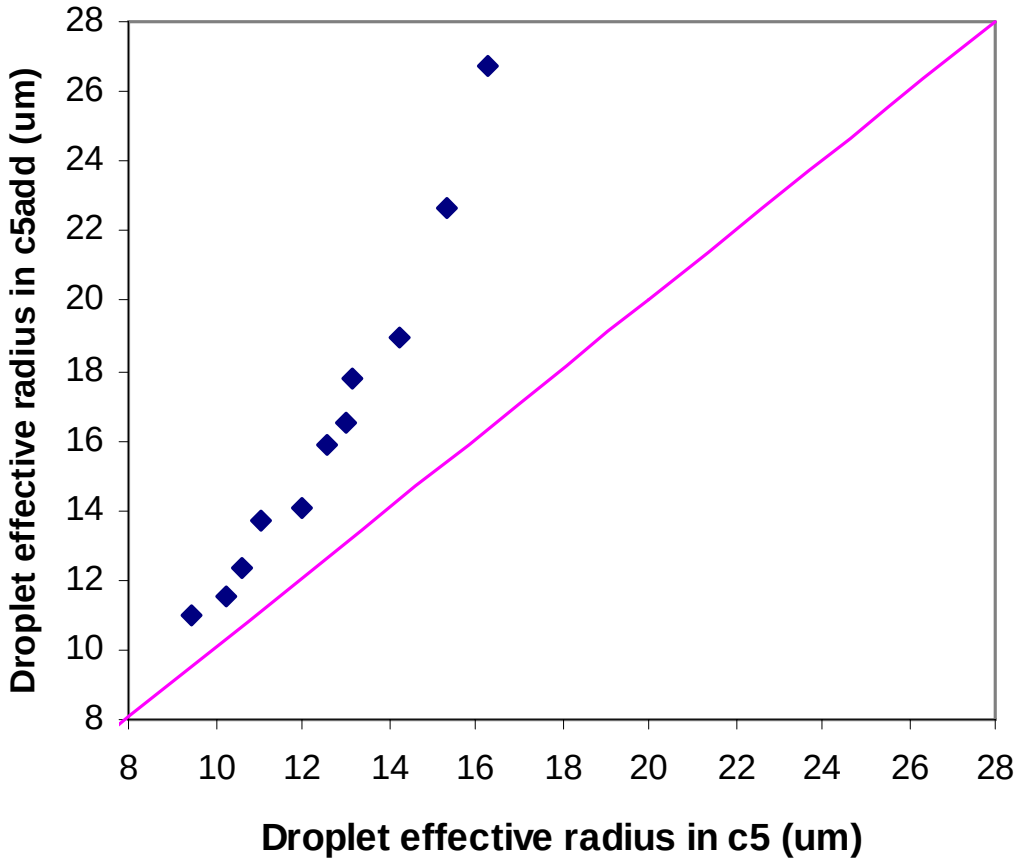

Fig. 17 Comparison of DER for two simulations at different times, 'c5' with only small aerosol particles (x-axis) and c5add with giant CCNs and more aerosol particles (y-axis).

Dusek et al. [2006] studied the cloud-nucleating ability of aerosol particles in terms of relative importance of chemical composition and size distribution using measurements made in Germany. They found that the particle size distribution plays a more important role than chemical composition. Without in-situ and coincident measurements of aerosol and CCN in our study region, it remains an open question if this is also the case for our study. In any event, the issue warrants a further investigation that requires acquisition of many in-situ observations.

2.6 Global Analysis

The inter-comparison results suggest distinct AIE behaviors at two regions that may be attributed to different aerosol types and environmental conditions. We further explore how aerosol types and cloud types may affect behaviors of AIE by expanding our analysis to the regions around the globe to include various aerosol types and mainly two cloud types.

Shallow stratocumulus clouds occur frequently within the marine boundary layer, especially over cool ocean waters west of coasts of African, South American and North American. As boundary layer deepens, stratocumulus clouds transform their organization from relatively homogeneous field of stratus to broken field of cellular form clouds [*Agee et al.*, 1973; Stevens, et al., 2005]. They can take two forms, open form with clouds forming around the edge and clear air in between, or closed form with clouds filling up the cell while clear air between cells. Closed

cellular stratocumulus clouds (CCSC) are better suited for our investigation because semi-collocated aerosol and cloud properties are available and because unlike open cells precipitation is light to none [Bretherton, et al., 2005]. Their cloud formation mechanism is dynamically different from continental fair weather cumulus. They are thus analyzed here as another type of cloud.

CCSC over Atlantic, Southern Pacific, oceanic trade cumulus over the Gulf of Mexico and the Caribbeans, and continental fair weather cumulus over Eastern China and India are analyzed in our global analysis using the aggregated scene-by-scene approach. For every region, analysis is done for a period of three months. The location, time period and number of samples are summed in Table 1.

In Figure 18 BT-DER profiles for CCSC over a region off coast of West Africa as defined in *Kaufman et al.* [2005], where air mass is under heavy influence of dust aerosols, show that AIE efficiency for these clouds is negative. Same results are found (not shown here) for CCSCs over Southern Atlantic that is under influence of biomass burning aerosols from Africa, and Southern Pacific off coast of Peru and Chile where aerosols are mainly natural sea salt and pollutions from industries along Peru coast. Negative AIE efficiency for these regions agrees well with previous studies over similar regions. Student's t-test analysis shows that most difference in mean DERs in each BT bin for different aerosol loadings are significant at the 99% level. Only exceptions are when the number of pixels that goes into averaging is too small, or when the mean DERs are nearly identical to each other like for the case of India (shown later), which may also indicate a 'saturation' effect of AIE as suggested by studies before [Kaufman et al., 1998].

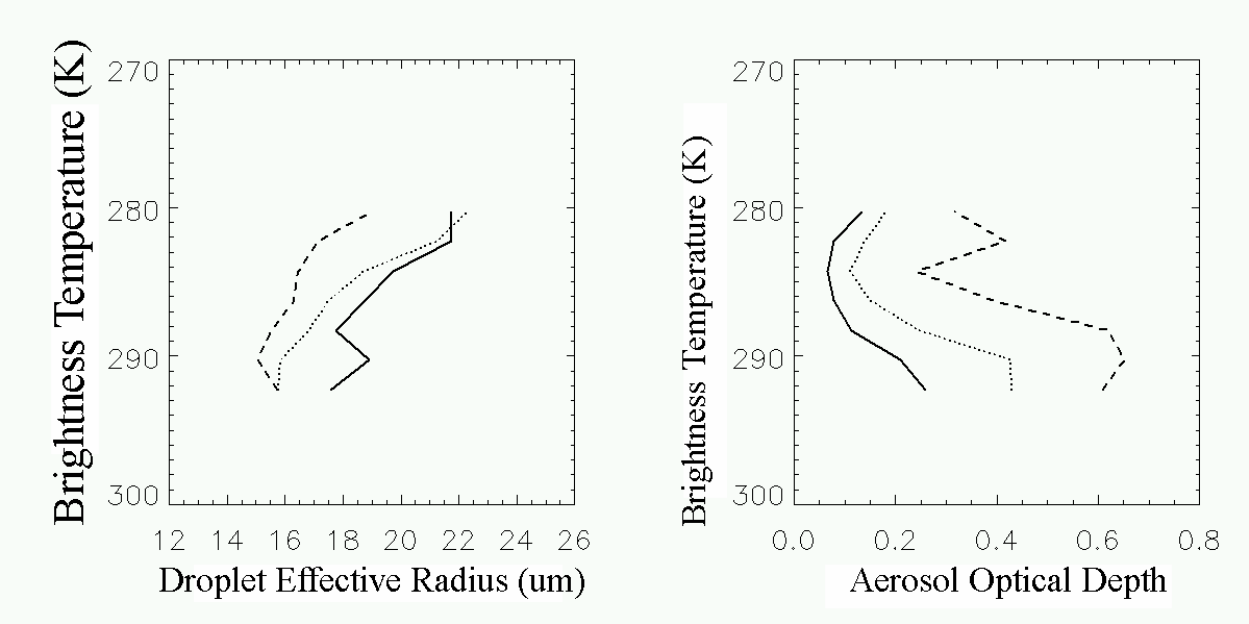

Figure 18 DER-BT profiles for stratocumulus clouds over the Atlantic off coast of west Africa. All clouds included have COD greater than 10 to minimize potential artifacts. Solid, dotted and dashed lines represent clean, normal and polluted conditions, respectively.

In Figure 19 results from the Gulf of Mexico and the Caribbean are presented and they show positive AIE efficiency. We think this might be related to the different cloud types and aerosol types. The cumulus cloud over the Gulf and the Caribbean are formed by surface heating, similar to the continental cumuli. On the other hand, CCSCs over ocean are maintained mainly by the radiative cooling at the top of the clouds which drives cooled air down along walls of the cloud cells, compensated by rising air in the middle of the cells [*Agee et al.,* 1973]. They are often decoupled from the ocean surface by cooling at lower layer from drizzle evaporation and by cooling of ocean sensible and latent heat, which stabilizes the boundary layer and suppress turbulent transport of vapor and energy [*Paluch and Lenschow*, 1991]. The difference will determine the water vapor supply for clouds and therefore liquid water path dynamics of clouds, which in turn may affect AIE. In addition, aerosols over the Gulf and the Caribbean may contain particles with continental sources similar to the Southern US as well as sea salt particles while over Atlantic numerous CCN particles like dust and smoke dominate.

The AIE efficiencies for fair weather cumulus clouds have geographic variations as manifested in the contrast between Amazon region and eastern US. They differ again for clouds over India and Eastern China. In India, the AIE efficiency is very close to neutral meaning that there are no detectable changes of DER among different aerosol loadings. It could be related to the extremely heavy loading of

aerosols during summer in India and aerosol signals saturate. In Eastern China, the AIE efficiency is found to be positive for the region south of 30N and slightly negative for the region north of 35N. The different effects between the north

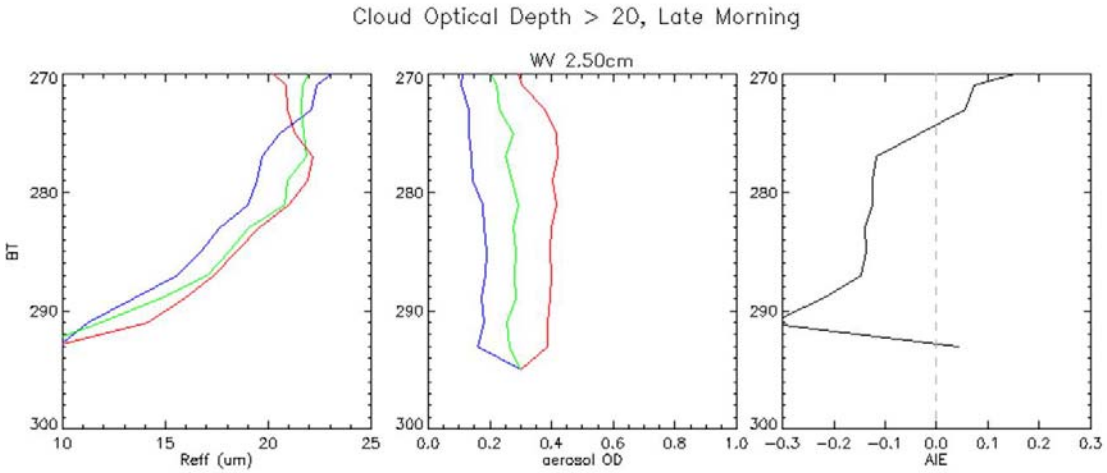

Fig 19 DER-BT profiles for cumulus clouds over the Gulf of Mexico and the Caribbean. AIE efficiency is positive for this region.

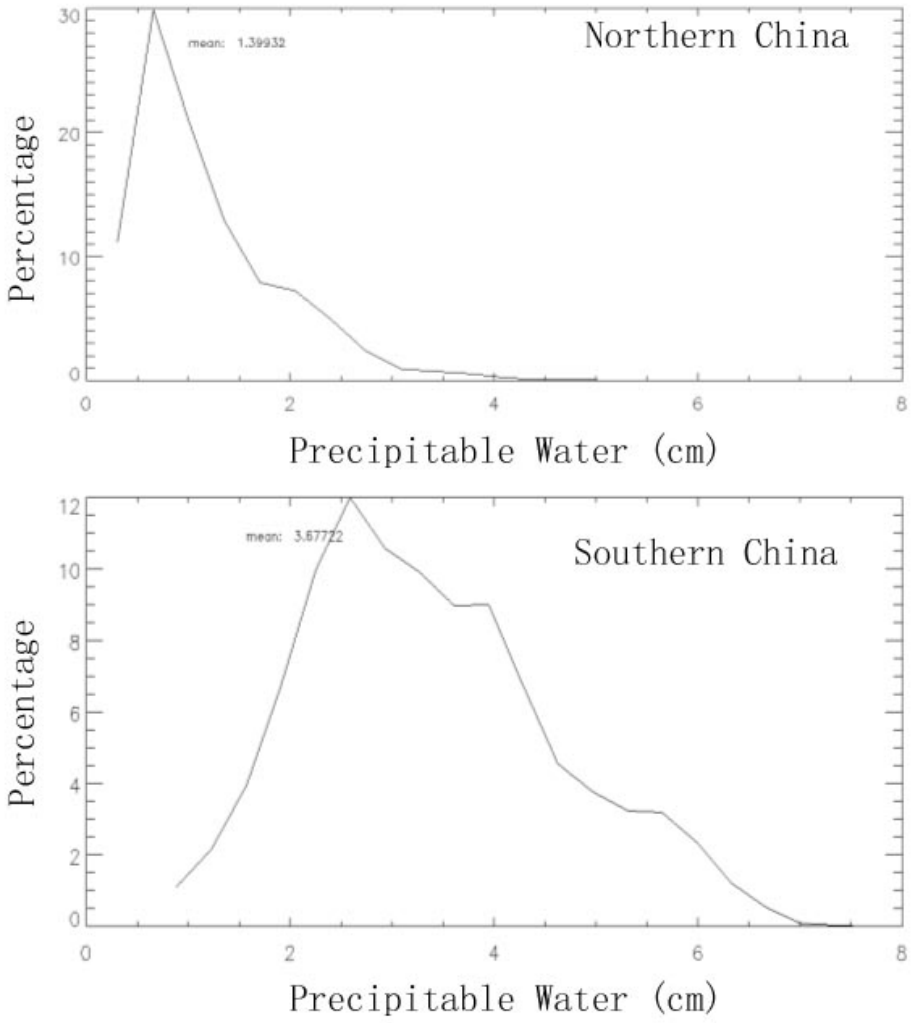

Fig 20 Precipitable water distributions for Northern and Southern China during summer 2002, June- August; PW is mostly less than 2cm in Northern China with mean about 1.4cm; it is however mostly greater than 2cm in Southern China with mean about 3.7cm.

and the south could be related to the distributions of PW for two regions as shown in Figure 20. These results are very similar to those from eastern US. We recognize the interesting similarity between atmospheric circulation patterns in southeastern China and US, both regions with a high pressure system sitting off the coast in the summer, the Pacific Subtropical High and the Bermuda High, respectively. The similarity may imply that the origin of the air mass may have strong influence on the cloud development and thus AIE, which has been noted by *Brenguier et al.* [2003]. There are various pathways through which cloud properties are affected by the origin of an air mass but there seems to be no direct link with the positive AOD-DER relation as found in this study.

We also investigate another cloud type that is trade cumulus clouds, but only for the Indian Ocean region. Experimental results have shown that aerosols reduce cloud droplet size for trade cumulus clouds [Ramanathan et al., 2001]. In Figure 21 our results suggest the same trend for Indian Ocean trade cumulus clouds.

Our global analysis results provide powerful evidence that negates the null hypothesis that our new findings are merely results of artificial correlations because if the phenomenon simply resulted from a 3-D or another artifact, we would see it everywhere for the same kind of clouds.

As noted in the introduction a cloud should be considered as a system. AIE can be any perturbations due to aerosol changes. These perturbations include cloud liquid water path changes as a result of aerosol-cloud interactions. Liquid water path is a quantity that is central to many processes like precipitation and cloud shortwave

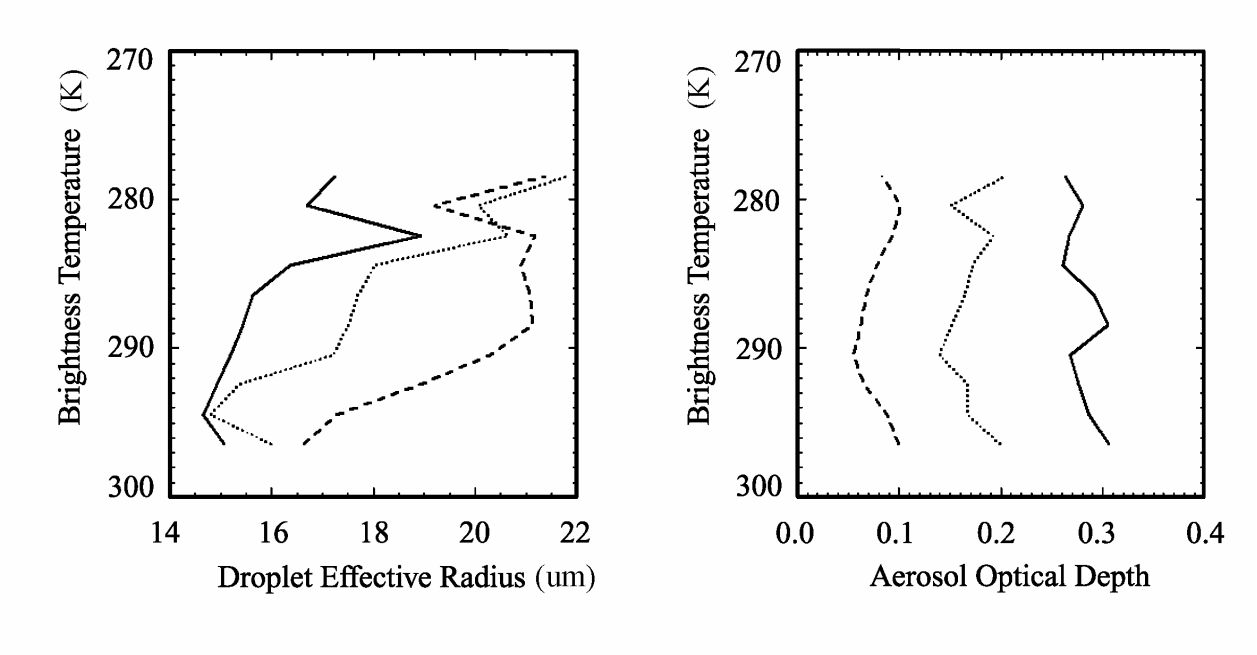

Fig 21 DER-BT profiles for Indian Ocean trade cumulus clouds. Significant negative AIE efficiency is observed for this type of clouds.

albedo. We investigate possible influence of aerosols on cloud LWP by plotting LWP (in log scale) against AOD based on ensemble data, where LWP is averaged over different AOD bins. Two examples are given in Figure 22 representing two cloud types, CCSC and continental fair weather cumulus clouds. The uncertainty is large for each AOD bin as seen by the large standard deviation (vertical bars). Standard deviations are calculated only when sample size for a bin is larger than 200. Despite this large uncertainty two different trends are observed from the data: an increasing trend of LWP with AOD for continental fair weather cumulus and the opposite for CCSC. AOD-LWP relationship for fair weather cumulus shows a saturation effect after AOD gets higher than about 0.65 in Fig 22. AOD-LWP relationships for these two cloud types are presented over all regions in Figure 23. We note the importance of cloud type because the AOD-LWP relationship for ensemble data is similar to individual areas shown in Fig 23 and shows a strong association with cloud types. LWP for fair weather cumulus cloud positively depends upon AOD when AOD is below a threshold and slightly decreases with AOD after passing the threshold, while LWP for CCSC decreases strongly with AOD when AOD is relatively low and becomes relatively flat after aerosol loading is higher than 0.25. We postulate that this different response is related to cloud formation mechanisms of these two cloud types. CCSC is formed in a marine boundary layer environment that is capped by a stable inversion layer. Aerosol induced decrease in DER may lead to stronger evaporation of cloud droplets at the top of boundary layer and thus have a detrimental effect on cloud LWP. On the other hand, aerosols induced microphysical changes may feedback to cloud development and increase LWP.

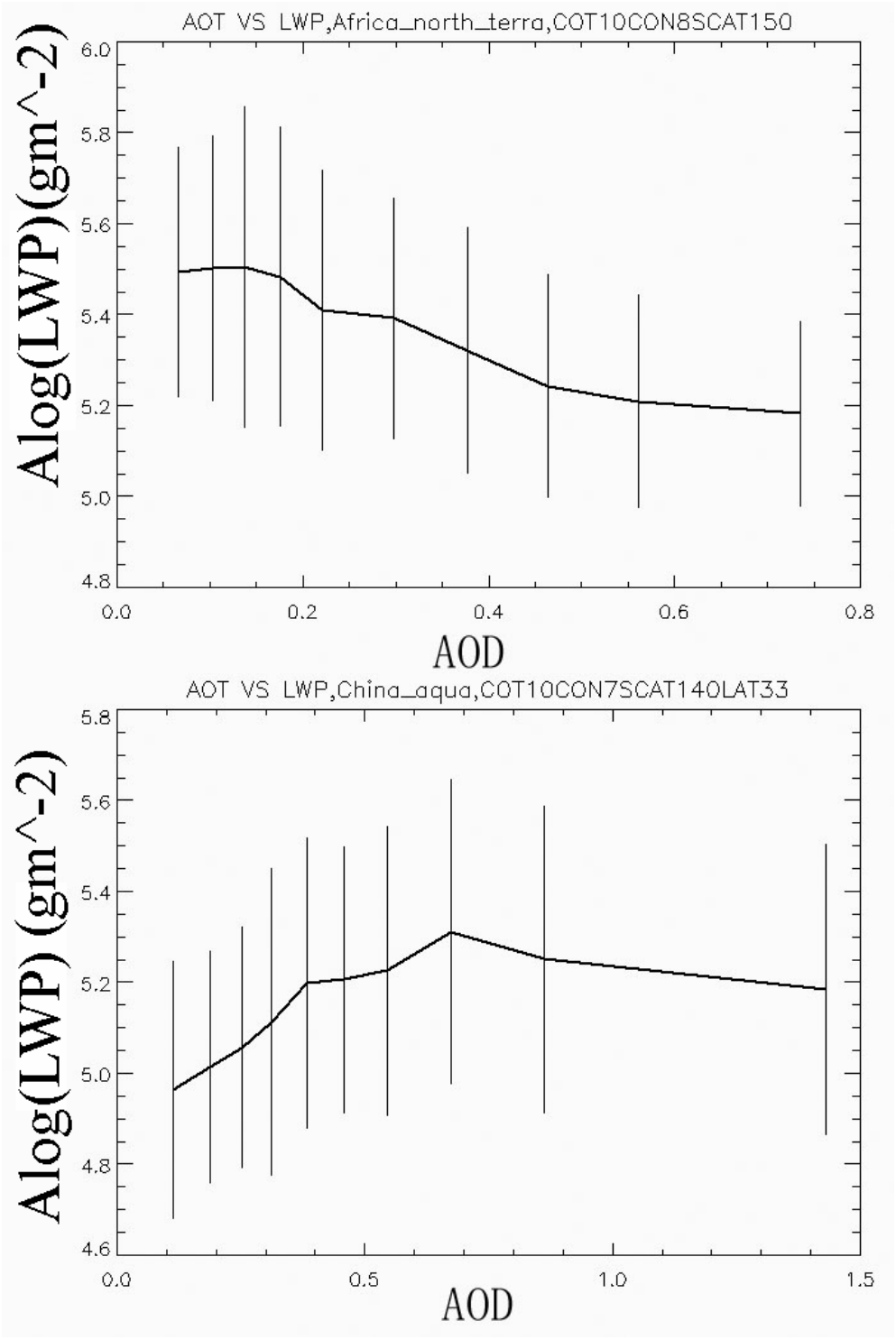

Fig 22 AOT-Log(LWP) plots. Upper panel: CSCC off coast of West Africa; lower: fair weather cumulus over China. Vertical bars represent one standard deviation range

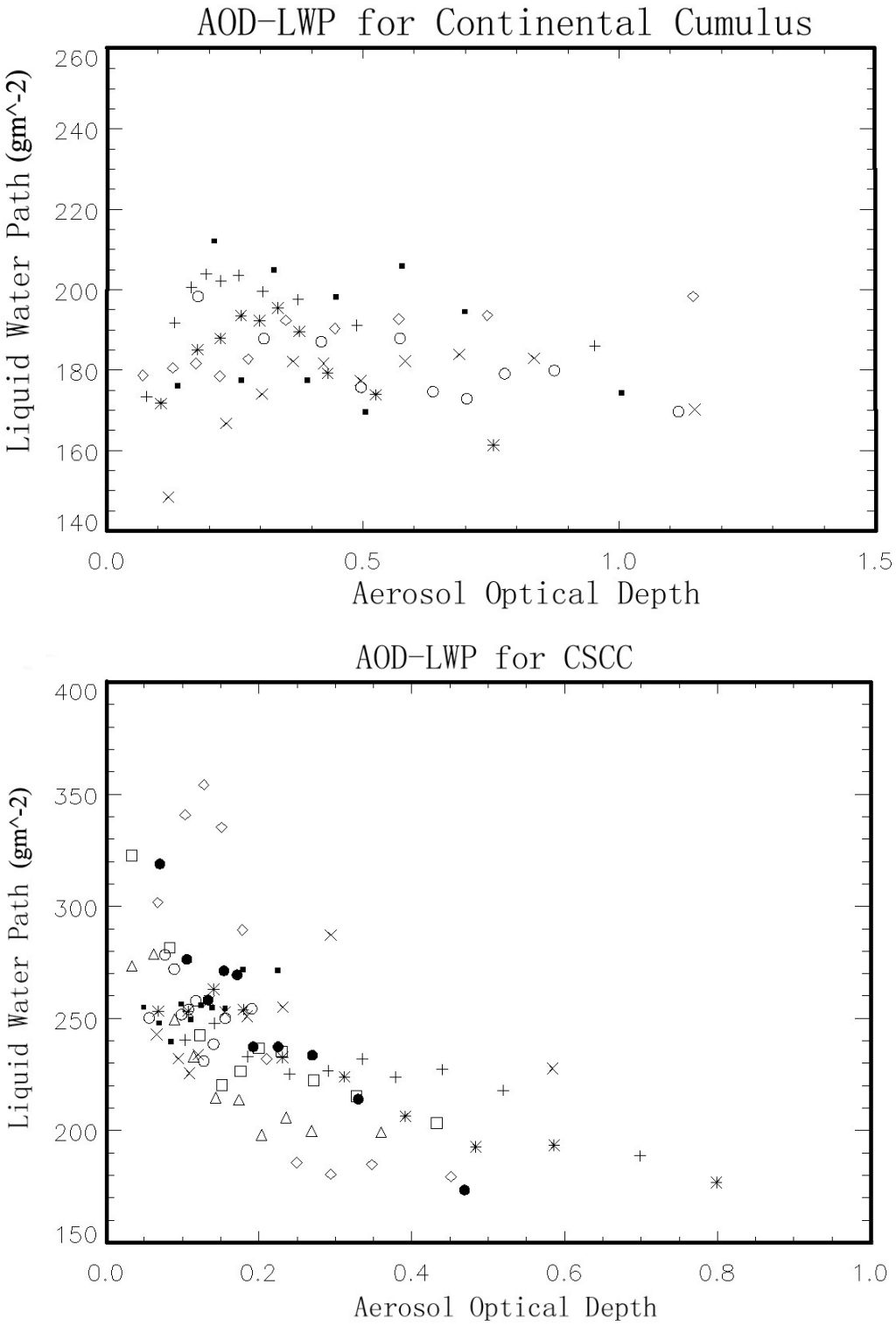

Fig 23 AOD-LWP for continental fair-weather cumulus (upper) and CSCC (lower). Different symbols represent different regions.

2.7 Summary

Aerosol indirect forcing (AIF) has the largest uncertainty among all forcing factors in our understanding of the climate system. Some estimates of the AIF were made based on empirical relationships between aerosol and cloud properties obtained under specific conditions, although cloud particle size is affected by numerous factors pertaining to aerosol, atmospheric environment and the dynamics. To date, the observed relationships between cloud droplet effective radius (DER) and aerosol loading which is often measured in terms of aerosol optical depth (AOD) were overwhelmingly negative with variable sensitivity. Presented in this study are extensive analyses of the aerosol and cloud retrieved products from the Moderate Resolution Imaging Spectroradiometer (MODIS) satellite. They revealed that the DER may increase or decrease with the AOD. While the vast majority of the regions selected around the globe exhibit negative relations between DER and AOD, a few locations show positive dependence including the eastern US that is scrutinized in this study. A major effort is devoted to separate real effects from artifacts.

Various artifact explanations are identified and analyses were conducted to evaluate their influence on the relationship between AOD and DER. First, we employed four techniques to assess the influence of partially cloudy effect, which can increase both DER and AOD retrievals in neighboring pixels because of partially cloudy pixels. It is demonstrated that this effect is unlikely to be the cause for the correlation between AOD and DER because neither the brokenness of clouds, nor the connectivity of clouds, nor cloud fraction has a dominating effect. The cloud 3-D effect could be the most serious problem in interpreting the results obtained across a

large range of scattering direction. However, little difference was found by using data from narrow strips of the MODIS images relative to the entire swath. The third potential artifact is concerned with the aerosol swelling effect, whereby AOD increases with PW. DER may also increase with PW due to water vapor availability. While positive correlations were found for a few cases, they are too weak and variable to explain the tight correlations between AOD and DER. Both AOD and DER can also correlate highly with cloud height because of air convergence and the dependence of DER on cloud height, respectively. We reanalyze the correlation between DER and AOD for narrow intervals of cloud brightness temperature, a proxy of cloud depth, and still get positive relationships. To minimize the influence of surface condition on the AOD retrieval, similar analyses were conducted using MODIS DER and AOD data over oceans and MISR AOD data over land, noting that the MISR retrieval of AOD is least affected by surface reflection. Similar correlations between AOD and DER are found. These analyses attest that the positive correlation found between DER and AOD is likely a true physical phenomenon.

This is reinforced by more compelling evidence revealed from a global survey. Negative relations consistent with previous studies were found for the majority of cases. Our global analysis also attests to the importance and need for taking into account factors like aerosol characteristics, circulation pattern and cloud types when studying the aerosol indirect effect (AIE). An examination of AOD-LWP relationship over the globe reveals that LWP positively depends upon AOD for fair weather cumulus clouds while it negatively depends on AOD for closed cell stratocumulus clouds. Both dependences saturate when AOD is high enough. We

hypothesize that cloud formation mechanisms and environmental conditions for these two cloud types may explain AOD-LWP relationship's dependence on cloud types.

We explored potential mechanisms that can explain observed positive AIE efficiency using a 2-D version of a state-of-the-art cloud resolving model, the Goddard Cumulus Ensemble (GCE) model [*Tao et al.*, 2003] that has detailed spectral-bin microphysics. The inputs to the model were selected based on the unique atmospheric environments of the region. For aerosols, special consideration was made to slightly soluble organics (SSO) that are particularly rich over the Gulf region. To take into account the effect of SSO on the aerosol activation process, the Köhler theory [*Fan et al.*, 2007] was reformulated. Using observed atmospheric sounding data, we are able to simulate cumulus clouds and the effects of several aerosol species. Positive relationships were found between cloud DER and aerosol optical depth or aerosol total concentration. The positive relationship appears to originate from a decreased number of activated cloud droplets with increasing SSO. Similar results were also obtained if giant CCNs are introduced in the model. The dependence of AIE efficiency on water vapor amount is also demonstrated in the model simulation.

Despite of the many painstaking investigations by means of observation and modeling, the utter complexity of the issue and inherent limitations of satellite data prevent us from reaching a definitive conclusion regarding both the effect and its causes. However, the study does present sufficient evidence to warrant further exploration of this important phenomenon using detailed field measurements of aerosol characteristics and cloud properties.

Chapter 3: Global Study of AIE on Deep Convective Clouds

3.1 Introduction

Deep convective clouds (DCC) are characterized by high vertical reach and relatively small areal coverage. Studies [Ramanathan et al., 1989; Harrison et al. 1990; Hartmann et al., 1992] using satellite data have shown that net radiative forcing for DCC systems on large scale is close to zero with large negative shortwave forcing canceling out large positive longwave forcing. *Kiehl* [1994] used a simple calculation to explain the cancellation, which results from a coincidence between tropopause temperature that determines outgoing cloud longwave flux and DCC cloud albedo that controls reflected shortwave flux. Further investigation [Hartmann et al., 2001] proposed that DCCs and associated cloud types must be considered as an ensemble to observe the cancellation. Departures from the cancellation are noted in other studies [e.g. Futyan et al., 2004] when data are not averaged over large area and/or long period of time. The intricate balance is crucial for climate studies and thus warrants further investigation as to why some DCC systems do not produce large net radiative forcing while others do.

Subvisible cirrus clouds are optically thin in the shortwave and thick in the longwave while geographically ubiquitous and temporally persistent, especially in the Tropics [Liou, 1986]. They impose a significant large-scale radiative forcing on the atmosphere [Hartmann, 1992]. These clouds reduce the solar radiation reaching to the surface by reflection. They also strongly absorb infrared (IR) radiation emitted by the Earth surface and lower atmosphere and emit IR radiation at much colder temperature

themselves, hence resulting a positive net longwave radiative forcing on the climate. The net radiative effects of these clouds depend on cloud ice microphysics among other factors like the surface reflectance, cloud height, cloud ice water content (IWC) and cloud lifetime etc [Stephens et al., 1990; Stephens, 2005]. Microphysical properties of cirrus clouds affect cloud lifetime in the atmosphere as clouds with large ice particles tend to precipitate out and dissipate while those with smaller ice particles may sustain themselves through radiative feedbacks to the upper stratosphere and stay in the air longer [Jensen et al., 1996]. These properties are also important in regulating the stratosphere moisture because smaller ice particles are more likely to remain in the air that enters stratosphere and thus provide more moisture for stratosphere [Sherwood, 2002]. DCCs and cirrus clouds are strongly connected as large amount of ice water mass is detrained from DCC systems as anvil clouds that are important sources of cirrus cloud formation [Mace et al., 2006 and references therein]. Ice microphysics for DCCs therefore has strong influence on characteristics and development of cirrus clouds.

Atmospheric aerosols are necessary for cloud formation and play a crucial role in regulating cloud microphysics, cloud lifetime and cloud fraction etc, known as aerosol indirect effects (AIE) [*Twomey*, 1977; *Albrecht*, 1989; *Kaufman and Fraser*, 1997; Ackerman et al., 2000; Kaufman et al., 2005]. Most previous studies concentrate on the shallow (liquid water) clouds to search for signals of albedo changes due to aerosol-cloud interaction. For deep (ice phase) clouds studies examining aerosol influence are mostly modeling efforts and seemingly contradictory results are reported. *Phillips et al.* [2002] demonstrated that by increasing CCN

concentrations ice crystal size is clearly smaller in DCC anvil clouds while simulations by *Fridlind et al.* [2004] show that DCC anvil cloud microphysical properties are only sensitive to mid-troposphere aerosols, not to boundary layer aerosols, according to observations in CRYSTAL-FACE [Fridlind et al., 2004 and references therein]. Observational investigations using in-situ measurements on aerosol-DCC interaction are rare, which may be due to the fact that in-situ measurements are expensive and limited, and at the same time, subject to large natural and artificial uncertainties. In addition to limited data our poor understanding of the baffling complexity of ice initiation and growth processes [Heymsfield et al., 2005 and references therein] inside DCCs contributes to the difficulty of extracting any aerosol related signals.

Remote sensing data could alleviate sampling problem because of their spatial and temporal coverage and thus provide ample samples that can be used to get statistically significant aerosol-DCC interaction signals, if any. For example, *Sherwood* [2002] analyzed patterns of Total Ozone Mapping Spectrometer (TOMS) aerosol index (AI) and angle corrected Advance Very High Resolution Radiometer (AVHRR) 3.7 μm reflectance for cold cumulonimbus cloud tops and hypothesized a connection between biomass burning aerosol and DCC top ice particle size; *Chylek et al.* [2006] averaged large amount of MODIS (Moderate Resolution Imaging Spectroradiometer) data over Indian subcontinent and surrounding areas for winter and summer and found a surprising systematic increase of ice particle size with increase pollution level, which they proposed to be due to a combination of meteorological regime change and heterogeneous ice nucleation due to aerosols;

Massie et al. [2007] tested the hypothesis that an AIE exists throughout the troposphere with MODIS cloud and aerosol products and found no apparent AIE signal associated with ice clouds, which seem to better agree with the conclusion of *Fridlind et al.* [2004]. These studies all seem to recognize the large uncertainty and employ large amounts of data to control the noise. Simple gross average may not solve the problem [Vant-Hull et al., 2007]. A more physically based approach is needed to get better handle on the data.

A few observational case studies on aerosol-precipitation interaction also show contradictory results where aerosols can either increase [Hindman et al., 1977] of decrease precipitation [Rosenfeld, 2000; Rosenfeld, 1999]. Modeling studies on this subject do not have a consensus either [Khain and Pokrovsky, 2004; Fan et al., 2007; Levin et al., 2005]. Part of the difference in modeling results could be attributed to the way how microphysics processes are treated in the models. Aerosol types, however, seem to be responsible for the difference in both observational and modeling results, with large aerosols like dust particles acting as giant cloud condensation nuclei (CCN) and increasing/accelerating precipitation and fine aerosols like pollution and smokes suppressing precipitation. To reconcile these contradictory results of aerosol-DCC-precipitation interactions, the first step would be to find the reason why they are different in order to further understand how.

High cloud microphysics parameterization in a climate model was pioneered by *Heymsfield and Platt* [1984] based on in-situ measurements of *Heymsfield* [1975] and lidar measurements of *Platt and Dilley* [1981] where ice particle size is dependant upon temperature and ice water content (IWC). The parameterization is

crucial for studying cloud feedbacks in the scenario of a global climate change [Platt, 1989] and different parameterizations may introduce large variation in model simulations as demonstrated by previous studies [Kristjansson, et al., 2000; van Zadelhoff et al., 2007]. Several parameterizations has been proposed [Ou and Liou, 1995; McFarquhar and Heymsfield, 1997; Donovan, 2003], most of which are based on in-situ and/or active instrument like lidar and radar measurements and ice effective radius (CER) are assumed to be determined by cloud temperature and/or ice water content. All of these parameterizations are heuristic and fixed globally regardless of the environment while they are based on a few cases. More physical insights are needed to better parameterize ice cloud properties. With the global coverage of remote sensing data it is possible to identify the spatiotemporal variations of ice properties and their dependence on temperature, which can serve as indicators for future field measurements to verify, and a first step towards better parameterization in models.

To gain more insight on the cancellation of DCC longwave and shortwave forcing we study several aspects of DCC top optical and microphysical properties using MODIS cloud products. With MODIS aerosol and cloud products and auxiliary information from other A-Train satellite instruments we then examine the aerosol influence on cloud properties. We will also investigate the possibility of using MODIS cloud product to formulate parameterization of ice particle size that varies geographically and give an explanation for it with a simple thermodynamic model. Data sets employed in this study is summarized in section 3.2. Methodology and regions of interest are discussed in section 3.3. Section 3.4 presents the major findings

of our work. Discussions and implications of our results are given in section 3.5. Section 3.6 summarizes this study.

3.2 Data and Quantities of Interest

The A-Train constellation is a succession of US and international satellites seconds to minutes apart having 1:30 pm equate crossing time, which includes EOS Aqua, CloudSat and Cloud-Aerosol Lidar and Infrared Pathfinder Satellite Observation (CALIPSO) satellites among others. Data and information from these three satellites provide unprecedented opportunities to study aerosol-cloud interaction because direct and nearly simultaneous observations of aerosol and cloud. At the time of this study, MODIS aerosol product (MOD04 and MYD04, note that the prefixes 'MOD' and 'MYD' are used for products based on MODIS measurements onboard of Terra and Aqua platforms, respectively), cloud product (MOD06 and MYD06) and L1-B radiance product are available from 2000 and 2002 for Terra and Aqua, respectively.

The bulk of the data used in this study come from MODIS level-2 granule data of aerosol and cloud from both Terra and Aqua. In addition, the Level-1 sub-sampled reflectance product (at 5 km resolution) helps us choose individual cases as explained in the methodology section. Channel 31 (11 μm) Level-1B 1km resolution radiance data are used to calculate brightness temperature (BT) as a proxy for cloud vertical development. Additional information from other A-Train satellite sensors are also used as explained below.

3.2.1 Cloud Properties

Utilizing the fact that near-infrared reflectance is sensitive to cloud particle size and visible reflectance to cloud water amount cloud particle size and cloud optical depth (COD) are simultaneously retrieved based on reflected radiation at these two wavelength bands for liquid-phased clouds [King et al., 1992; Platnick et al., 2003]. Ice crystal habits complicate the retrieval process applied to ice clouds mainly because of the sensitivity of reflectance to crystal shapes. Better characterization of bulk ice properties is thus critical for improving the quality of retrieved quantities. The latest Collection 5 MODIS product is substantially improved by incorporating more comprehensive crystal habits based on newly available in-situ measurements and radiative transfer model calculation [Baum, et al., 2005] among other changes as summarized by *Yang* et al. [2007]. Furthermore the sensitivity of retrieved ice effective radius (CER) to ice crystal habit is alleviated in this study since DCC optical depths are sufficiently large that crystal shape variance should not be as important [Baum et al., 2000]. It is also worth noting that CER values used in this study should not be interpreted in absolute sense, but rather as a relative indicator of particle size differences.

For DCCs cloud top pressure (CTP) is retrieved using the so-called CO_2-slicing method. The method utilizes the partial absorption in MODIS infrared bands within the 15-μm CO_2 absorption region [Platnick et al.,

2003]. Each MODIS band is sensitive to a different atmospheric layer. All three cloud parameters, COD, CER and CTP, are quality controlled in MODIS cloud product and in this study only the highest quality data pixels as indicated by quality control flags are used. Brightness temperature estimated using 11-μm L1-B radiance is served as the proxy for cloud vertical reach and a crude estimation of the convective strength [*Rosenfeld and Lensky,* 1998].

3.2.2 Aerosols

It is necessary to examine the spatiotemporal variations of cloud condensation nuclei (CCN) and ice nuclei to assess the impact of these variations on the DCC properties. Though no direct measurements of CCN from space are available, the column integrated aerosol optical depth (AOD) can be retrieved globally with the MODIS bands. The effectiveness of aerosol as CCN depends on their chemical and physical properties, or generally their types. Common aerosol types include sulfate aerosols from natural or anthropogenic sources, mineral dust, and carbonaceous aerosols. Some geographic regions have their signature aerosol types at specific time [Jeong et al., 2005 and references therein]. During a fixed period of time for a specific region we could assume that CCN concentration to AOD ratio is fixed. Under this assumption relative variation of AOD can be used as a proxy of variation of CCN. MODIS AOD is retrieved at three wavelengths: 0.47, 0.56 and 0.65 μm at a spatial resolution of about 10 km [*Remer et al.*, 2005] for MODIS aerosol product. The resolution is degraded from the original 1 km or less following several cloud screening tests [*Remer et al.*, 2005]. The

collection 5 MODIS aerosol product is significantly improved especially over land by incorporating better surface reflectance characteristics and aerosol models among others [Levy et al., 2007]. We use MODIS AOD at 0.56 μm in our study as a proxy of CCN, which is probably the best currently available and has been shown to be quite reasonable for some regions [Hegg and Kaufman, 1998] though no extensive survey is done over the globe.

We are particularly interested in dust's effects on DCC microphysics given its unique ability to act as both CCN and IN [Desalmand 1987; DeMott et al., 2003; Levin et al., 2005]. A significant portion of dust particles resides in the coarse mode of aerosol size distribution, especially those over source region. The larger size makes dust possible source of giant CCNs that are shown to have special effects on microphysics and precipitation process of deep clouds [Levin et al., 2005]. The existence of dust and its characteristics are detected and estimated from the Cloud-Aerosol Lidar with Orthogonal Polarization (CALIOP) onboard CALIPSO, the Ozone Monitoring Instrument (OMI) onboard Aura, and data from the aerosol robotic network (AERONET). CALIOP is an active Lidar instrument that measures backscatter at two wavelengths, 532nm and 1064nm and orthogonal polarization at 532nm. We use imagery of backscatter intensity at these two wavelengths to separate aerosol and cloud layers and estimate the size of aerosols by the contrast between two wavelengths. CALIOP depolarization images together with aerosol source information are used to identify non-spherical dust particles. The Sun photometers of AERONET provide comprehensive ground-based

remote sensing data of aerosol properties at more than hundreds of sites globally [Holben et al., 1998]. The latest AERONET algorithm utilizes both sky and direct beam radiance measurements to retrieve aerosol optical depth at six wavelengths (0.34, 0.38, 0.44, 0.67, 0.87 and 1.02 μm) and infer the volume distribution (dV/dlnR) for 22 size bins [Dubovic et al., 2006]. Size distribution and AOD at longer wavelength i.e. 1.02μm contain information on the fraction of coarse mode aerosol, which serve as another indicator for the existence of large dust particles at specific location and time. OMI instrument measures backscattered radiation in both the visible and ultra-violet (UV) and provides a suite of atmospheric parameters that includes aerosol index (AI) for UV absorbing aerosols like smoke and dust [Herman et al., 1997]. AI is an indicator of existence of dust on a much larger spatial scale.

3.2.3 Environmental Conditions

The European Centre for Medium-Range Weather Forecasts (ECMWF) ERA-40 reanalysis provides state-of-the-art meteorological fields that are used to characterizing the general condition of atmosphere. Column integrated water vapor amount, or precipitable water (PW), vertical relative humidity and temperature profiles can be retrieved using hyperspectral measurements from the Advanced Infrared Sounder (AIRS) onboard of Aqua. These variables are used to give us a near simultaneous view of the atmospheric state along with aerosol and cloud measurements mentioned above.

3.3 Methodology and Regions of Interest

3.3.1 Data Screening

We noted that ice cloud properties have significant natural variations, in addition to which uncertainties in the remote sensing retrieval process may lead to artificial variations. It is necessary to minimize artificial variations in order to achieve better signal to noise level. MODIS cloud product has internal flags used for indicating the quality of retrievals that are based on a series of testing as discussed in detail by *Platnick et al.* [2003]. We employ four flags to ensure that each pixel used is 99% cloudy; retrieval is marked as useful and with highest quality; cloud phase is ice. Cloud phase is extremely important as water and ice cloud particles have completely different optical properties [Platnick et al., 2003]. Treating water clouds as ice clouds, or vice versa, will inevitably lead to huge errors in the retrievals, which needs to be avoided for our purpose.

Since we are interested in cloud properties and aerosol-cloud interactions in the summer, when deep clouds are frequently formed and dissipated, cloud contamination on aerosol retrieval processes is likely to happen, which can potentially lead to artificial correlations that have no physical base [Yuan et al., 2008]. We use quality flags and internal cloud fraction data to alleviate the potential problem. All aerosol data used in our

study are marked as having the highest quality as indicated by the quality assurance flags in the aerosol product. Ideally we want to include only retrievals with zero cloud fractions to eliminate potential contamination, while this severely limits sample size. To balance these two factors we limit aerosol retrievals to have internal cloud fraction no greater than 20% over land and 50% over ocean.

3.3.2 DCC Definition

There is no precise definition of a deep convective cloud from the passive remote sensing point of view. In practice brightness temperature (BT) from satellite IR window channels has been used to define DCC by setting a threshold of low BT, T_c [Houze, 1989; Sherwood, 2002; Liu et al., 2007]. For different purposes T_c can range from as low as 210K to select only the most vigorous convective clouds [Zipser et al., 2006] to as high as 245K to study the general population of DCC systems [Kubar et al., 2007]. Cloud optical depth is retrieved mainly based on reflected visible solar radiation and is another possible proxy for cloud vertical development. For this purpose it, however, suffers from its poor dynamical range, especially when clouds are optically thick like DCCs, since MODIS COD saturates at 100. Using BT alone cannot differentiate two apparently cold cloud pixels, one of which is part of a real DCC while the other may result from a combination of clear sky and cirrus clouds [Chang and Li, 2005]. We thus combine BT and COD to

give us more confidence in selecting out only cold clouds that are associated with DCCs. We define cloud pixels with BT no greater than 243K and COD no less than 40, which further screens out relatively thick cirrus clouds not associated with an active DCC system, as DCC (including its anvils) pixels.

3.3.3 Methodology

As noted in the Introduction the strength of satellite data is its extensive spatiotemporal coverage. Statistics of aerosol and cloud properties like AOD and CER etc are derived from the screened data set for each region to study the gross characteristics of aerosols and clouds and their geographical variations. Geographical maps of aerosol optical depth and cloud properties are used to investigate their connection with environmental conditions, which will be further utilized to filter out natural variations associated with environmental conditions to constrain the data when investigating aerosol's effect. To detect signals of aerosol related cloud property variations either special condition, for which clouds can be otherwise assumed to be uniform (e.g. ship tracks), or a sufficiently large data set is required. In our study we follow the latter approach taking advantage of the strength of satellite data. Recognizing the danger of simple averaging of data that may lead to false conclusions [Vant-Hull et al., 2007], in our approach we first establish a physically sound relationship between CER and BT that is universally observable. We then attribute perturbations to this relationship to aerosols

with appropriate constraining of other environmental conditions. The understanding of natural variations and the consideration of a physical relationship are key steps for us to better extract the signal associated with aerosols in addition to advantage of ample sampling.

We also develop a method to do case studies of an individual DCC system, which is used to test the robustness of the physical relationship and gain further insight on the microphysical structure of these DCC systems. Individual DCCs are manually selected based on 5-km resolution MODIS reflectance data to include only those that span sufficiently large area for carrying out meaningful statistical analysis and are completely covered by MODIS swath to avoid incomplete sampling of a system. Once a DCC system is selected cloud state variables like BT and microphysical properties like CER are collected using the same filtering process discussed above. Characteristics of individual DCC system will be compared to ensemble data.

3.3.4 Regions of Interest

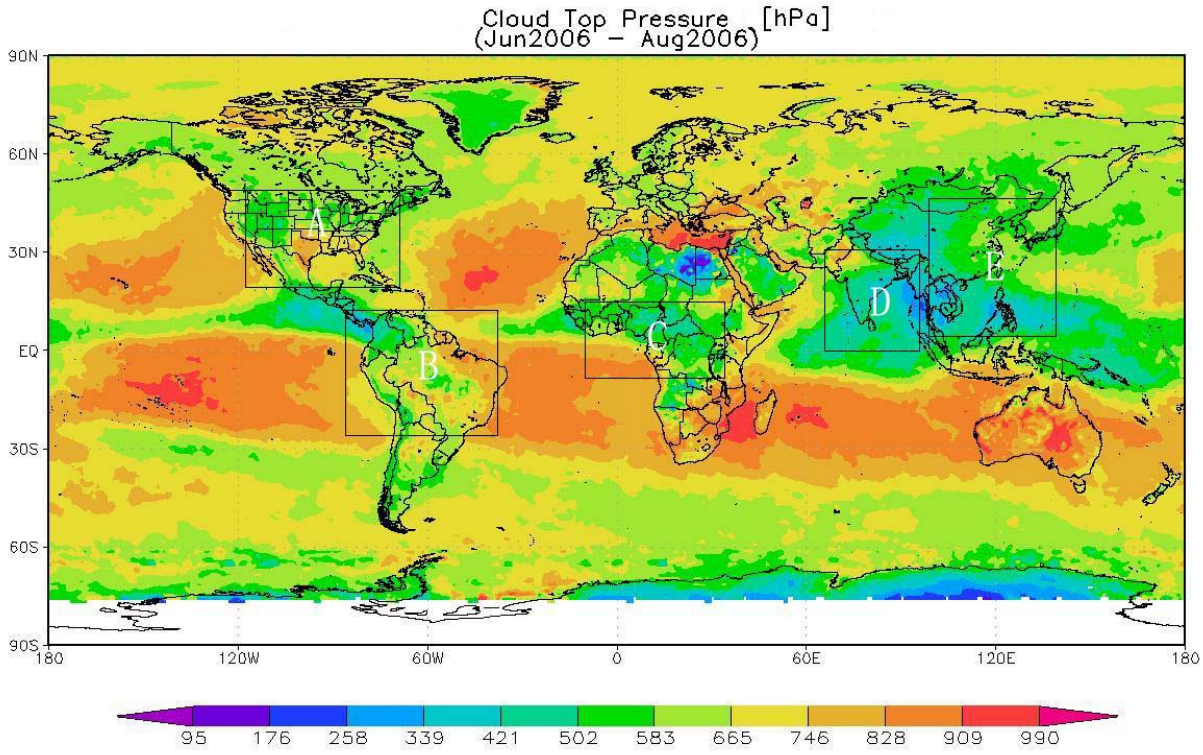

Figure 24 Five study regions are (A) North America (B) South America (C) Central Africa (D) Indian Monsoon and (E) East Asian Monsoon as roughly outlined with five boxes. The map is a global distribution of cloud top pressure averaged between June and Aug, 2006 using MODIS data.

The tropics and continental areas in extratropical zones at summer time are active regions for deep convective cloud formation with the tropics being the dominant source [Gettelman et al., 2002; Liu et al., 2007]. The regions (Fig 24) of interest in our study include southwest Indian monsoon region (Indian subcontinent, Bay of Bengal, Arabian Sea and tropical Indian Ocean), China and East Asian Monsoon region, continental North America, South America and central Africa. These regions are shown to be active in forming DCCs and they span a wide range of different environmental conditions. In particular, for aerosol loadings India and East Asian regions are among the most heavily polluted regions in the world while North America regions are relatively cleaner. Similar aerosol loading contrast exists for South America regions between wet season and dry season and between 'green ocean' area and smoke-laden area [Andreae et al., 2004]. Those regions that have high contrast in aerosol loadings and active in forming DCCs, which is ideal for aerosol-DCC interaction study, are strategically chosen to enhance our signal to noise ratio. The Indo-Gangetic Basin region is investigated in our study to assess the dust particle's influence since during pre-monsoon and monsoon periods this region is under influence of dust aerosols that originate mainly from Tsar Desert, a local desert located at the Northwestern Indian-Pakistan boarder, and Arabian Peninsula. Special attention is paid to the region surrounding the Tsar Desert where meteorological conditions like precipitable water, relative humidity, temperature are similar to the rest of Northern India during monsoon season while heavy load of dust particles may

distinguish itself from other regions in aerosol type, which provides the best condition to assess the influence of dust particles.

3.4 Results

3.4.1 General Properties of DCCs

a) Geographical Patterns

The geographical distribution of DCC frequency during summer 2002 is displayed in Fig 25a for Asian region. The map is made up of 2.5 X 2.5 degree grid cells and the frequency is calculated as the sum of number of DCC pixels during the summer over each grid cell. Three major areas of active DCC formation are readily identified from the map, the southeast Indian Monsoon region (IM), the East Asian Monsoon region (EAM) and the Pacific Warm Pool region (PMP), which are all associated with the large scale summertime monsoon circulation and environmental conditions such as high sea surface temperature [Liu et al., 2007]. In addition the summer time heating of the Tibet Plateau (TP) makes it also an active DCC region as indicated by the local maxima in the frequency map [Chen and Liu, 2005]. DCC frequency maps of other study regions like summertime North America continental region and South America rainforest region show the same close relationship to large circulation pattern and high elevation areas are usually active in producing DCCs in the summer time due to solar heating of the landmass.

Cloud top pressure (CTP) distribution map for the same period is shown in Fig 25b. The CTP is averaged the same way as frequency data. There is a good negative correlation between the pattern of CTP and the pattern of frequency, indicating active DCC regions also form the deepest clouds. There exists a general south-north gradient in CTP distribution, in part due to the troposphere top height distribution that is higher in the

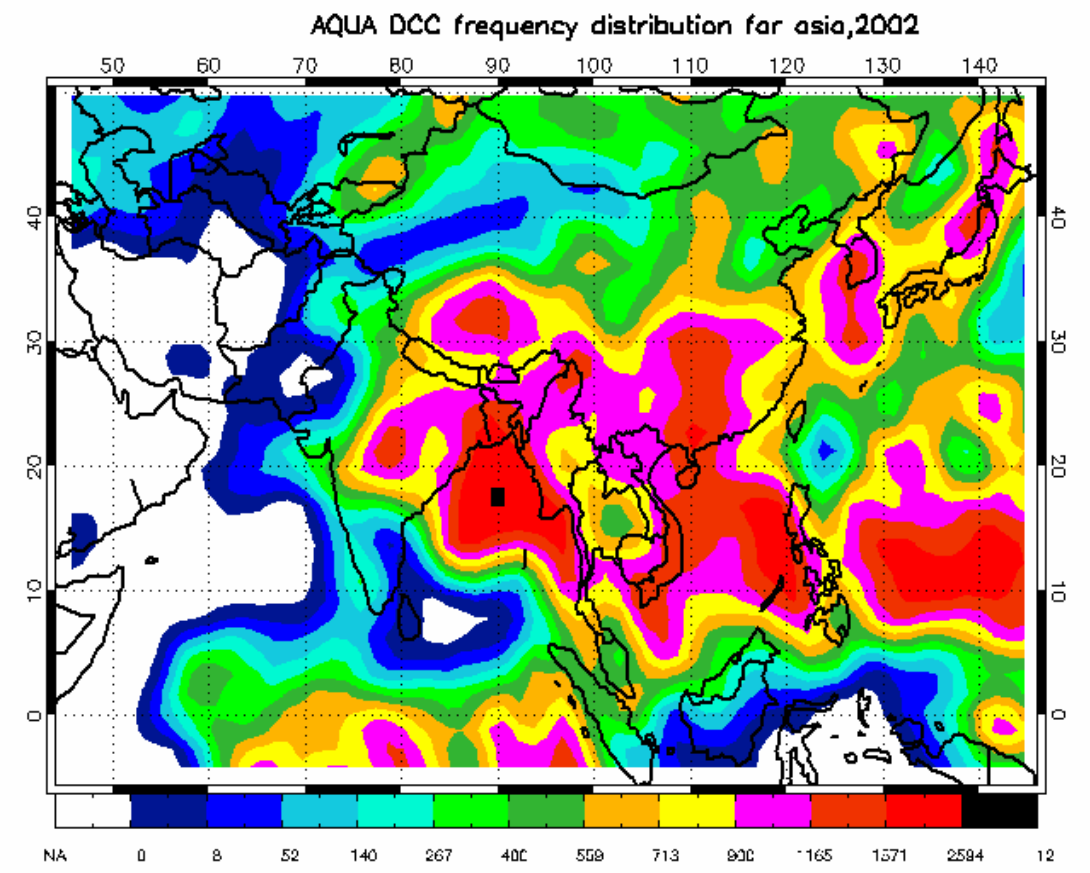

Figure 25a DCC occurring frequency over Asia for year 2002. The resolution of the map is 2.5 by 2.5 degrees.

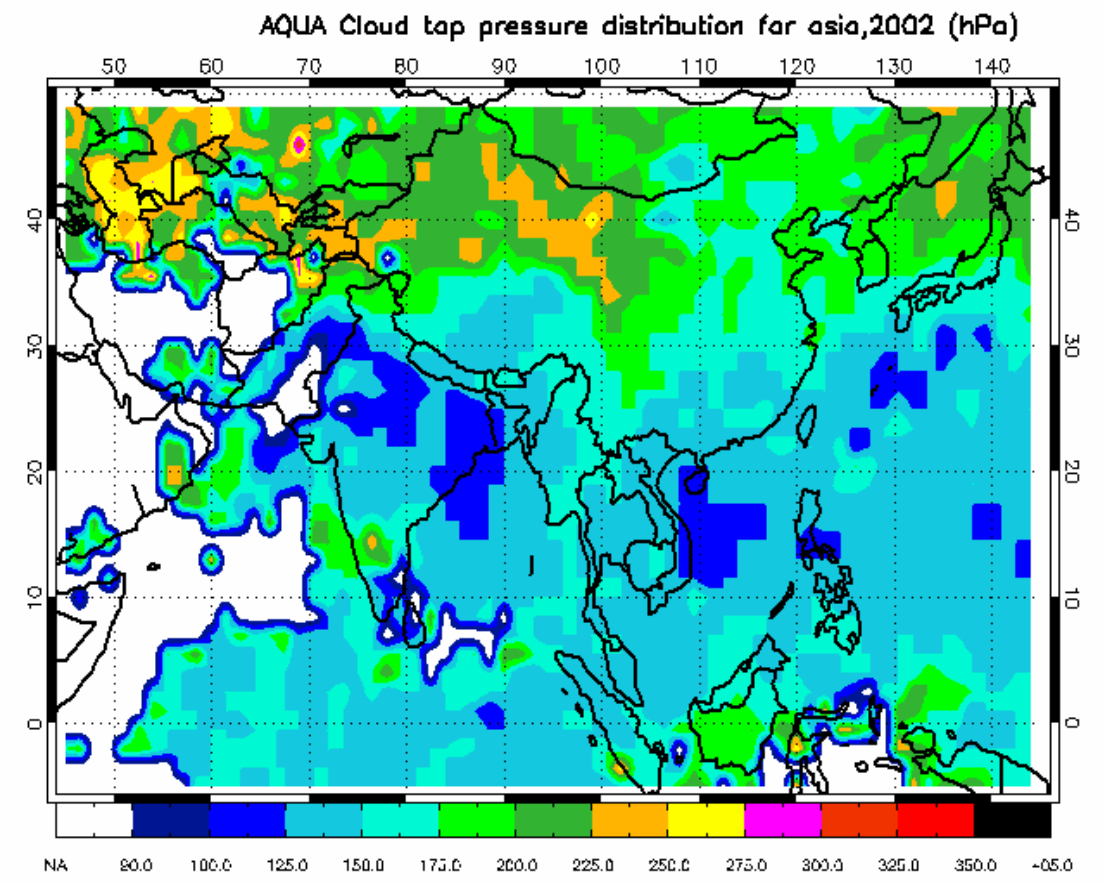

Figure 25b: Cloud top pressure map averaged over Asia during summer 2002. The blank areas indicate no data. South to north gradient in CTP is noted and several hot spots of deep convection are discussed in the manuscript.

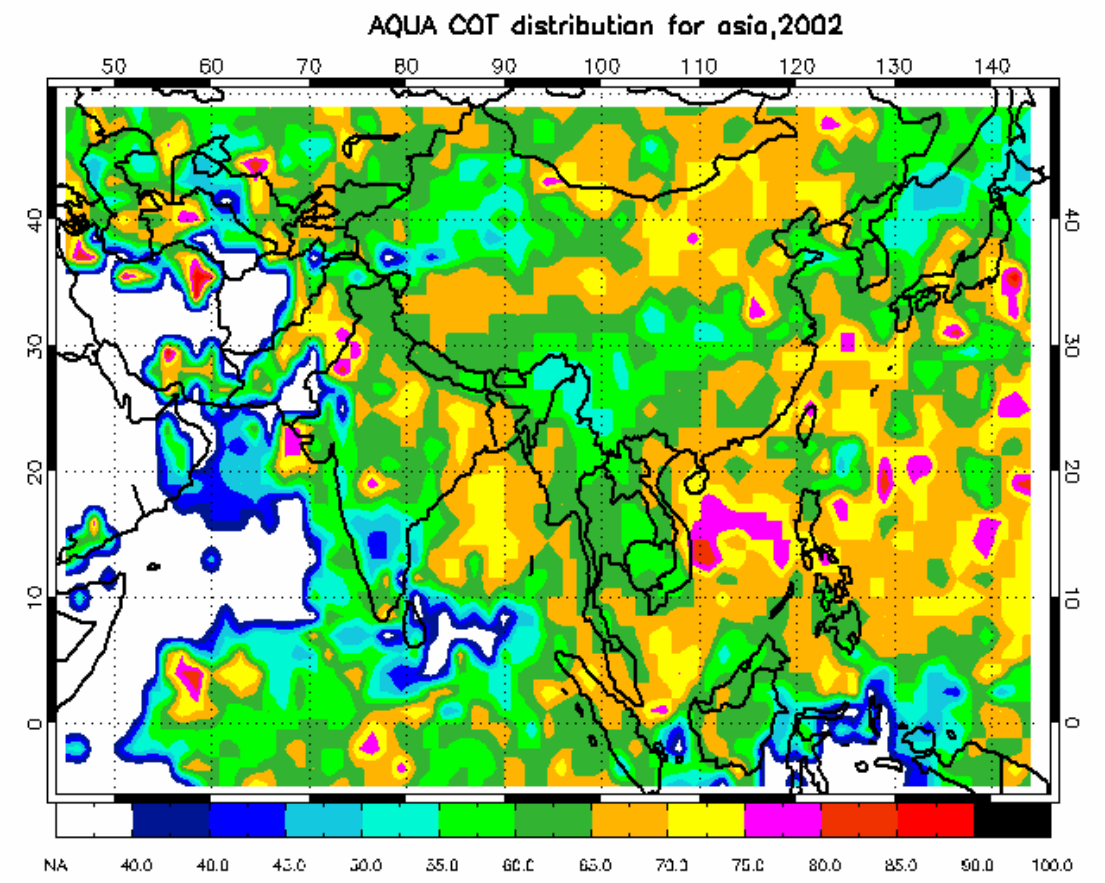

Figure 25c: Cloud optical depth distribution over Asia during summer 2002.

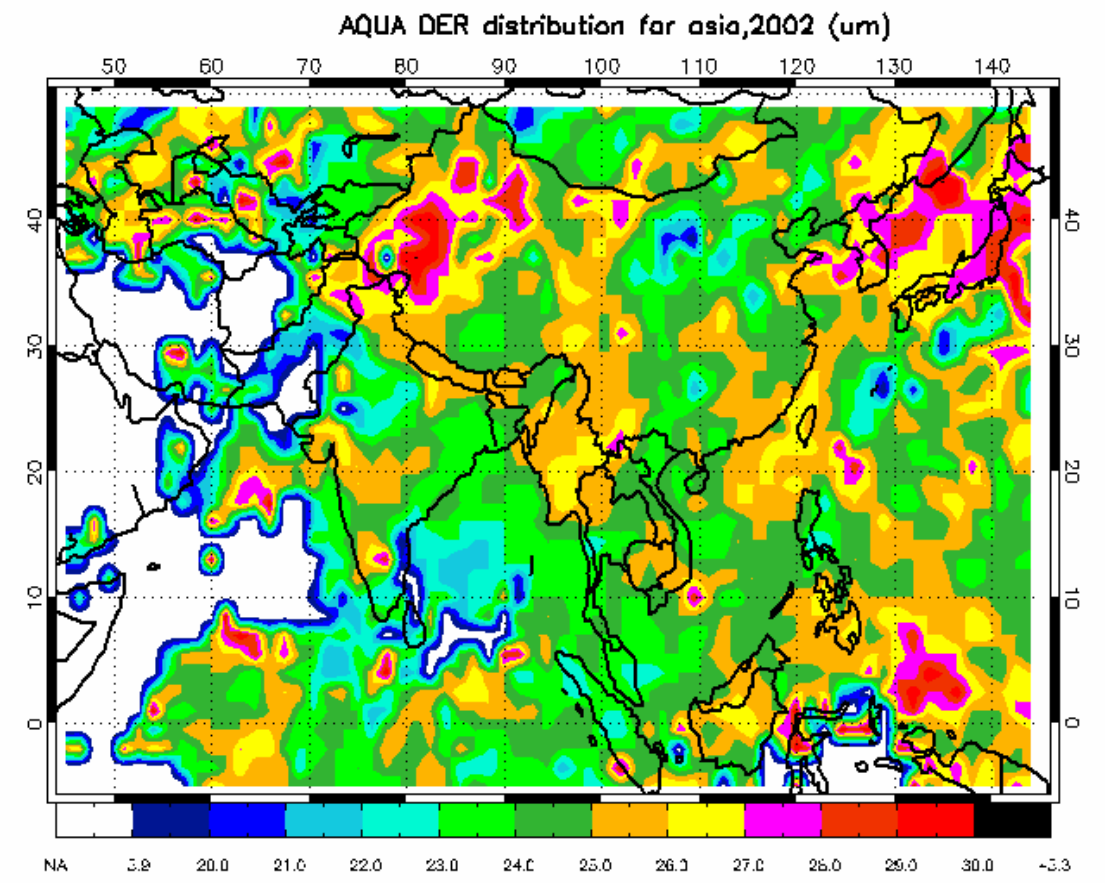

Figure 25d: Crystal effective radius distribution over Asia during summer of 2002.

No Clear pattern can be identified.

tropics and decreases to the north. According to this map the deepest clouds can be found over Northern Indian, South China Sea and to the south of Japan, where average CTP is between 125 and 100 mb and clouds probably have reached to the tropopause region frequently. This is in agreement with previous studies using different instruments. A map of cloud optical depth for the same region and period is shown in Fig 25c. The COD is generally greater over areas that produce deeper, more clouds like IM, EAM, PMP and TP. However, an extensive area over Northern China has optically thick clouds but of relatively shallow vertical extent as indicated by the CTP values, whose cause will be further discussed in following sections. Distribution of CER is plotted in Fig 25d and its pattern is not as well defined as that of frequency or CTP, which indicates that CTP or COD alone would not explain the variability of CER and indeed, CER is a microphysical quantity that is under influence of many factors as discussed in the introduction section. Simply using the data as it is and correlating the pattern with one factor like aerosols would lead to false correlation. Instead, we have to first filter out natural variations associated with environmental conditions to constrain the data; the two most important factors will be discussed in the following paragraph.

b) Cloud Brightness Temperature and Topography

In-situ and active remote sensing measurements [Heymsfield and Platt, 1984 and reverences therein; Martins et al., 2007] have demonstrated that ice particle sizes for high clouds strongly depend upon the environment

temperature and they are shown to positively correlate with each other, meaning ice particle size increases with temperature, which is opposite to the relationship between droplet size of liquid phase clouds and brightness temperature [Rosenfeld and Lensky, 1998]. This positive dependence is postulated to result partly from size sorting [Heymsfield, 1975] and from implication of Clausius-Clapeyron equation (CCE), which determines the saturation water vapor amount for a given temperature. When temperature is as low as around 200K further rising of air parcel, therefore decrease of temperature, would limit the amount of water vapor for growth of ice water content as indicated by CCE [Hartmann, 1994]. This physical relationship between cloud temperature and ice particle size will serve as basis of our study. The data we employ in this study shall obey the same relationship to be physically sound and meaningful. We apply two methods to examine the data, one comparing time series of BT and CER and the other probing the relationship between averages of BT and CER with both methods targeting a fixed region and time span. An area is selected based on the frequency map to contain significant amount of data to increase the statistical robustness. Then time series of BT and CER for this selected area is plotted for a time period and an example is provided in Fig 26a. Each point in the plot represents the mean value of either quantity over the area for one day. BT positively correlates with CER extremely well agreeing with the

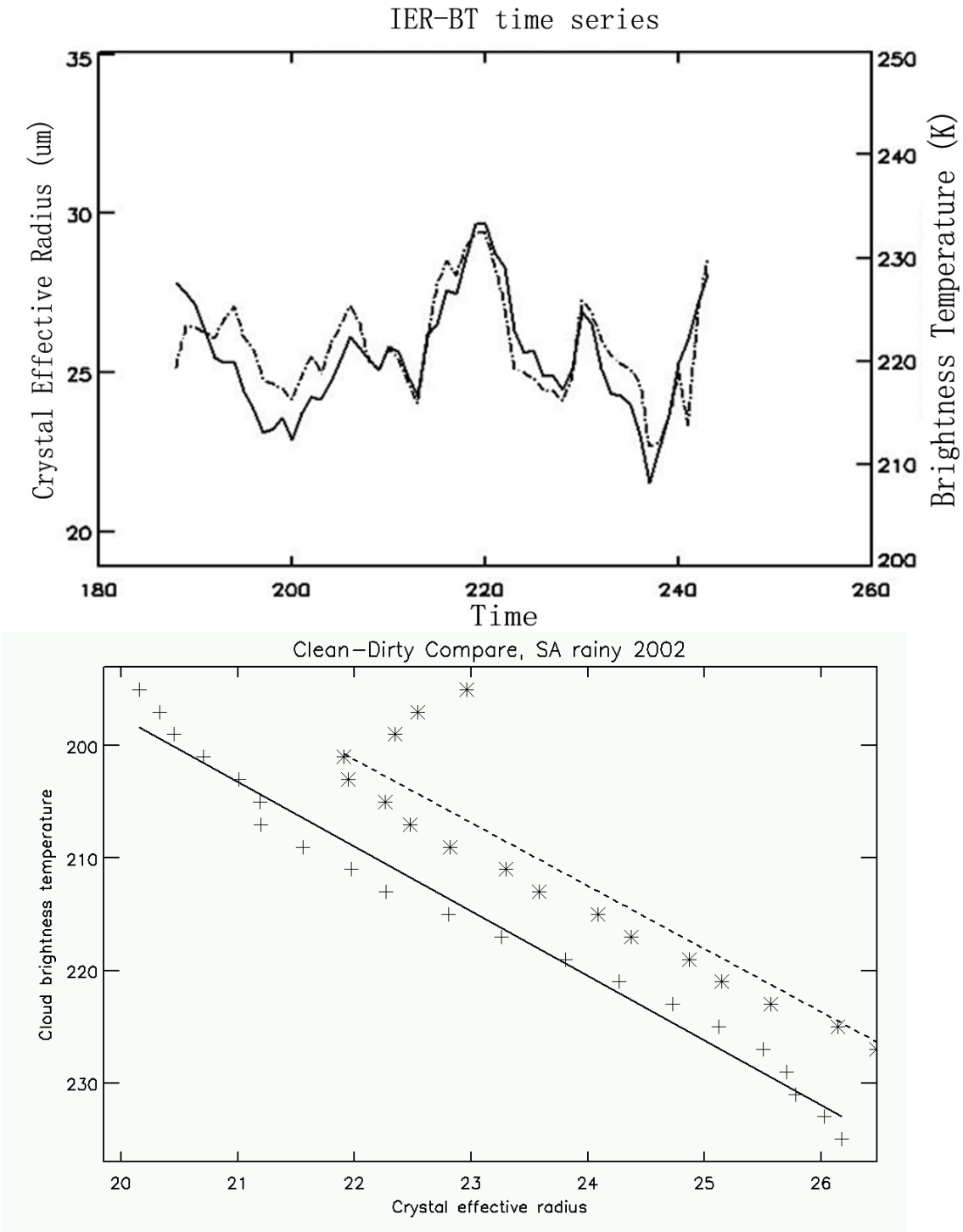

Figure 26: Top: time series of CER, left vertical axis, and BT, right vertical axis, are presented in the same plot. They are highly positively correlated with each other; lower panel: CER-BT profiles, from both Aqua and Terra, over South America during 2002, two lines representing Aqua (+) and Terra (*) data.

in-situ observed relationship. CER is plotted against BT in Fig 26b where BT is divided into equal sample size bins and CER is averaged over each bin and this produces a mean CER profile for certain area over a period of time. The BT-CER profile again shows good agreement with established results, which lends further confidence that the retrievals are physically sound in relative values regardless of their absolute accuracy. This relationship is observed in our data all over the global and appears to be a universally obeyed relationship, which serves perfectly as our physical base of further discussions of the aerosol effects on DCCs.

The influence of cloud temperature on CER is universally observed with little exceptions. However, there are several aspects of this relationship that vary geographically, which will be discussed further in later sections. Another source of variations of CER is topography as shown by Fig 27a and Fig 27b. Fig 27a shows the geographic distribution of CER from Aqua over North America in 2003 and Fig 27b is a digital elevation map for this region. A pronounced minimum is present in the CER map corresponding geographically well with the location of the Rocky Mountains. We propose several environmental conditions that favor smaller ice particle sizes over high elevation areas. From reanalysis data and AIRS retrievals (not shown) both total column integrated water vapor (precipitable water) and relative humidity are lower over plateaus as expected. The dry condition increases the cloud base height for cumulus clouds and therefore lower cloud base pressure and temperature, which are shown to be favorable for activating more droplets

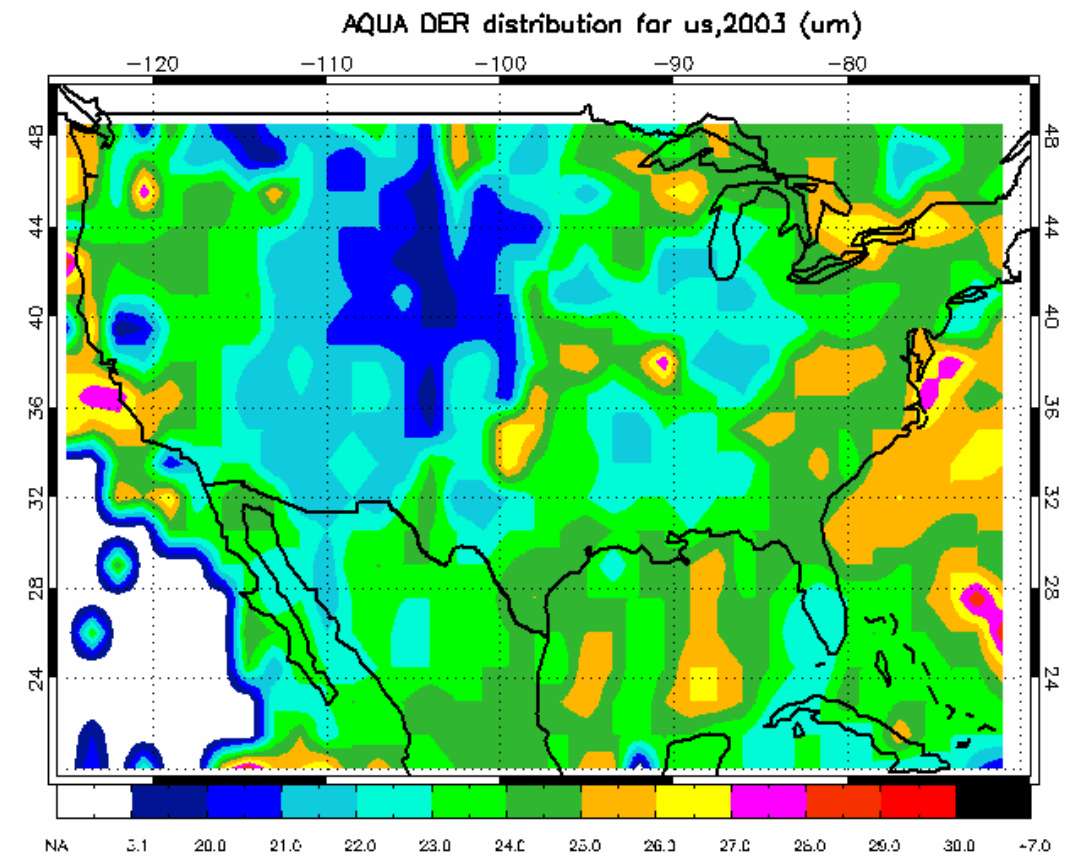

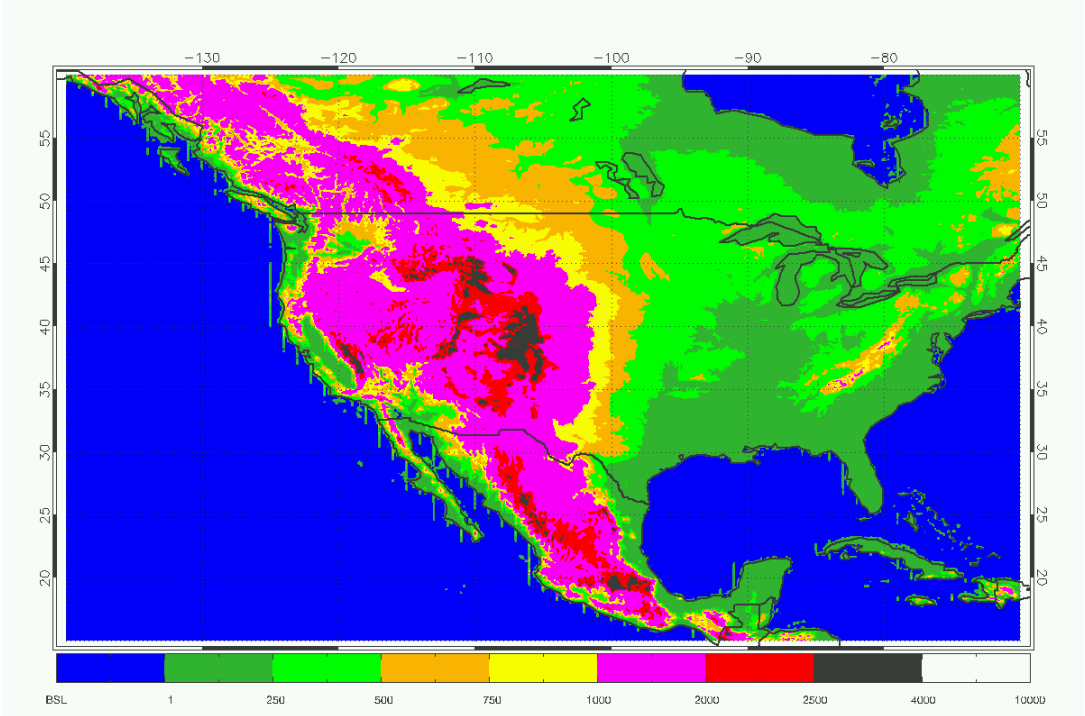

Figure 27a (upper panel): CER distribution map over US for summer, 2003;

Figure 27b (lower panel): Digital elevation map for North America in meters.

because of higher achievable maximum supersaturation level [Johnson, 1980]. We define in-cloud Lagrangian time, T_p, as the time it takes for droplets to rise from the cloud base to homogeneous freezing level (HFL) that is taken as -38 C. T_p is determined simply by two factors, vertical velocity and cloud depth of base to HFL. Low humidity directly contributes to shallower cloud depth by increasing cloud base and the land heating of mountains raises the potential temperature of surface air over plateaus, which is favorable for more energetic convection and thus increases updraft velocity [Houze, 1993]. These two conditions combine to reduce T_p and thus the time for droplets to grow. More activated droplets and shorter growth time significantly reduce the size of cloud top ice particles as observed in our study. The arguments are summarized in Fig 28 as a flow chart. The correspondence between high elevation and small ice particle size can be observed not only in North America but globally in our data set. This means that in addition to cloud height (BT) topography is another dominant factor that influences ice particle size and this topographical connection cautions against use of simple geographical pattern matches to study aerosol influences [Sherwood, 2002].

c) Histograms and Cloud Structures

Only a very small fraction of clouds in nature belongs to deep convective cloud category as defined in our study because the cloud occurring

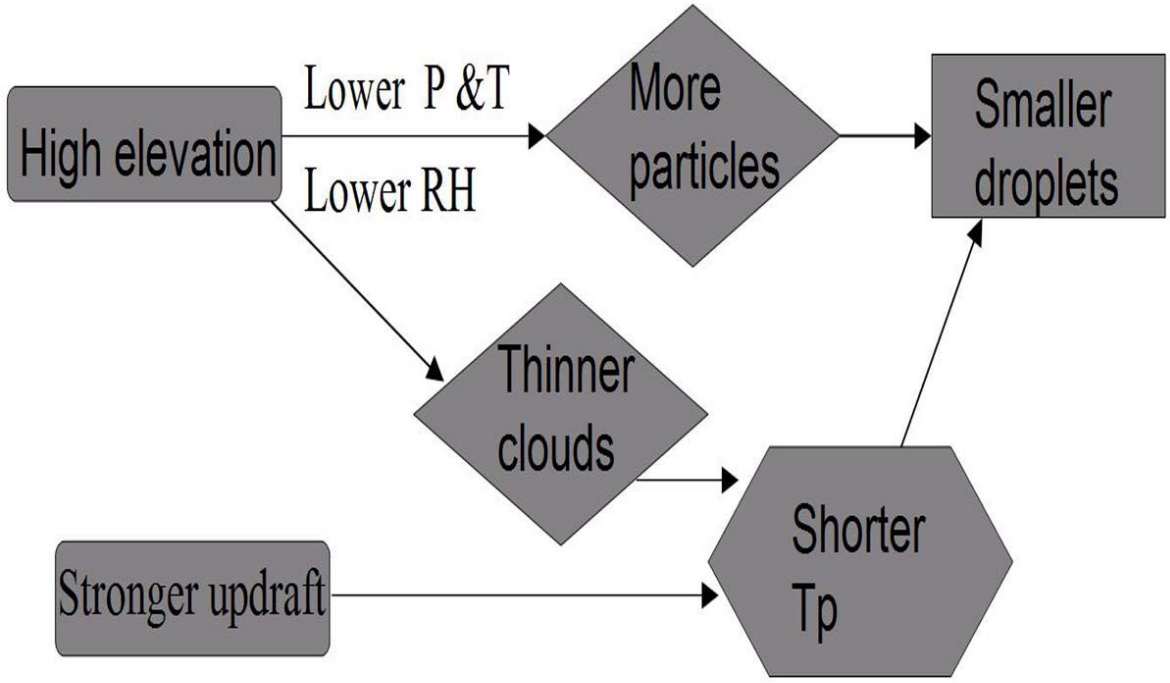

Figure 28: Flow chart of factors and processes that are favorable for smaller cloud droplets over highland areas and therefore smaller ice particles. Detailed discussion is presented in the manuscript.

frequency decreases exponentially with decreasing cloud top BT [Gettelman et al., 2002; Liu et al., 2007]. Although DCCs as defined in this study occupy only the very tail of cloud occurring frequency distribution they are mostly made up of convective cores and the thickest part of anvils [Roca and Ramanathan, 2000]. They are core components of complex convective systems and thus extremely important for many processes that affect climate as discussed in the introduction. The structure for this particular set of clouds is worth exploring to get more insight into these processes. For example, the FAT (fixed anvil temperature) hypothesis proposed an important constraint on the temperature of DCC anvils resulting from a sharp decrease of clear sky radiative cooling because of sharp decrease of water vapor saturation ratio through Clausius-Claperon relationship [Hartmann and Larson, 2002]. In Fig 29 BT histograms of four regions are constructed for both Terra and Aqua data. Histograms of all regions show a peak around 200K and the distribution is non-Gaussian and is right-skewed to low BT. The frequency of extremely cold clouds drops off rapidly once they are colder than the peak as evident by histograms, which agrees well with previous studies [e.g. Gettelman et al., 2002]. This exponential drop is due to the constraint that the tropopause puts upon convections and severely limits further vertical growth of DCCs, from which we may infer that the peak in BT distributions is attributable to DCC anvils that are formed because of the constraint and spread under the stable tropopause region over much larger areas than the convective cores do because convective cores overshoot into tropopause region and turn colder

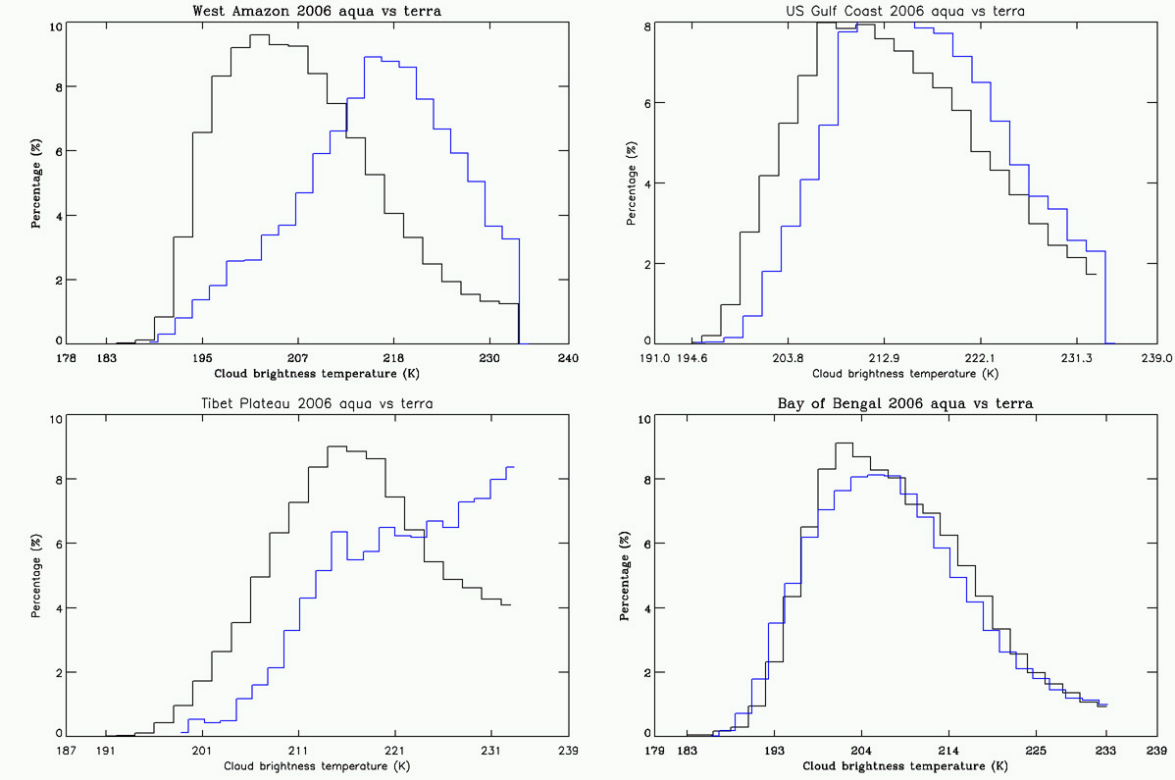

Figure 29: Four pairs of BT histograms for four regions as noted in each panel's title in 2004. They include, clockwise, West Amazon that is a tropical forest; US Gulf Coast that is continental; the Bay of Bengal that represent almost tropical ocean in the summer and the Tibet Plateau area that is a highland area. A preferential detraining level at around 200K is manifested in the structure of DCC BT histogram. Blue lines are for Terra data and black lines for Aqua. The difference between these two is due to diurnal variation.

over limited spaces, which makes them only occupy the tail of BT spectra. Analyses of individual large DCC systems show similar structure of DCC BT distributions and therefore support our postulation. From Fig 29 it is also noted that peak temperature in the distribution, corresponding to the temperature where DCCs detrain their mass and anvils form, has geographical variations that are probably associated with large scale circulations that determine the temperature of the tropopause region and therefore the preferential detraining level. The peak temperature also has year-to-year variations for a fixed area possibly because of local circulation change. Our observations seem to support the FAT hypothesis in that DCCs generally have distribution peaks around 200K. However, our observations suggest significant variations both geographically and temporally and 200K is not a universal number. Even for a fixed region significant diurnal and annual variations of the detraining level are implied by changes in BT distribution from Terra and Aqua data as in Fig 30, which further indicates that detraining levels are not fixed as if there were under a solid lid.

As far as radiative forcing of DCCs is concerned cloud optical depth (COD) is important in regulating shortwave forcing of these clouds while BT largely influences outgoing longwave radiation. These two quantities are often used together in radiation models to calculate radiative forcing with additional assumed conditions [Hartmann et al., 2001 and references therein]. We therefore carry out similar analyses for COD as those of BT. There have been arguments on whether the near cancellation of LW and SW forcing for

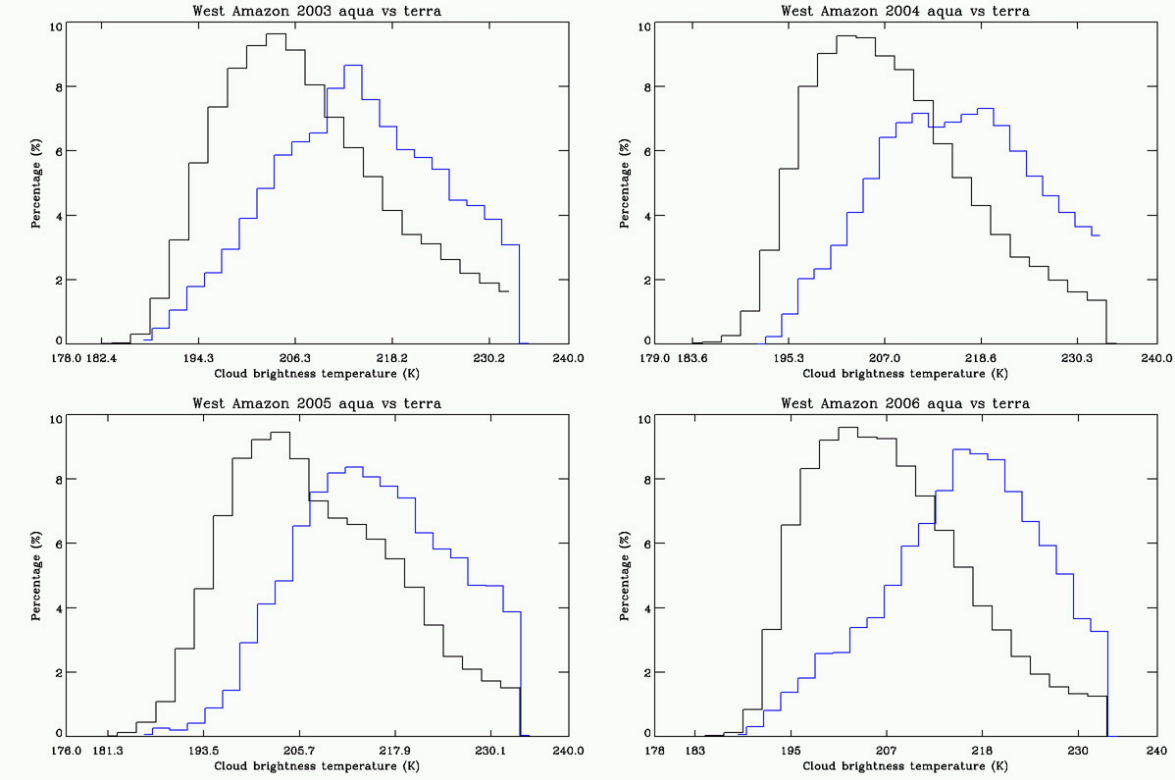

Figure 30: Four years of BT distributions for the West Amazon region. This region is marked by both the diurnal and the annual variations in peak temperature. As implied in Fig 29, some regions like the Bay of Bengal has almost constant peak temperature.

tropical DCC active regions is due to DCCs alone or it is rather due to the distribution of the whole cloud system that include both DCCs and other shallower clouds accompanying them [Hartman et al., 2002 and references therein]. Only the deepest clouds are included in our study and therefore examination of these clouds will shed light on whether high, thick clouds alone lead to cancellation of LW and SW forcing or the whole spectrum of clouds needs to be considered to have the cancellation. In Fig 31a multiyear COD histograms of four regions are presented for Aqua data. The peak at the right end of COD distribution is due to the combination of two facts: one is that MODIS COD product has an upper limit of 100; the other is that thick anvil clouds cover large areas as shown in BT distribution. The peak is especially pronounced for distributions over the tropical regions, which we think is ultimately caused by the structure of individual systems: DCC systems formed in the tropics tend to have larger and thicker anvils associated with convective cores compared to those over subtropics or high elevation areas. This difference can be clearly seen by comparing two regions that have two extreme distributions: the Bay of Bengal and the Tibet Plateau, where COD distribution for the Bay of Bengal region has only one pronounced peak at the high end while that of TP shows no sign of peak at high COD values. We may conceptualize these extremes as two types of DCC organizations: one umbrella like structure in the tropics and the other more turrets like over highland areas. As a result of this organization difference the means and standard deviations for the tropical DCC systems are generally larger. We also

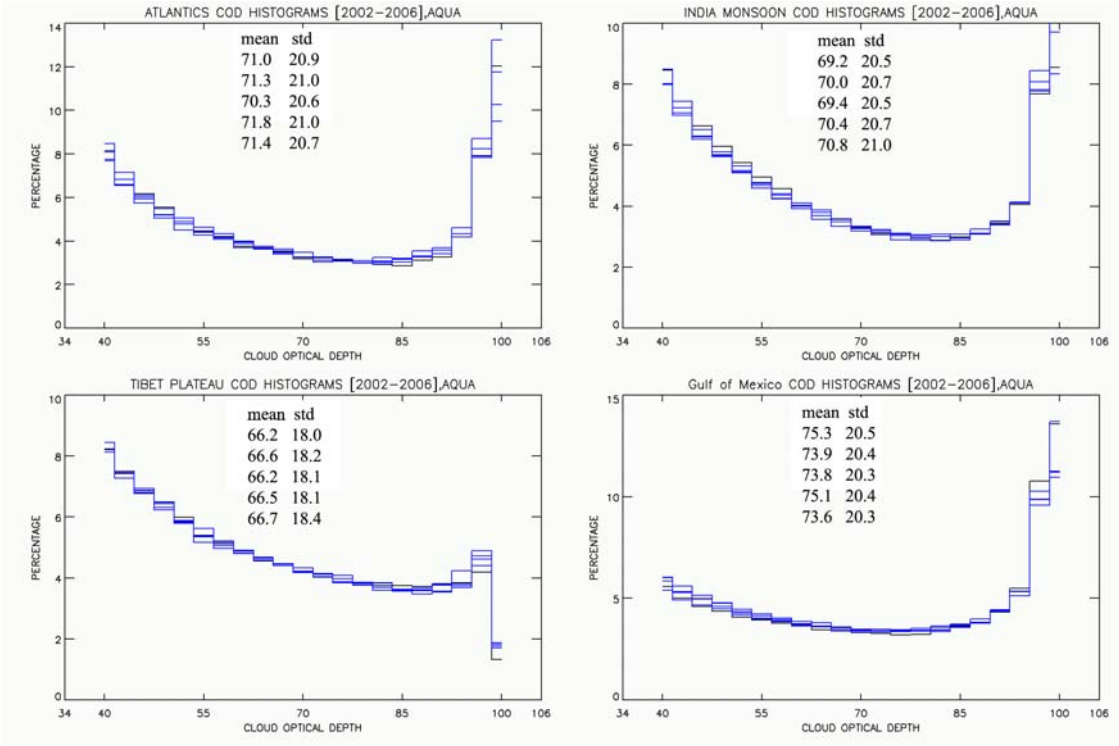

Figure 31a: Aqua COD distributions for four regions are shown.

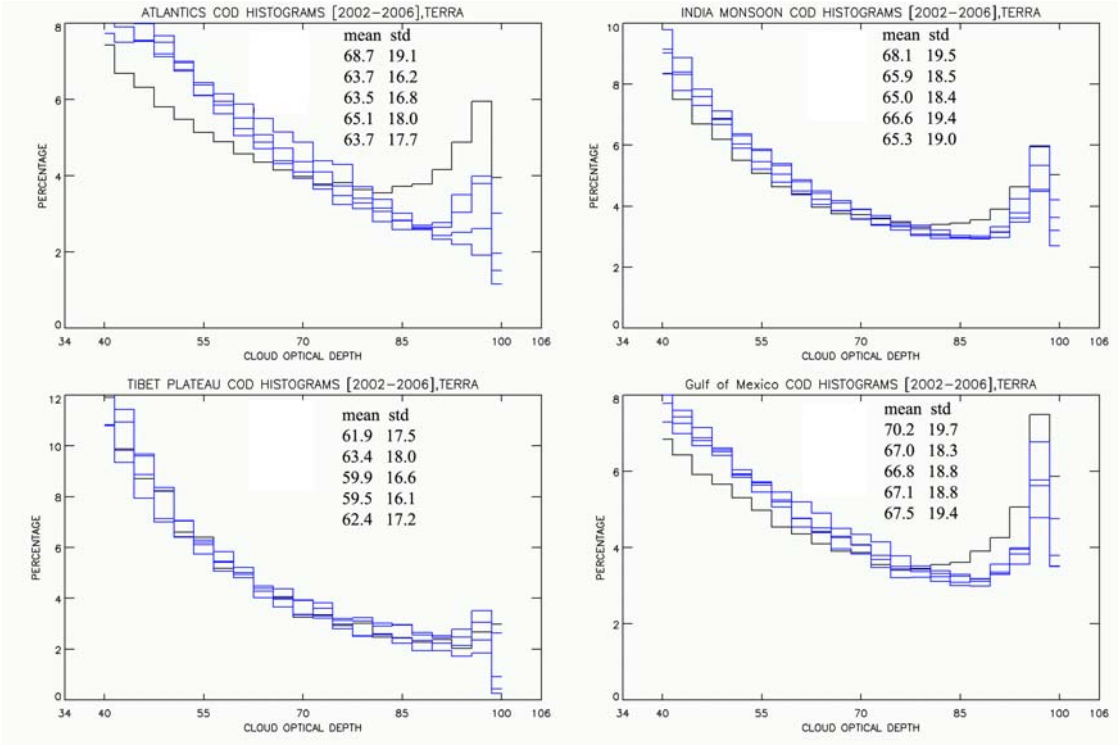

Figure 31b: Terra COD distributions for the same four regions.

note that for individual regions COD distribution structure is well-defined and the shape is extremely stable for all the years we analyzed, which is manifested by the almost constant means and standard deviations. The stable statistics of COD for each region suggest that a special kind of organization of DCC systems exists for each region despite yearly variations in local circulations. In other words, DCC systems have local signature structures, at least statistically. Despite the stable local signature structures for individual regions significant variations are observed not only between the tropics and the subtropics, but within themselves as suggested in the figure. This geographic variability is perfectly in line with findings in previous studies using direct energy flux measurements [Hartmann et al., 2001; Futyan et al., 2004] and suggests a strong locality of DCC systems that may be associated with their distinct local environmental conditions, which agrees with previous studies that found systematic differences among DCC active regions [Kubar et al., 2007 and references therein]. The mechanisms behind these different organizations warrant further investigation and are beyond the scope of current study.

In Fig 31b multiyear histograms of four regions using Terra COD are presented. We note that in contrast to the stable statistics of Aqua COD data, COD histograms from Terra show a different picture. We know Terra and Aqua overpass times are in the mid morning and in the early afternoon, which can be crudely used to represent part of diurnal change. It is known from different kinds of observations that DCCs show significant diurnal change

over some regions [Yang and Smith, 2006]. The diurnal change can be seen by comparing Figs 31a and 31b. Clouds generally become thicker in the afternoon as indicated by the higher mean values and the real difference between these two is probably greater considering MODIS treats all COD greater than 100 as 100. The shapes of COD distribution are sometimes altered in some cases like for over the Rocky Mountain region where a peak in the high COD end is present only in the afternoon. Another intriguing result to note is that although the statistics of Terra data still falls within a narrow range, significantly larger yearly variations than those of Aqua COD histograms are recorded. This suggests that clouds become mature and better organized into a local signature structure only in the afternoon but they are relatively immature in the mid morning, which explains why the Terra statistics is not as stable. This implies that instead of stable near neutral cloud radiative forcing we may observe significantly larger yearly variation for morning clouds than those in the afternoon since 'mature' DCCs tend to have near neutral radiative forcing. This implication poses direct challenge to our understanding and interpreting the results by satellite observations of the Earth's radiative energy budget. One study by *Wielicki et al.* [2002] shows that radiative energy budget for the tropics is more variable than previously thought using measurements from different satellite platforms and sensors. If indeed the cloud statistics and therefore organization undergo significant changes diurnally results from that study would come as no surprise since the instruments were measuring clouds that are bound to have yearly variations

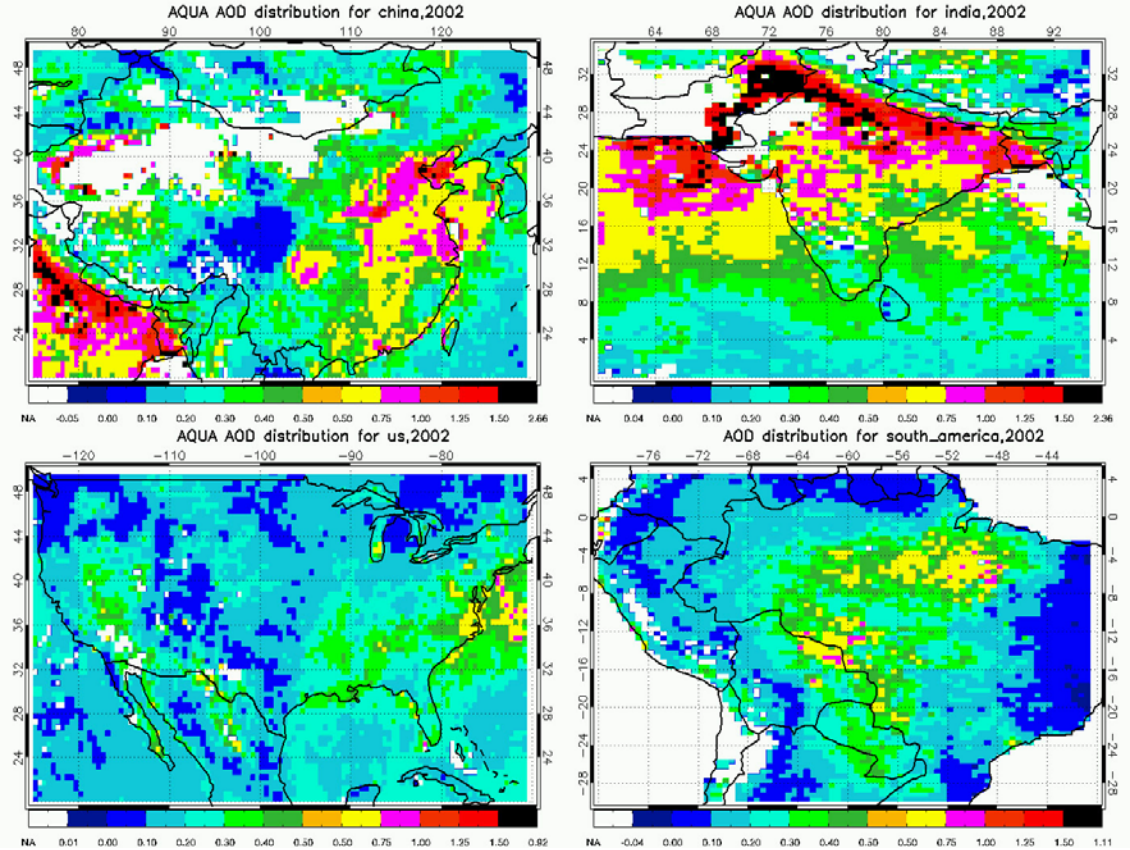

Figure 32: AOD maps in 2002 for four regions with the same scale. Maps of US, India and China are AOD averaged during the summer (June-August) and the South America AOD map is the average during September-November.

according to our analysis. Our study suggests that sampling and comparing the well organized clouds may offer more insights on this issue.

3.4.2 Aerosol Effect

Aerosol optical depth spatial distributions for four DCC active regions are shown in Fig 32. India and Eastern Asia stand out as the two most polluted regions and high degrees of heterogeneity are observed for each region, which is desired in our study to investigate aerosol effects. For example, the Indo-Gangetic Basin (IGB) located in the northern India is home to a huge population that produces large amount of anthropogenic aerosols in the summer together with dust from natural sources like the Tsar Desert at the border between Pakistan and northwestern India. IGB is surrounded by the Himalaya to the north and hills to the south, which, together with ample sources [Guttikunda et al., 2003], makes this strip of land highlighted in the AOD map as one of the most polluted over India [Jethva et al., 2005], especially in the spring and summer. Ground observations have indicated that aerosol sources are so strong and persistent that after a rain out the aerosol level goes up immediately [Ganguly et al., 2006]. Due to the summer Indian monsoon DCC systems are frequently organized over this region as shown in previous plots, which coupled with the persistent level of aerosols provides great potential for aerosol-DCC interactions. The lower part of the Indian subcontinent is also loaded with intermediate AOD values that can still be

considered high when compared with the rest of the world. In the summer the southwest Indian monsoon system has prevailing southwesterly winds over the lower part of Indian subcontinent that carry pollutions from land to over part of Bay of Bengal as evidenced by the patch of high AOD over the ocean adjacent to the land. These geographical and circulation conditions coupled with aerosol source distributions are configured to create patterns of AOD that have strong contrast and heterogeneity, which are desired for our study and can be said to AOD patterns over other regions.

Since we are using AOD as a proxy for actual cloud condensation nuclei (CCN) and we assume a fixed AOD to CCN ratio for a specific region. The existing contrast and heteorogeneity in AOD maps create a large dynamical range of CCN and are ideal for investigating aerosol effects. From visual examinations of CALIPSO imagery we make sure that for a study region most of aerosols are confined to planetary boundary layers, which is crucial for our usage of AOD as the proxy for CCN because otherwise aerosols seen from MODIS are not those entering clouds and activate. This is an advantage over previous studies that use other CCN proxies like aerosol index that is only sensitive to elevated UV absorbing aerosols that are less likely to active as CCN and may not interact with cumulus clouds. Most DCCs are generated locally by atmospheric instability and therefore air parcels in the boundary layer are active in the process of cloud forming. This ensures aerosols and clouds are interacting with each other. We confirm this by inspections of near simultaneous imageries from MODIS, CALISO and

CloudSat for many cases. We first identify individual DCC systems that are relatively isolated towers from MODIS images, so that enough clear sky area is present for CALISO to take measurements. From CALIPSO lidar backscattering images we can know where the aerosol layer is and cloud base is readily available from CloudSat radar images. Since the spatial scale of aerosol variation is on the order of 100km we may extrapolate the aerosol signal from clear sky area to under nearby cloud bases and thus we can confirm from these two measurements that aerosols and clouds are interacting.

a) Time Series

One conventional method to investigate aerosol effects is to simply correlate time series of CCN amount, which is approximated by AOD here, and a cloud parameter, which is CER in our study. Two examples are shown in Fig 33 where we select one region in Eastern China and the other in Eastern Amazon, each covering an area about 5 degree by 5 degree, and plot out daily averages of AOD and CER for each region. AOD is negatively correlated with CER as expected from the Twomey like aerosol effect that argues for decreased droplet sizes as a result of increased CCN concentrations [Twomey, 1977].

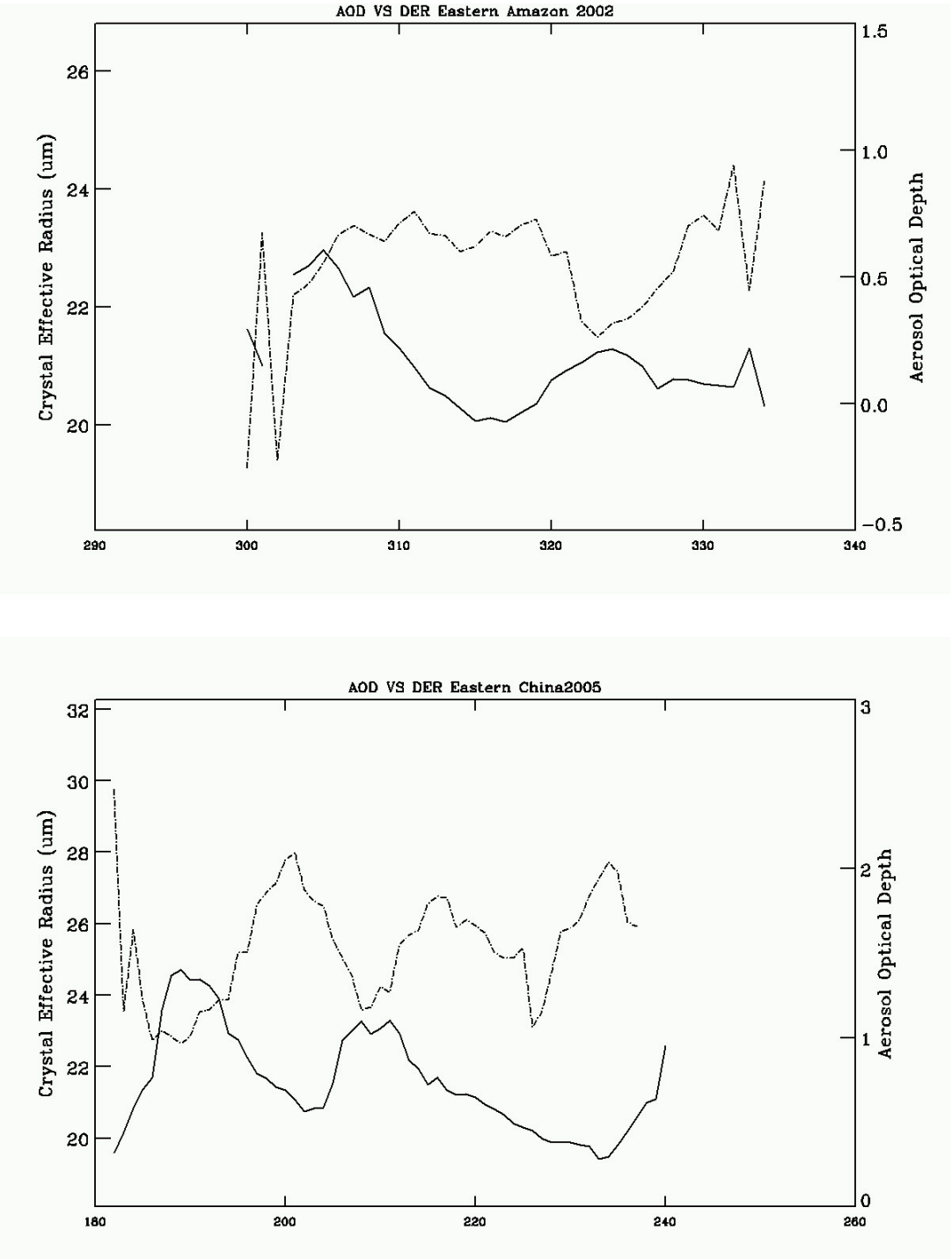

Figure 33: AOD-CER series of two areas over Eastern China and Eastern Amazon. Solid lines are for AOD; and dash-dotted lines are for CER. Note that AOD can be below 0 in MODIS collection 5 product. The x-axis is the day of the year.

However, this method suffers from three major shortcomings that prevent it from being convincing enough. Firstly, in this method no proper constraints on cloud formation's thermodynamic and dynamical conditions that dominate cloud formation and determine their properties are applied. The natural dynamic range of ice cloud microphysics due to these dominant factors overshadows any aerosol signal, if it exists. Secondly, because these two retrieval quantities are exclusive to each other and we have strict quality control on both AOD and CER data, sample sizes of either AOD or CER for one day over a limited space are often too small to arrive at any definite conclusions, which again makes them vulnerable to natural variations. Lastly, active cloud (not only DCC) formation in the summer may lead to false correlation between AOD and CER resulting from cloud and aerosol retrievals performed at the same time and over the same location [Yuan et al., 2008] although we have applied strict filters to the data to lower the possibility of a false correlation. Because of these unfavorable reasons we do not adopt this method as our investigation tool. In fact, many of our analyzed areas show sporadic or no correlation because of either lack of data or reasons discussed here.

b) Spatial Patterns

Another conventional way to interpret the data and detect possible signals from aerosol effects is inspect spatial patterns of both aerosol and

cloud properties [e.g., Sherwood, 2002]. We have noted the disadvantage of this method in previous discussions because spatial variations are largely influenced by environmental condition variations in topography and circulation that would overshadow any aerosol signals. In general we found little evidence that suggests patterns of AOD and CER are correlated. One could find spurious correlations between them over a few specific areas if looking closely. For example, the ice particle sizes are smaller for IGB region and they are accompanied by higher AOD. However, this correspondence is weak and is neither temporally nor spatially consistent, which is exactly what one should expect realizing the strong control that environmental conditions have on cloud properties. We apply two constraints on the data to homogenize these conditions to carry out spatial pattern analysis. First the topography of our target area must be relatively homogeneous to eliminate the influence of elevation. The influence of cloud height is controlled by binning the data based on cloud vertical reach. Within each data bin clouds have similar BTs or CTPs. An example is shown in Fig. 34 where the IGB region and the nearby Bay of Bengal is selected as our target area as elevation for this region is lower than 250m and relatively flat. Fig. 34a shows the spatial CER pattern of

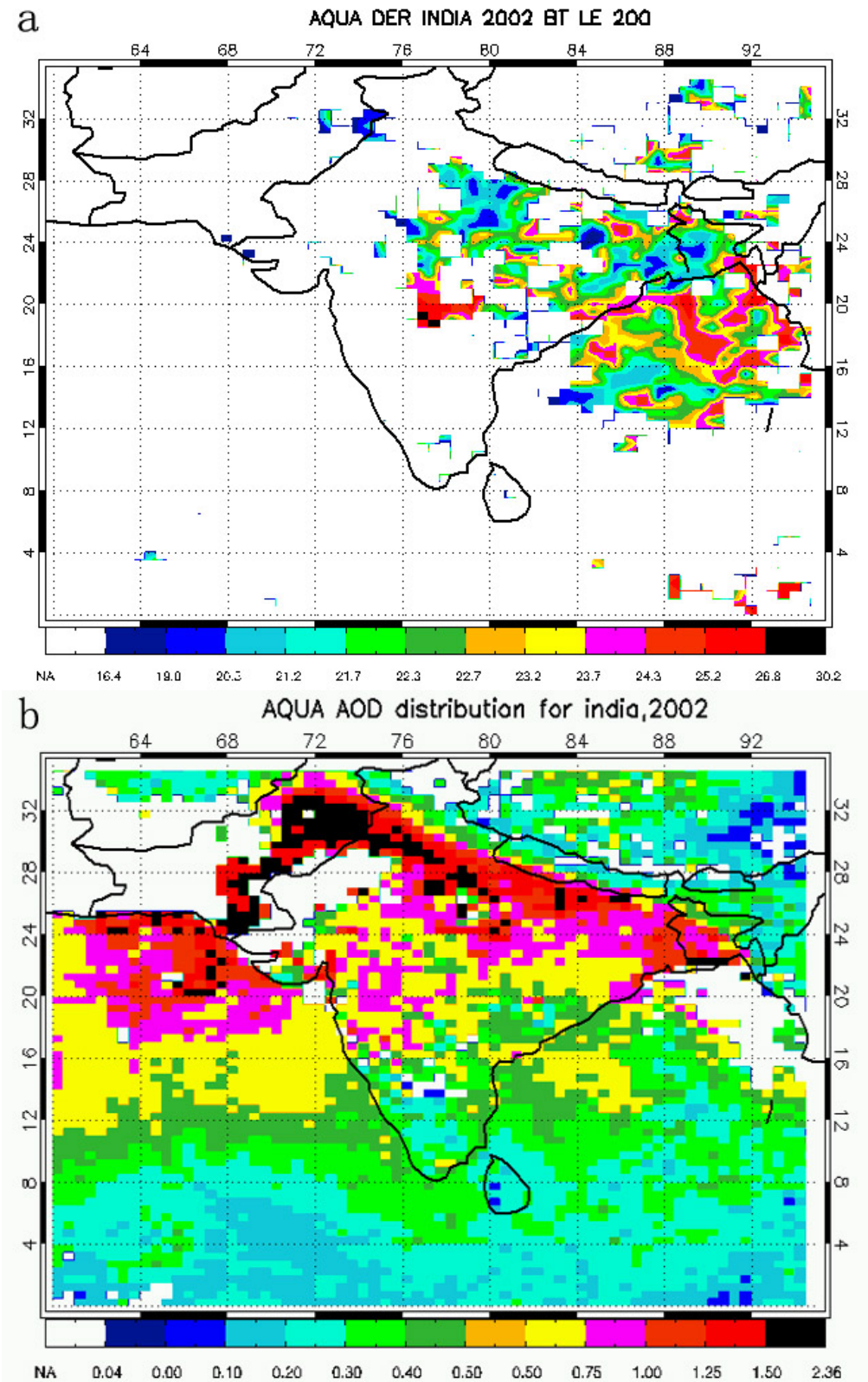

Figure 34: a) CER distribution map for only clouds having BT less than 200K in 2002; b) Aqua AOD distribution map for summer 2002.

clouds that include only those with cloud top pressure higher or equal than 200mb for this area and corresponding spatial pattern of AOD is plotted in Fig 34b. We choose 200mb as a threshold for binning the data because these clouds have are reached closely to the tropopause and likely in the same mature stage of development. Clouds that belong to other bins lower than this level may be in different development stages, with some already mature while others reaching the same height but still developing. The AOD pattern negatively and strongly correlates with CER pattern in Fig. 34. The strip of low CER area over IGB is heavily polluted as indicated by the high AOD and over the ocean ice particle sizes are generally larger, but are decreased where a patch of heavy pollution area resides, which probably is due to transportation from the land by the prevailing southwestly wind. There is a blank area in the AOD map over the Bay of Bengal that is caused by extremely high cloud cover. Surrounding that area a few 'hot spots' with high AODs are present although the number of pixels going into average is under 10 and bear little statistical significance.

One shortcoming of this method is that proper filtering and binning process decrease significantly the sample size that is required to beat down 'noise' level caused by natural variation especially over regions with weak AOD heterogeneity. Besides it does not offer any more insights to aerosol effects other than a qualitative check.

c) CER Profiles

In this method our main tool is the physically sound CER vertical profiles constructed by collective measurements of a number of collocated and simultaneous CERs and BTs from MODIS. These CER-BT profiles serve as base of our analysis. In this method we first choose two target areas that are DCC active in order to get significant sample size. Two target areas must also have similar environmental conditions to single out only aerosol signals. These environmental conditions we check include important atmosphere state variables and derived parameters like temperature profile, precipitable water vapor (PW) amount, relative humidity, lifting condensation level (LCL) and convective available potential energy (CAPE). They need to be comparable in seasonal means since our analyses are carried out for seasonal ensemble data. Among them PW, relative humidity and temperature profiles data are from the MODIS and AIRS instruments whose seasonal maps are conveniently available through the GIOVANNI website. LCL and CAPE are calculated from ECMWF analysis data. In addition to atmosphere state conditions we may also compare two areas having similar topography or favorable topography configurations that will be discussed later. To enhance aerosol signals we choose target areas with large contrast in aerosol loadings. After two target areas are selected through these screening steps two CER-BT profiles are constructed. The difference between the profiles is our aerosol signal since within each BT bin clouds have almost the same BT and other environmental conditions are also controlled in the screening process. We will

first propose a conceptual model for our analysis and then outline a few scenarios that are ideal for investigating aerosols' impact.

i) Conceptual Model

From bases of DCCs cloud hydrometeors typically undergo four stages of evolution. First, cloud droplets are activated at the base and as a parcel rises, extra water vapor is condensed onto these droplets, the so called condensational growth stage. This growth process is characterized by slow growth rate because the supersaturation ratio inside clouds is never large enough to sustain fast growth. On a diagram of cloud hydrometeor effective radius (ER) against cloud BT condensational growth will show up as a line with steep slope. Condensational growth of droplets eventually triggers the coalescence process as a few large droplets grow sufficiently large to collect other small droplets because of the difference in their fall velocities. Coalescence process is a much more efficient process at increasing cloud droplet effective radius than condensational growth and thus it is characterized by a flatter slope in the ER-BT diagram. As the air parcel continues its ascent temperature decreases accordingly and drops to much colder than 273K while cloud water remains in the liquid phase and becomes supercooled. Other conditions being the same larger droplets freeze more easily than do small ones. As such, the coalescence process in a sense facilitates both warm rain process and initial freezing of cloud water as a few extremely large droplets

may freeze under supercooled conditions. Once a few ice crystals are created they can grow at the expense of supersaturation of water vapor by deposition and supercooled liquid water by accretion. Cloud water then enters into a mixed phase stage where both liquid and ice phase are present and raindrops are also likely to exist in this stage due to warm and/or cold rain processes. This stage is again characterized by a relatively steep line in the ER-BT diagram since competing effects of rain out, ice crystal growth and ice multiplication keep the effective radius from increasing very fast. Cloud water becomes fully glaciated after either ice process completely deplete liquid phase cloud water or the air parcel reaches the homogeneous freezing level. Because of size sorting and entrainment ER evolution after air parcels are fully glaciated is characterized by a line of negative, steep slope in the ER-BT diagram as that shown in Fig 26. These four stages are summarized schematically as profile C (clean) in Fig 35.

The evolution profile for a microphysically continental cloud differs from profile C in that the concentration of droplets is so high that it effectively delays coalescence process by slowing down the condensational growth process due to competition for water vapor among more numerous droplets. Manifested in the ER-BT diagram is a longer, steeper condensational growth line and therefore colder temperature where coalescence process is started, assuming a similar ER threshold for initializing coalescence growth. This then leads to colder initial freezing temperature, or $T_{fD} < T_{fC}$, where T_{fD} and T_{fC} are freezing temperatures of dirty and clean clouds, respectively. Another

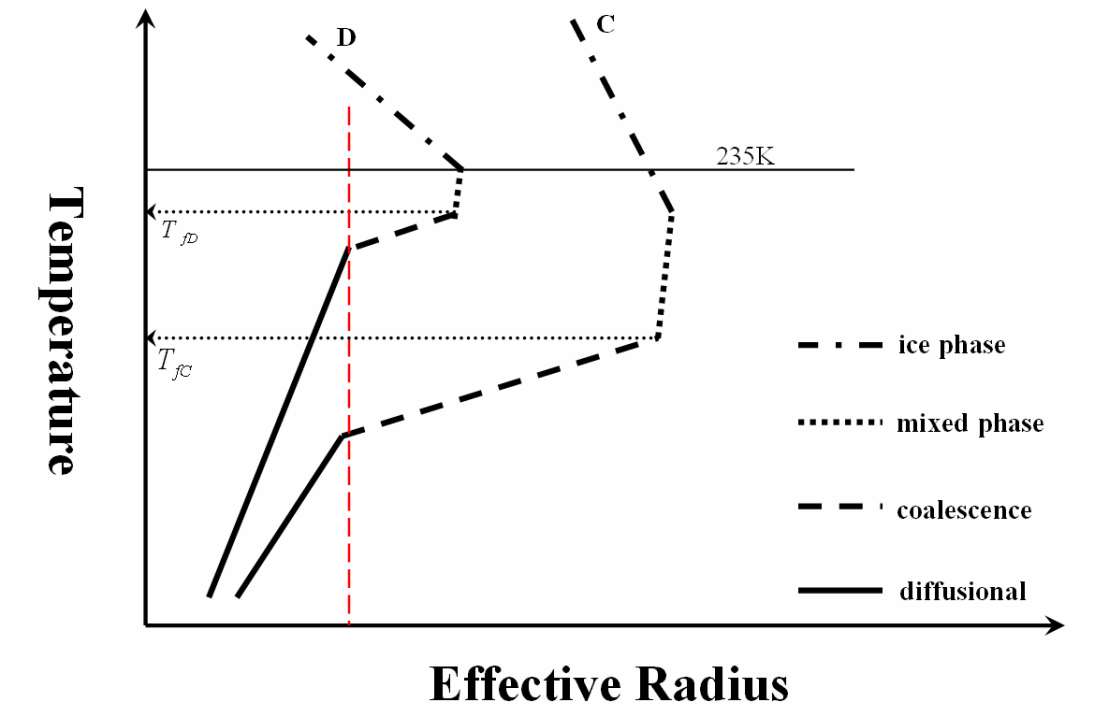

Figure 35: A conceptual model illustrating cloud hydrometeor evolutions inside microphysically continental (D) and clean (C) clouds. The horizontal solid line indicates the homogeneous freezing level at around 235K. Two dotted lines show temperatures of initial freezing of droplets.

effect of delayed coalescence and elevated freezing level is a shorter time for coalescence growth because at colder temperature relatively small droplets can be frozen. Under extremely polluted conditions coalescence process may never take effect and homogeneous freezing is wholly responsible for glaciating cloud water as indicated by *Andreae et al.* [2004]. This microphysical effect of pollution is illustrated in Fig 35. The end result of this effect is that under similar environmental conditions ensemble of clouds under polluted conditions shall have smaller ice particle sizes than relatively pristine clouds do. This conceptual model of cloud hydrometeor evolution and microphysical effects of aerosols serves as our theoretical base for investigating aerosol effects on DCC microphysics in real observations.

ii) Offshore Transport

One case is shown in Fig 36 for two areas over the Bay of Bengal. Fig 36a shows the AOD map for the Indian Monsoon region and two selected areas that have distinct aerosol loadings are indicated in the map. The high AOD level over our polluted area is due to aerosol transport from the land by the monsoonal wind as aforementioned. The other area is relatively unaffected and remains clean as indicated by the low AOD value. These two areas are very close to each other and other atmospheric conditions are nearly identical. They also fall within an extremely DCC active region and plenty of samples are available. A pair of CER-BT profiles is shown in Fig 36b with BT

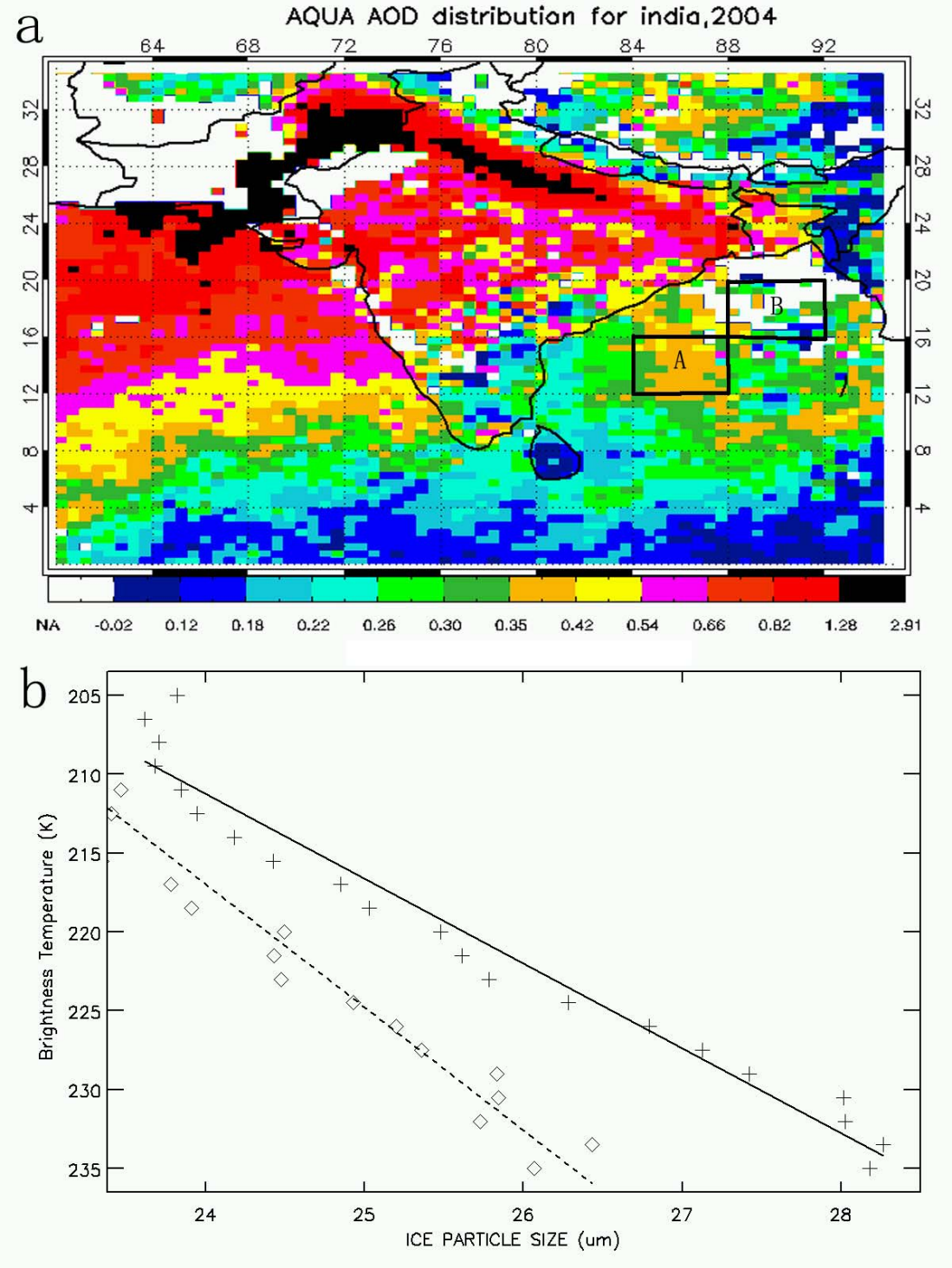

Figure 36: a) AOD map of Indian region in 2004; "A" is an offshore polluted area and "B" is relatively clean area. b) CER-BT profiles for areas A and B. The solid line is for clean area B and the dashed line is for polluted area A.

bin size equal to 1.5K. These two profiles are consistently separated by a difference of about 1 to 2 μm at every cloud height level. This case represents a scenario where heterogeneity in the AOD over ocean is created because of transport of pollutions over land while other conditions are relatively homogeneous. This scenario can be applied to not only over the Bay of Bengal but also over waters close to coast of eastern China and over the North Atlantic Ocean off US east coast, where strong heterogeneities are created by the same offshore transport of pollutions to over the ocean. Indeed, our analyses carried out for these two regions indicate the same aerosol effect.

iii) Aerosol Loading Dipole

Fig 37 shows a case for two areas over Southwestern China, one polluted and the other clean. The polluted area is over Sichuan Basin that has high aerosol loading and because of its topography aerosols are trapped in this basin whose elevation is below 500m and its surrounding areas are above 2000m. The seasonal and spatial mean AOD from MODIS for this area exceeds 0.6 that is among the most polluted regions over China and shows up as a local maximum in our AOD distribution map, Fig 37a. The clean area sits just to the northwest of Sichuan Basin that is almost pristine and its elevation is above 1000m. These two areas create a dipole in aerosol loading while they are quite close to each other. Despite higher elevation that is favorable for smaller ice particle sizes, CER over high elevation, clean area is consistently

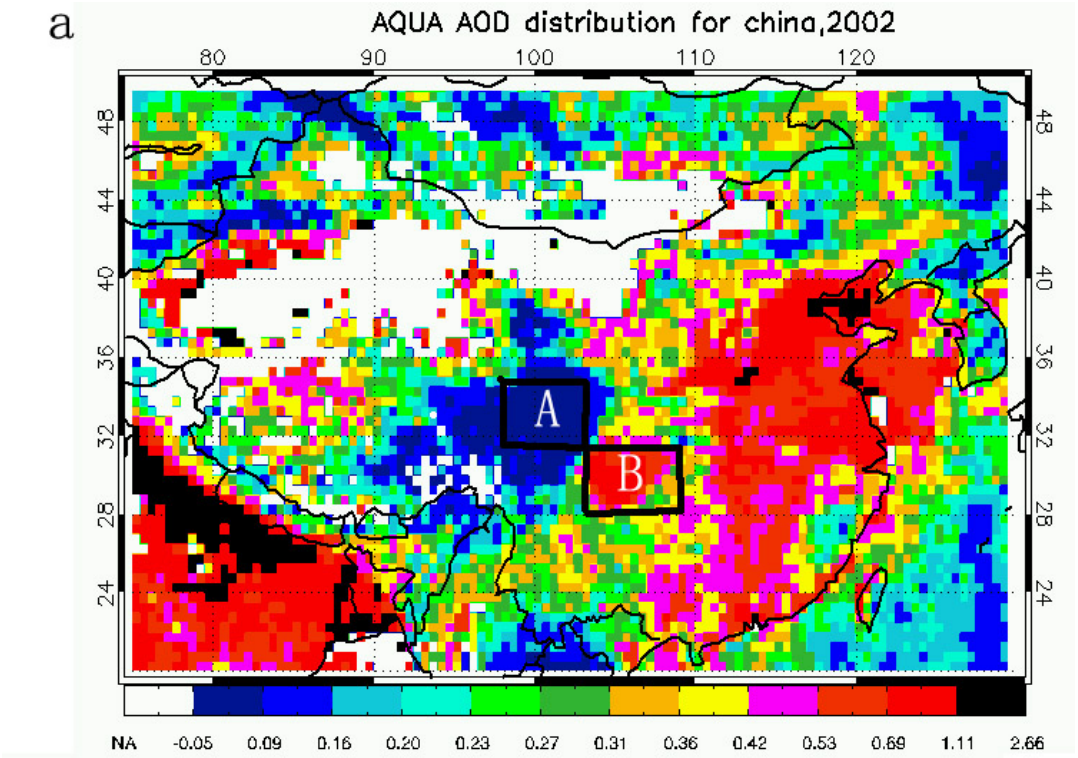

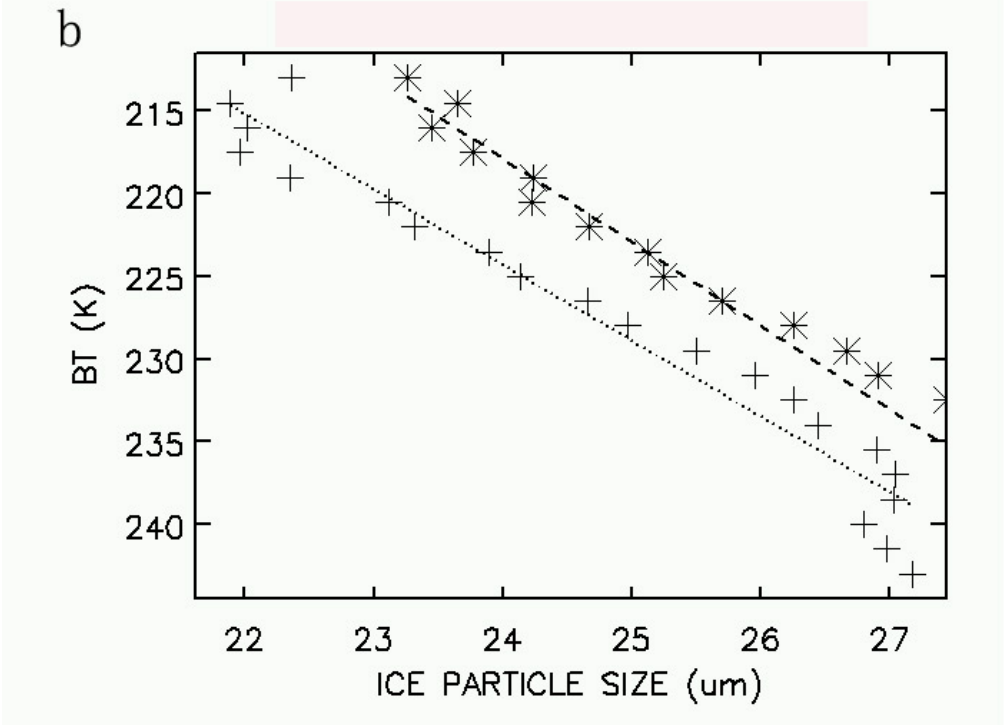

Figure 13: a) Two areas are selected as indicated in AOD map over China in 2002; Area A is clean area and area B is polluted Sichuan Basin. b) CER-BT profiles for these two areas, dashed line for area A and dotted line for area B.

larger at any given cloud BT than over polluted area as shown in Fig 37b. In other words the extremely high level of aerosol loading may have overpowered the influence of environmental conditions, in this case the high elevation. The difference in CER between two areas is about 1 μm consistently at all levels. This case represents a scenario where an extreme contrast exists between two areas in aerosol loading that creates a dipole. These dipole areas can be found over South America, the Southern US, India and our analyses support aerosol effects for all these areas (not shown here). Also we note here that in this example there is a favorable configuration of topography where the clean area is over highland so that if CER of clouds developed there is consistently larger over the lowland, highly-polluted area it then strongly implies aerosol's dominant effects.

In previous two cases we demonstrated that anthropogenic aerosols can reduce ice particle sizes. We argue that the underlying process responsible for this size reduction is delayed coalescence and prolonged condensational growth. Natural aerosols are the other component of our total aerosol loading and they include smoke and dust. We will discuss dust effects on DCCs in next section. Smoke is found to reduce cloud particle sizes and as a result they may change precipitation characteristics of these cloud systems over Amazon region and other places [Andreae et al., 2004; Rosenfeld, 1999; and references therein]. However, these studies are based on a few cases using either in-situ or remote sensing data, usually with extreme conditions. Here we want to assess on a seasonal time scale how statistics of

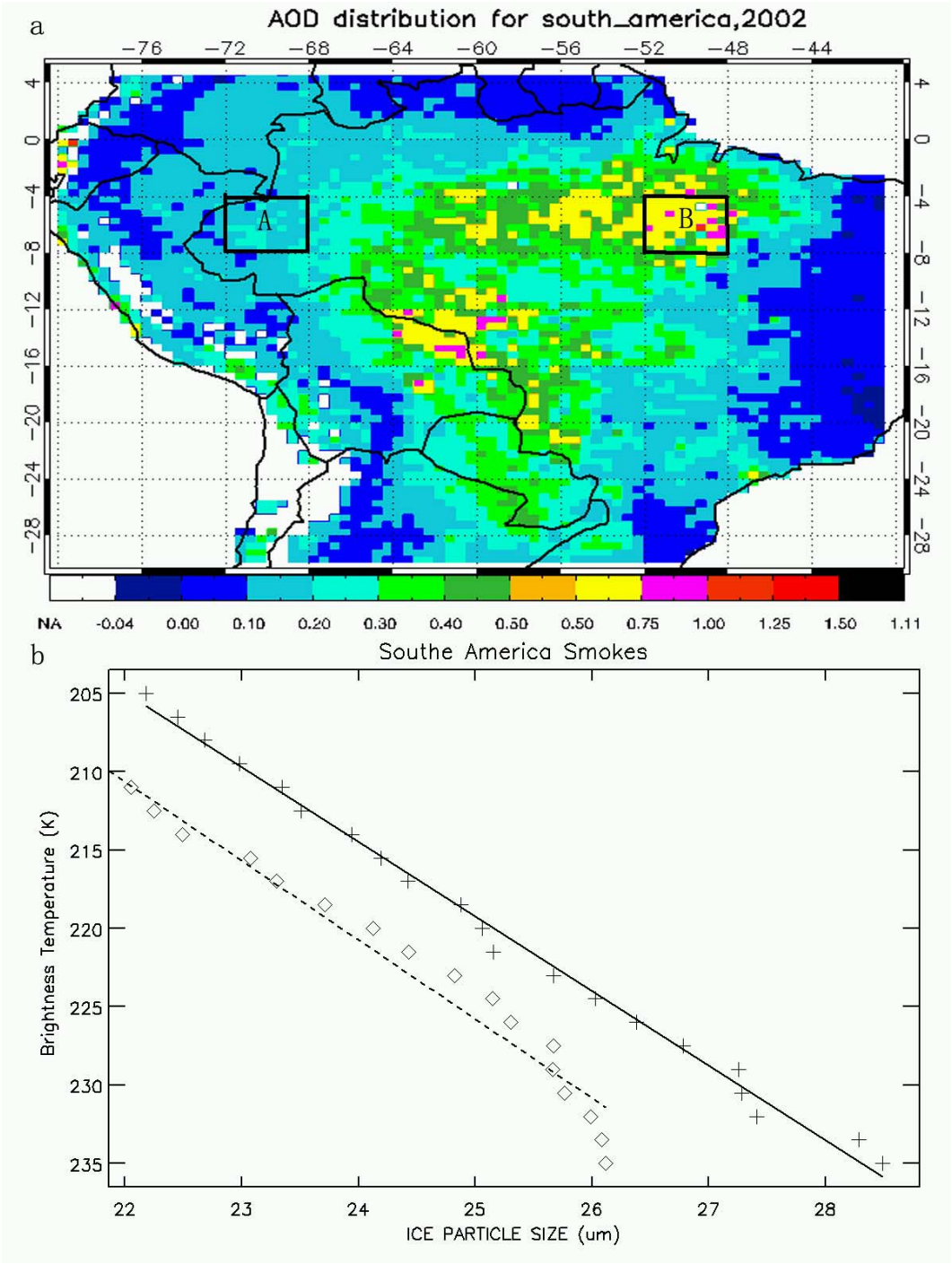

Figure 38: a) AOD map over South America in 2002; Two areas are selected as A and B with distinct aerosol loadings; b) CER-BT profiles for the two areas, solid line is for area A and dashed line is for area B.

cloud ice particle sizes responds to smoke aerosols. Our focus region is South America where solid in-situ evidence has been presented in support of smoke's effect on cloud microphysics. Our clean area is located at the western Amazon where AOD map, Fig 38a, reads mostly between 0.1 and 0.2. This area has a low, flat topography with elevation lower than 250m. The polluted area is selected over the eastern Amazon that also has a relative flat, low topography with elevation mostly under 250m. Aerosol loading is heavy for this area with mean AOD reaching as high as 1 and mostly over 0.6 due to manmade burning activities. DCCs formation is active for both areas providing enough sample size to carry out our analysis. The two CER profiles are shown in Fig 38b. Our ensemble data show significant impact of smokes on mean cloud microphysical properties. The clouds over polluted areas have consistently smaller ice particle sizes at all levels with a difference of about 1 μm. This agrees qualitatively well with result of the case studies from in-situ case studies. The same effect of smokes on DCCs is also noted over Africa, another major smoke source region. This reduction effect of smoke aerosols is likely due to the same underlying process responsible for pollution aerosols' impact on DCC microphysics.

iv) Homogeneous Freezing and Aerosol Invigoration Effect

Cloud droplets can remain in the liquid phase at temperature colder than 0 °C and they do not freeze till temperature drops to as cold as -37.5 °C

in deep convective clouds for some cases [Rosenfeld, 2000]. These 'supercooled' droplets are thought to be due to their small sizes and lack of ice nuclei. They only freeze at extreme cold temperature by homogeneous freezing, which does not require any ice nuclei. Once homogeneous freezing takes effect numerous small droplets may freeze, which shall reduce ice effective radius. At levels below homogeneous freezing the mixed phase cloud parcels keep rising and thus cloud droplets/ice particles keep growing. As a result the homogeneous freezing level shall leave a signature on the CER-BT profile as a turning point, where the dependence of cloud particle size on cloud height switches sign from increasing with height to decreasing with height as shown in the conceptual model. In Fig 39 we present CER-BT profiles for four individual storms. A kink is noted in the profile where CER stops increasing with decreasing BT and switches to the opposite, and the temperature of the kink is about 238K, -35°C. From our arguments homogeneous freezing level (HFL) for these storms may be close to this temperature. The homogeneous freezing level thus identified ranges from temperature higher than 243K (cutoff temperature in selecting our data) to as low as 235K in our case studies. We also note a strong contrast between maritime storms and continental ones in the level of homogeneous freezing level. Maritime DCCs generally have lower HFL than continental ones do. This is because maritime clouds droplets grow faster [Levin et al., 2005] and larger cloud droplets can freeze at warmer temperature compared to smaller

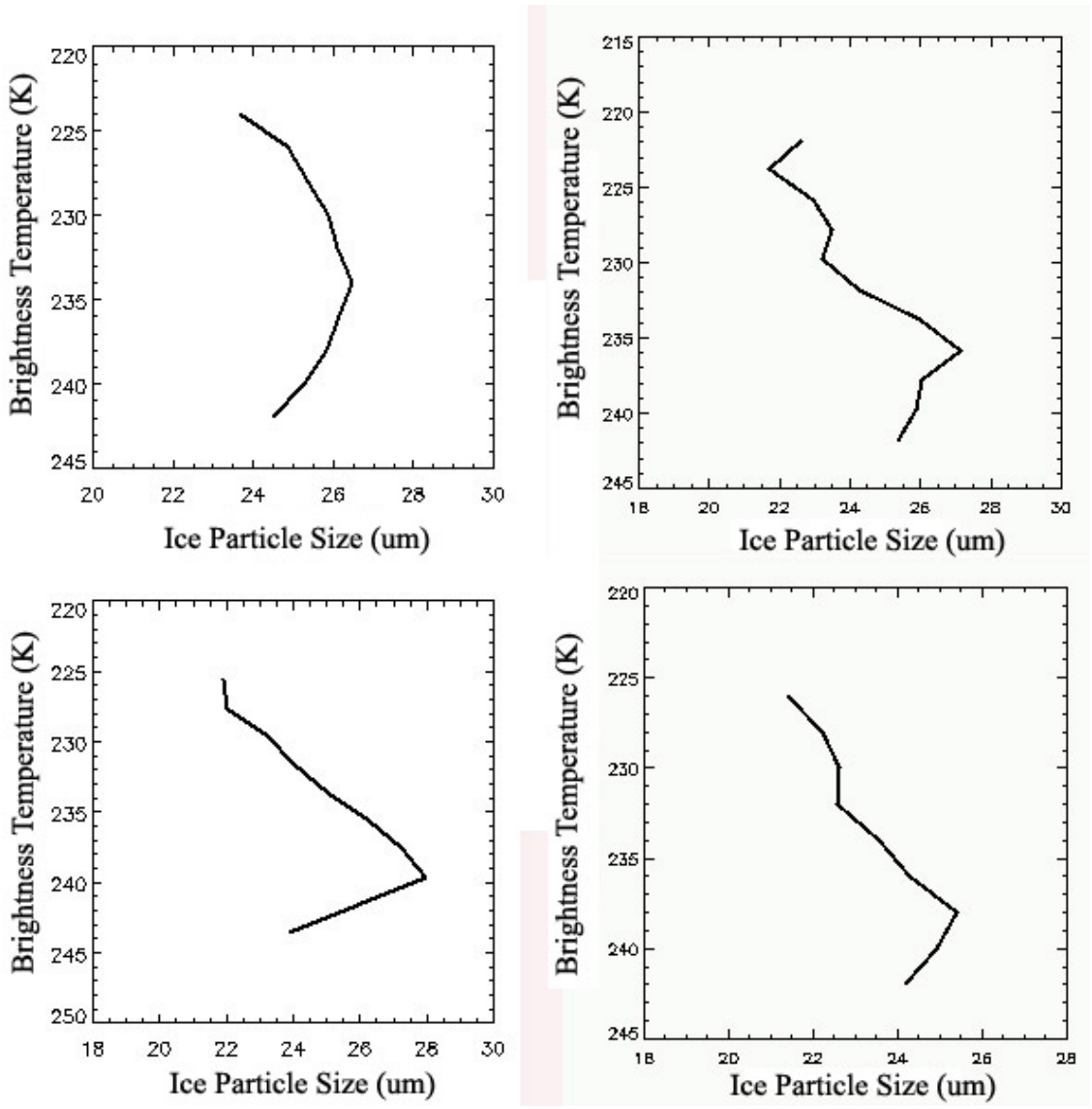

Figure 39: Four examples of CER-BT profiles for individual continental storms. The kink temperature in these profiles falls between 235K and 240K.

ones, which at least partly explains the land-sea contrast in ice particle sizes that are observed.

It has been postulated that injecting numerous aerosols into DCCs may severely suppress cloud droplet size growth and delay the freezing process [Andreae et al., 2004]. We have demonstrated previously that biomass burning and anthropogenic aerosols can reduce cloud particle sizes. It is argued that reduced cloud particle sizes and prolonged condensational growth is unfavorable for the coalescence process and therefore delays the creation of large drops/ice particles that can precipitate out. The delay in turn decreases the downward drag applied by large droplets/ice particles that have fall velocity faster than the updraft. The end result would be more cloud water mass is raised higher without precipitating out or freezing [Tao et al., 2007], and later at colder temperature the freezing process would invigorate cloud development by releasing large amount of latent heat. This chain of reactions of DCCs to increased level of aerosols can be investigated by numerical models where perfect control of environmental conditions is obtained [Tao et al., 2007 and references therein], but it is hard to find evidence in nature where no two DCCs are identical and thus prevent one from attributing observed changes in cloud height to aerosols in a decisive fashion [Koren et al., 2005]. We circumvent this problem by again utilizing the ample statistics. In Fig 40 we compare two CER-BT profiles that are based on data from the two areas we select in Amazon, one polluted and one clean, but with extended range of BT up to 243K. We note there is a kink in the mean CER-BT profile

similar to that of individual cases. From our arguments this is the mean level of homogeneous freezing for that area. The mean homogeneous freezing level for the polluted area is several degrees colder than that of the clean area. This result strongly suggests that aerosols increase the height of HFL, which is at least in part due to aerosols' ability to reduce ice particle size as demonstrated previously, and according to our chain of reactions it would more than likely invigorate cloud development.

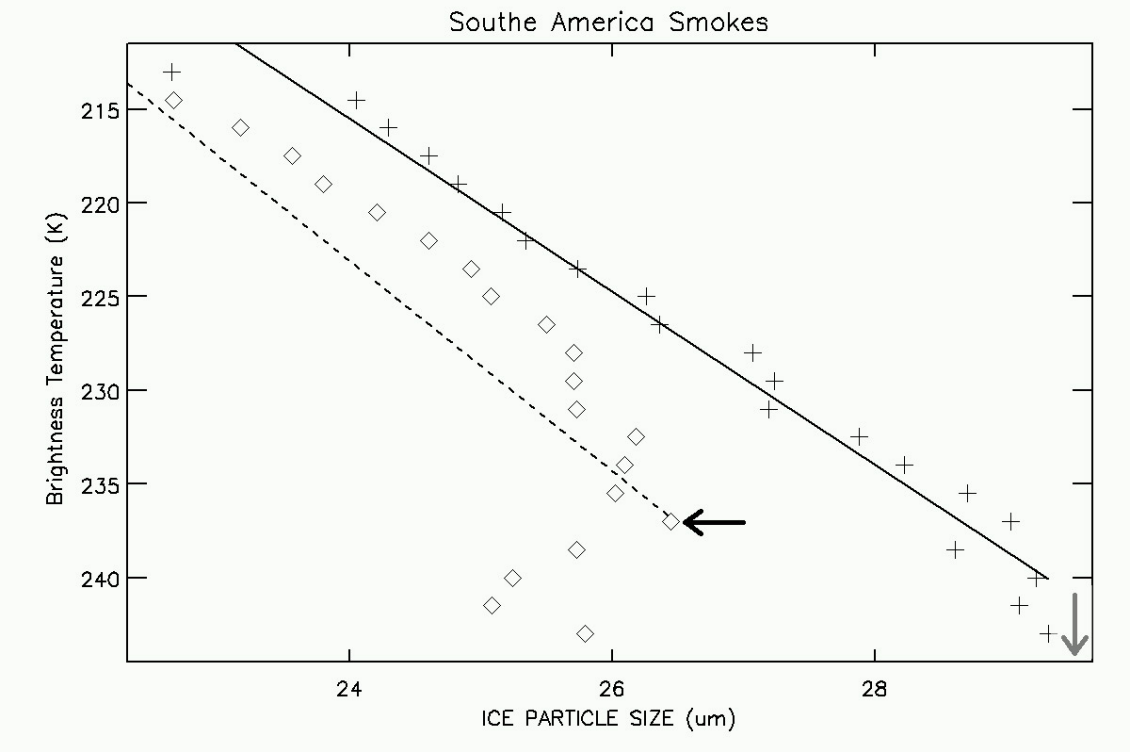

Figure 40: CER-BT profiles for the same two areas in Fig 14. The arrows in the plot indicate where freezing level is. Freezing level for polluted area (diamonds) is around 237K while that for clean area (plus sings) is warmer than 243K, our data limit.

3.4.3 Interaction between Dust and DCCs

Dust particles are another important source of aerosols in addition to anthropogenic aerosols and biomass burning smokes. Dust particles are largely considered to be in the coarse mode meaning their sizes are usually larger and significant amount of their mass falls in the supermicron range [Dubovik et al., 2002]. Because of physical and chemical properties of dust particles we now know that they can act both as CCN and/or giant CCN, and IN. For example, a study by *Levin et al.* [1996] shows that dust activate as giant CCN when they are coated with hydrophilic materials. It is also confirmed that relatively pure mineral dust particles are effective heterogeneous IN by both laboratory studies [Knopf et al., 2006 and references therein] and in-situ measurements [DeMott et al., 2003 and references therein]. Because of dust's dual roles their indirect effect on cloud properties and precipitation characteristics is regarded as uncertain. Modeling studies have shown that dust particles coated with air pollutants acting as giant CCNs can enhance the coalescence process and increase precipitation [Levin, et al., 1996; Yin, et al., 2000], while others show just the opposite, that is, dust particles are likely to decrease the cloud droplet size and suppress rainfall, e.g. *Rosenfeld et al.* [2001]. A study by *Fridlind* et al. [2004] show that unless long distance transported mid-troposphere dust particles are activated as INs their cloud resolving model could not reproduce the observed size distribution of anvil clouds [Heymsfield et al., 2005]. Consideration of dust's role both as giant CCNs and INs by a model study is shown to enhance graupel sizes [Levin et al., 2005], which seems to be backed up by another modeling study that also considers dust's dual role as giant CCN and IN [van den Heever et al., 2006].

To reconcile these seemingly controversial findings we focus our analysis on an area encompassing northern India and southern Pakistan to study the interaction between dust and DCC. It is necessary to make sure that dust particles are both abundant for this region and indeed interacting with DCCs. There are two major dust sources for this area, the local Thar Desert and the distant Arabian Peninsula. Both can be clearly seen from OMI AI data as shown in Fig 41. We also analyze AERONET data from a few stations that are located close to this region in 2006. Only the station at Kanpur, 26N and 80E, in Northern India have significant amount of data. Our analysis suggests that during the summer aerosol Angstrom exponent is very low and a significant number of aerosols have effective radius larger than 1μm for this area. Both of these two characteristics strongly indicate the presence of dust aerosols, which is also confirmed by studies using in-situ measurements [Jayaraman et al., 2006]. These lines of evidence give us confidence on the existence of dust particles. It is further supported by the CALISO images, e.g. Fig 42. Fig 42a shows a polarization image where a layer of aerosols with strong depolarization signal is noted in the center of the image. The strong depolarization suggests that aerosols are of irregular shapes and for this region dust are the most likely and maybe the only irregularly shaped aerosol type. Examination of the images in the lower panels that are images of attenuated backscattering intensities at the two wavelengths, 532nm and 1064nm, suggests that this aerosol layer has low angstrom exponent, another indication for existence of dust. The backscattering signal is completely attenuated by

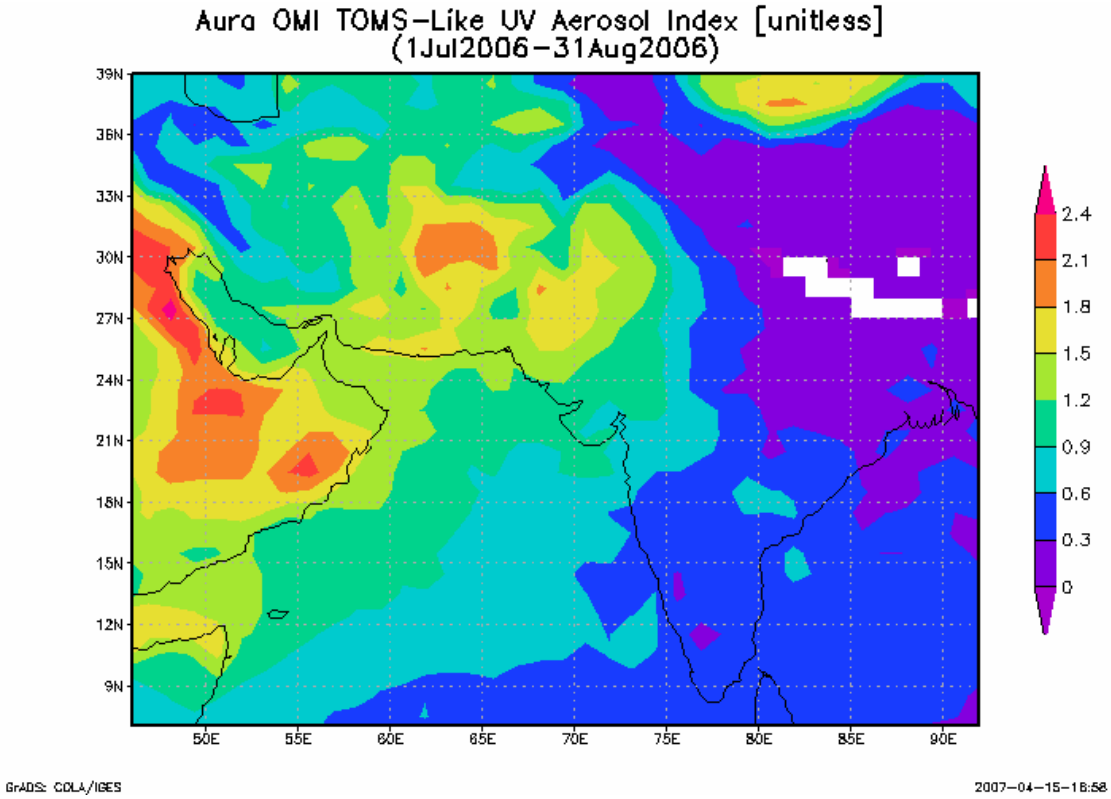

Figure 41: Aura OMI observed Aerosol Index averaged for summer season in 2006 over Indian Subcontinent and Arabian Sea.

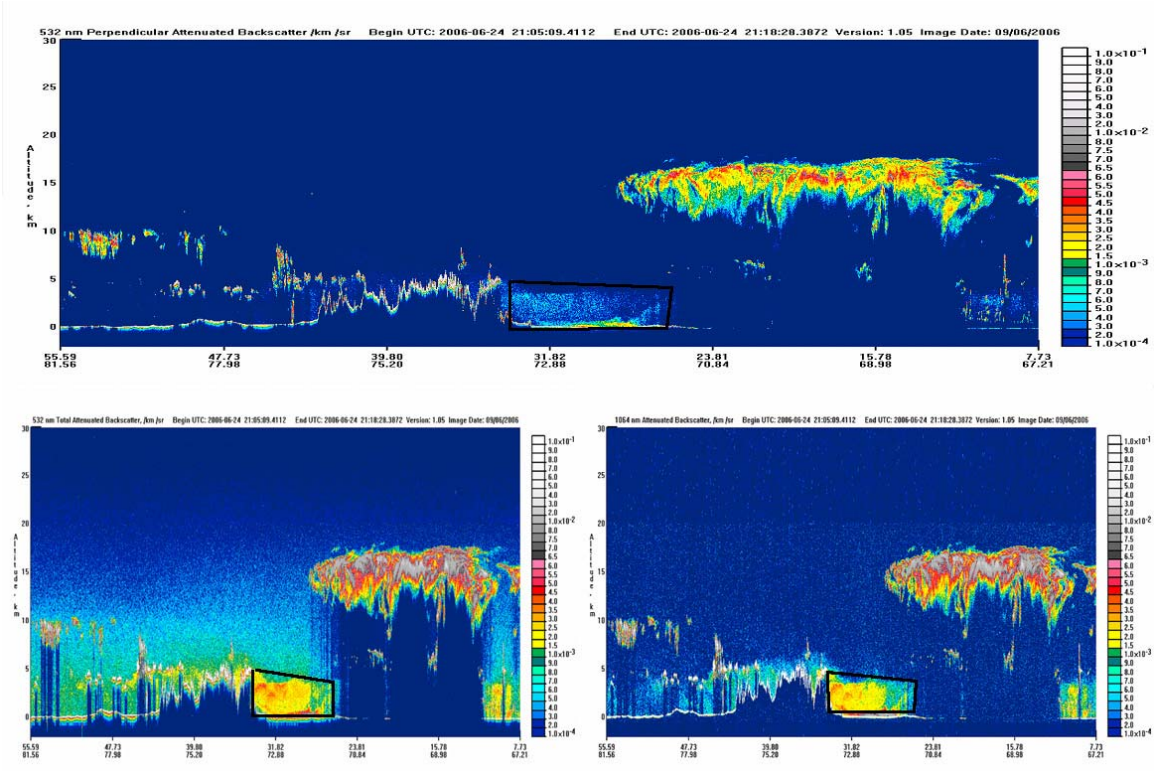

Figure 42: CALIPSO images of a dust-DCC interaction case. The boxes are showing a thick dust layer nearby a storm. Upper panel is an image of depolarization ratio; lower left is an image of 532nm attenuated backscatter; lower right is an image of 1063nm attenuated backscatter. CALIPSO locations are indicated in the x-axis and they go from north to south (left to right in the image).

the cloud system just to the right (south) of the dust layer. This system is confirmed to be a DCC system as suggested by near simultaneous image from CloudSat and MODIS images. We infer that the dust layer is very likely interacting with the DCC system to its right from Fig 42.

We argue that one major point of concern for previous studies of dust-cloud interaction is the neglect of consideration of air mass characteristics. Major global dust sources are all large deserts over which air is extremely dry and thus dust storms are usually imbedded within dry air mass. When the dry air mass meets moist air dust may interact with clouds if they are at the right altitude. However, at the same time the dry air accompanying dust will also mix with moist air and more than likely to alter the properties of clouds. It is hard to dissect the effect of potential dust on cloud microphysics from the effect of air mixing on cloud macro and micro properties since these two effects are entangled with each other. The entanglement potential is especially large for fresh dust storms that interact with cloud systems because their air mass characteristics remain intact and dry, while for aged dust plumes the problem can be alleviated as they may have undergone enough mixing with the new environment already. We select the Thar Desert area to remove this entanglement because of its relatively small size and the overwhelming moist transport of the summer monsoon as indicated in Fig 43 where a map of total column water vapor is drawn from AIRS data averaged for the monsoon period over the India subcontinent. Clearly the air mass over desert area is under dominant influence of monsoonal flow

and is as moist as the surrounding area. Similar data set from MODIS water vapor product suggests the same thing.

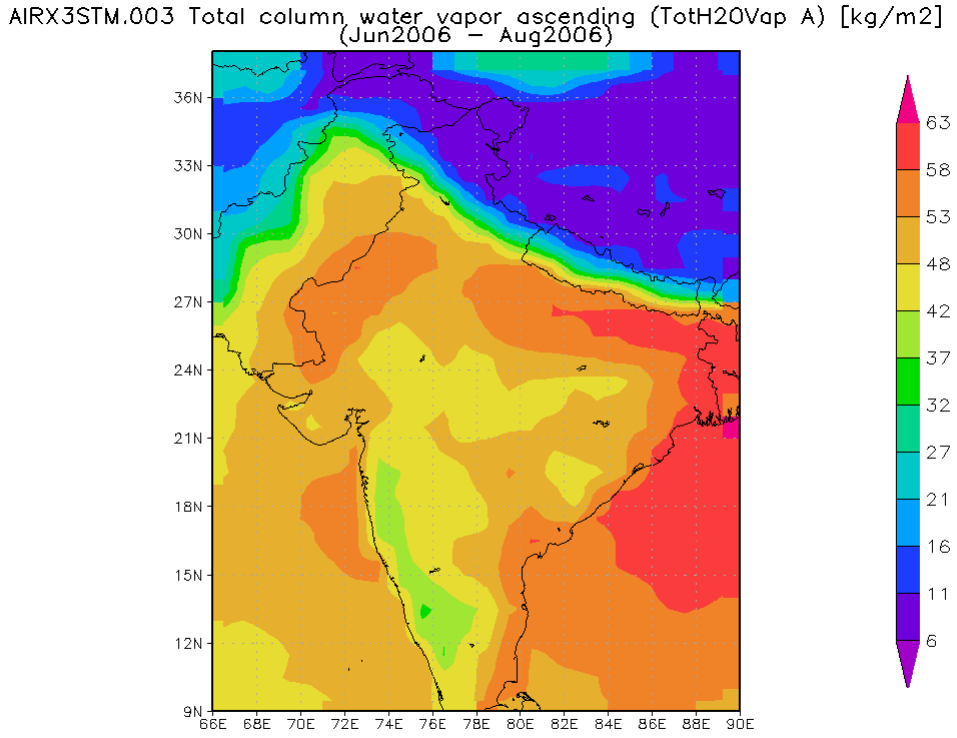

Figure 43: Precipitable water distribution averaged during the summer 2006 over Indian Monsoon Region. The Thar Desert is located in the orange patch at the India-Pakistan boarder.

Our hypothesis is that local dust particles can be active as large-sized heterogeneous INs that freeze droplets at warmer temperature, which help increase ice particle size by accretion processes like riming and limit homogeneous freezing by depletion of water vapor. To test this hypothesis we select two areas, one within the influence of local dust from the Thar Desert and one without influence of local dust, as indicated in Fig 44. We select the area close to local source to make sure dust particles are relatively pure and thus are good INs. Otherwise, once dust is coated with hydrophilic compositions like sulfate or nitrate they may act as giant CCN, which will be discussed later. The area with no influence from local dust source may still be affected by dust transported from sources at the Arabian Peninsula as suggested by the AI map (not shown), but we know from past studies that long range transported dust particles may actually decrease ice particle sizes by acting as IN at the mid-troposphere level [Fridlind et al., 2004]. These two areas are within the same branch of the Indian Monsoon and have similar atmospheric conditions. Their elevations are also similarly flat and low, less than 250m. Fig 44 shows two CER-BT profiles for these two areas. The ice particle sizes for dust laden area are consistently larger than those for the other area for about 2 μm, which agrees with our hypothesis. In addition to the larger ice particle sizes we note a warmer homogeneous freezing level for the dust laden area, which is also in line with our proposed hypothesis since heterogeneous freezing takes place at warmer temperature. This early freezing resulting from dust acting as heterogeneous IN can also be noted for areas close to the Takalamakan Desert in western China compared to other areas of China. An example

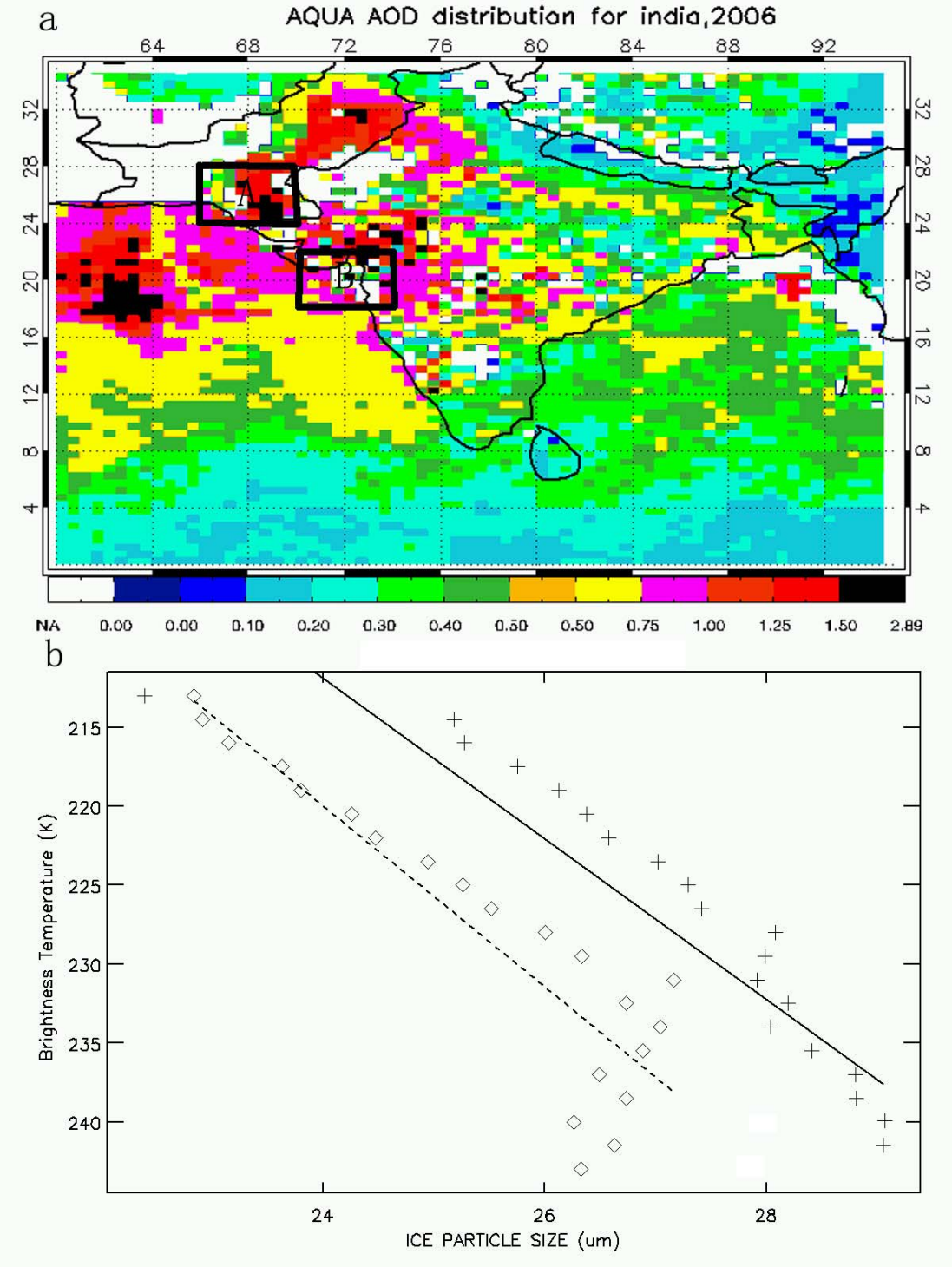

Figure 44: a) AOD map of Indian Monsoon region; two areas are selected, A within influence of local dust and B without local dust b) CER-BT profiles showing solid line for area A and dashed line for area B.

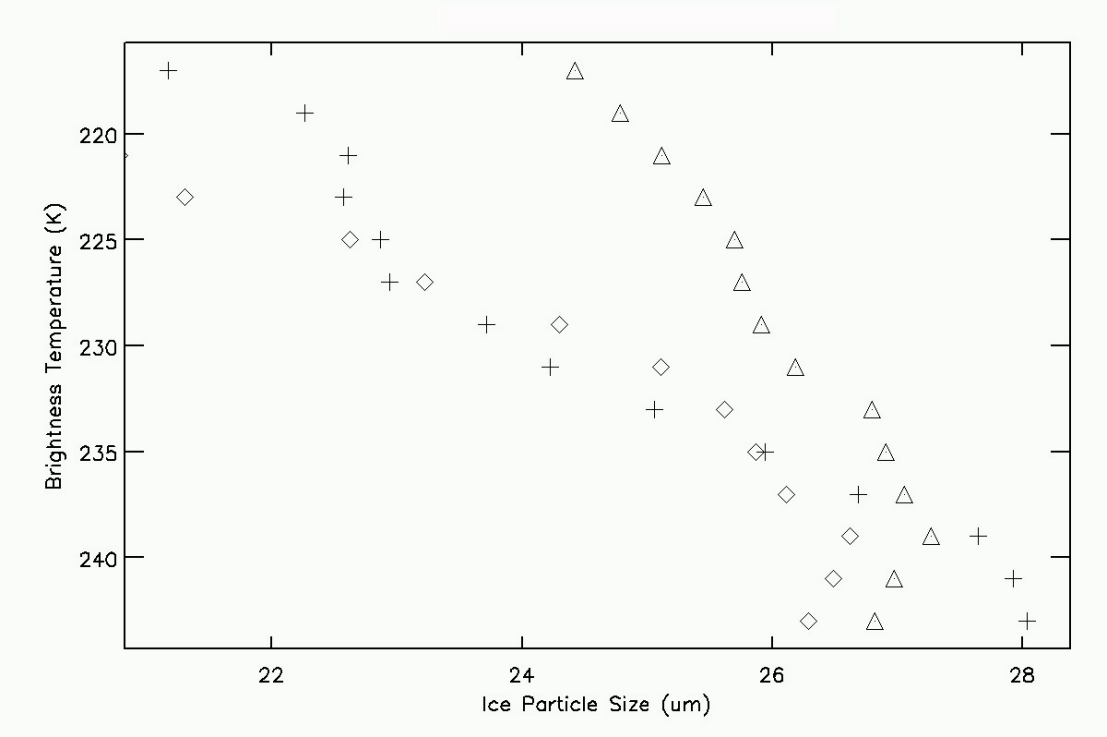

Figure 45: Three regions are selected over China in 2006. The diamonds and the triangular represent two non-dust laden areas and the plus signs represent local dust laden area.

is shown in Fig 45 where three profiles are shown. The local dust laden profile does not indicate freezing warmer than 243K while the other two areas show freezing level colder than 240K. The two dust free areas include one over northern China that is located at the same latitude as the dust laden area and the other over southern China. The dependence of CER on BT systematically varies with latitude, which will be discussed in later section, and thus we note the huge difference in CER between profiles of high latitude areas and the low latitude area.

As aforementioned, dust can also act as giant CCNs to affect cloud microphysical and macro properties. We propose that coarse mode dust particles once coated with hydrophilic materials they are active giant CCNs. These giant CCNs foster droplet coalescence process and increase droplet sizes. Given that larger droplets are also more likely to freeze at a warmer temperature the net effect of giant CCNs is to transform otherwise continental clouds into more maritime ones. The area in the IGB region that is downwind of the Thar Desert is chosen to study this pathway of dust influencing DCCs. AERONET size distribution retrievals for this area suggest major presence of coarse mode dust particles in the summer monsoon season, which is also noted by in-situ measurements [Jayaraman et al., 2006]. The area is also heavily loaded with anthropogenic aerosols. Dust coated with these hydrophilic aerosols is an easily conceivable scenario for this area and thus it is an excellent choice for our purpose. An example is given in Fig 46 where we select one dust laden area downwind of the Thar Desert in the IGB region and the other dust free area over the open Indian Ocean under pristine, maritime conditions. Fig 21 shows that

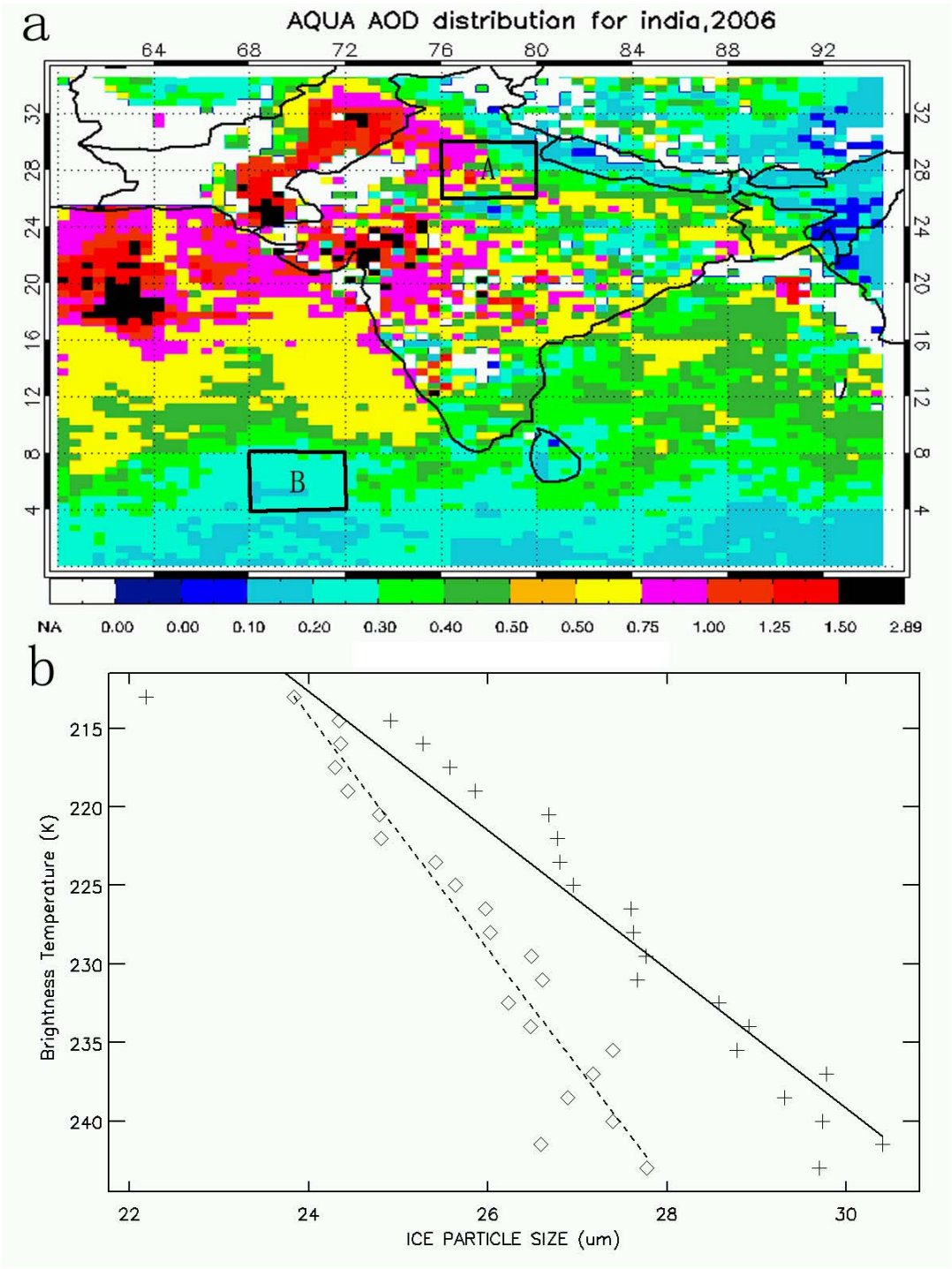

Figure 46: a) AOD map for Indian Monsoon region in summer 2006. A is an area affected by local dust source and B is an area over pristine Indian Ocean; b) CER-BT profiles for these two areas, with solid line for area A and dashed line for area B.

although the profile for dust laden area has a steeper slope CER at any given cloud height is generally larger than that of the profile for dust free, maritime area. Neither profile suggests freezing colder than 243K, which means cloud droplets inside DCCs at both locations grow fast in a maritime fashion. Considering the heavy pollution level of dust laden area this can only be explained by dust's ability to act as giant CCNs and transform the cloud properties.

3.4.3 Latitudinal Dependence of CER-BT Slopes

We have mentioned in previous discussion of aerosol effects that the slopes of CER-BT profiles seem to depend upon latitude of the study region. This dependence is indeed systematically observed over the globe in our analysis. To avoid the turning point that is caused by phase change of cloud particles in our estimation of CER-BT profile slopes we construct the profile only using data whose BT is colder than 235K. At 235K (-38°C) most cloud droplets will freeze homogeneously based on previous studies [Rosenfeld and Woodley, 2000]. In Fig 47a we show a number of profiles constructed for different areas over the Indian Summer Monsoon and East Asian Summer Monsoon regions. Two clusters of profiles can be noticed, one with steeper slopes and the other with slopes distinctly flatter. The first cluster with steeper slopes, meaning slower decreasing rate of CER with cloud top height, is associated with lower latitude areas like the South China Sea, the Indian Ocean and the Pacific Warm Pool; the other cluster is associated with mid-latitude areas like central China and Yellow Sea. Further data restriction is applied to keep only those clouds with BT between 200 and 235 to have meaningful number of data points at each BT bin. Four

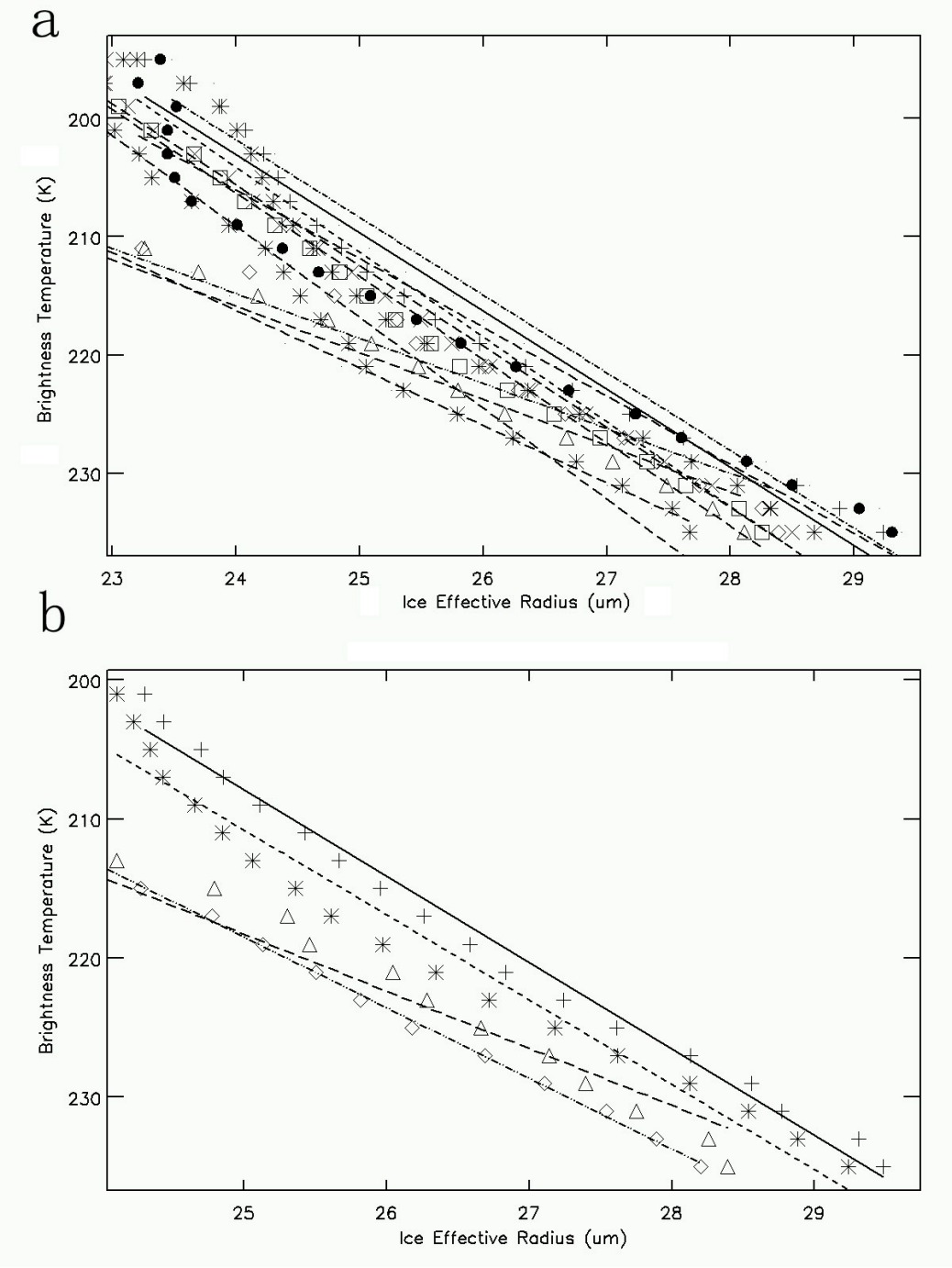

Figure 47: a) Several areas are selected over Indian and East Asian Monsoon regions. Two clusters for CER-BT profiles that have distinct slopes are noted. b) Four areas are selected over East Asian Monsoon region. Plus signs and stars are for two tropical areas: Pacific Warm Pool and South China Sea; and the rest two are for the Yellow Sea and Central China.

representing large areas are selected to quantitatively assess slope change. These four profiles are shown in Fig 47b. Tropical areas like the Pacific Warm Pool and the South China Sea have CER-BT slopes of around $6\,K\mu m^{-1}$ while mid-latitude areas like the Central China (mean latitude 29 N) and the Yellow Sea (mean latitude 33N) have slopes of 5 $K\mu m^{-1}$ and 4 $K\mu m^{-1}$.

This latitudinal dependence of CER-BT profile slope can be also observed over other part of globe. An example is given in Fig 48a where we select four areas sequentially with lower latitude, eastern US (mean latitude 28N), the Gulf Coast (mean latitude 24N), the ITCZ (mean latitude 8N) region near the equator and the tropical Amazon (mean latitude 8S). The slopes changes from around 4.8 $K\mu m^{-1}$ and 4.4 $K\mu m^{-1}$ for two tropical areas to 4.3 and 4.1 $K\mu m^{-1}$ for two mid-latitude areas. We note that after BT becomes colder than about 208K profiles of the two mid-latitude areas reverse their trends. We argue that this trend reversing may be caused by overshooting of convective cores associated with strong continental convections. These overshooting cores carry with themselves strong momentum that can lift larger ice particles. In addition the convective cores are relatively less prone to entrainment mixing that is extremely important for ice particle size at such cold temperatures. These arguments are in line with previous studies that show generally higher reach of convective cores for the mid-latitude continental DCCs than tropical maritime DCCs [Zipser et al., 2006; Liu et al., 2007]. Furthermore, the occurrence of these points is very low, only accounting for less than 0.5% of the total data that have BT colder than 235K. Therefore we want to remove the influence of reversing trend on our calculation of slopes. Data points that have BT colder than 210K are excluded for our

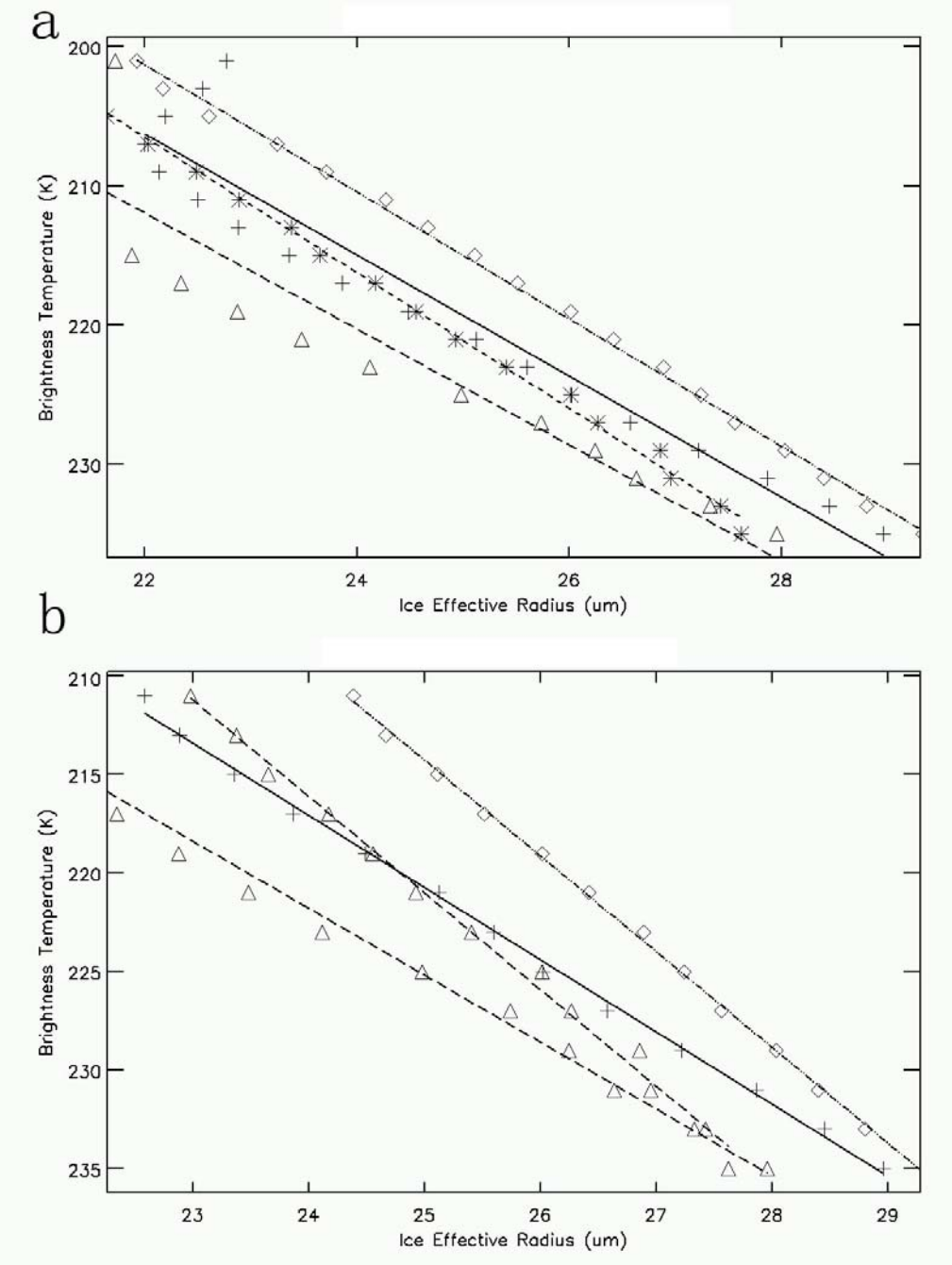

Figure 48: Four areas are selected over the Americas: Eastern US (pluses), Gulf Coast (stars), the ITCZ (diamonds), and Amazon (triangles). a) CER-BT profiles including temperature colder than 210K where CER starts to increase with decreasing BT for some areas. b) Profiles including only temperature between 235K and 210K.

purpose and profiles are reconstructed. The operation creates stronger contrast between slopes of low and mid latitudes areas. Slopes of low latitude areas are changed close to 5 $K\mu m^{-1}$ and those of mid-latitude areas are 3.7 K/μm and 3.4 $K\mu m^{-1}$, Fig 48b. Slope magnitudes for this part of the world are comparatively flatter than those of Asian region although the general decreasing trend of slope with latitude holds at both regions.

The slope of CER-BT may be affected by many processes and conditions like entrainment mixing, high level aerosol source, updraft velocity and ice crystal habits [Heymsfield et al., 2005]. Our data contain no relevant information to these processes and thus do not permit further investigation on these probable causes. We attempt to explain part of variation based on a simple thermodynamic consideration of a parcel experiencing adiabatic ascent whose water vapor is saturated with respect to ice. We use the quantity $\Gamma_i = -\frac{dw_s}{dz}$ that is negative vertical gradient of the saturation mixing ratio, w_s and thus is the vertical gradient of ice water mixing ratio since we assume an ice phase parcel. The saturation mixing ratio can be calculated from $w_s = \varepsilon e_{si}/(p - e_{si})$, where p is the air pressure, e_{si} is the saturation vapor pressure as calculated from Clausius-Clapeyron equation and ε=0.622. With similar steps in *Albrecht et al.* [1990] we can derive $\Gamma_i = \frac{(\varepsilon + w_s)w_s l_i}{R_d T^2}\Gamma_{si} - \frac{g w_s p}{(p - e_{si})R_d T}$ where l_i is the latent heat of sublimation, Γ_{si} is the lapse rate if an air parcel undergoes a moist adiabatic with respect to ice, R_d is the specific gas constant for dry air and T is temperature. Fig 49 shows Γ_i as a function of temperature and pressure of the

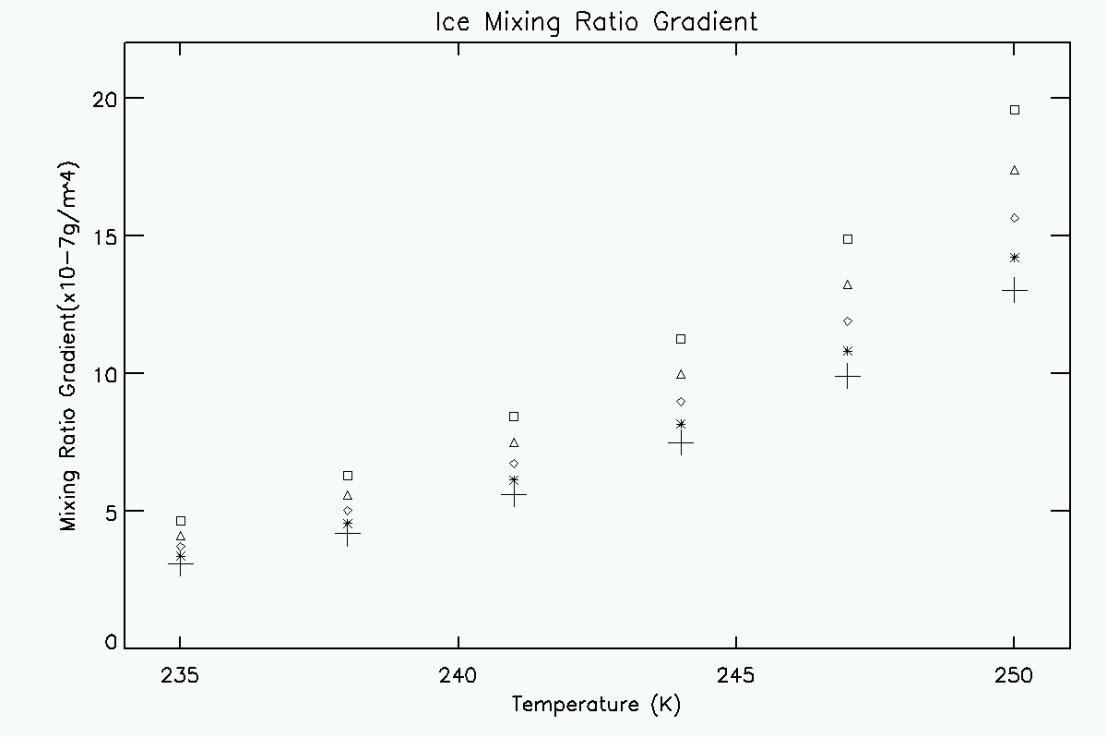

Figure 49: Ice mixing ratio gradient as function of air parcel starting temperature and pressure. Different symbols represent different pressures.

parcel starting level. Γ_i positively depends upon the temperature at which air parcel starts to ascend. It increases from about 5x10-7 gm^{-4} to about 2x10-6 gm^{-4} with temperature increasing from 235K, the cold end of freezing level, to 250K. Γ_i also has a strong positive dependence on the initial air parcel pressure. An increase of 100hPa from 200hPa to 300hPa at temperature 250K is accompanied by an increase in Γ_i from about 1.3x10-6 gm^{-4} to nearly 2x10-6 gm^{-4}.

Given the general north-south increase in temperature and moisture we argue that cloud base is generally lower in both temperature and pressure for low latitude areas. This is confirmed by our estimate of lifting condensation level from ECWMF reanalysis data. Also because of geographical distribution of land and ocean most of the tropical areas with active DCCs are in maritime conditions. Maritime conditions are favorable for early droplet freezing as mentioned before. The early freezing means higher freezing temperature and pressure and therefore larger Γ_i. It can be reasoned that with other conditions and processes being equal the decreasing rate of CER with height is slower for parcels with larger Γ_i, which means higher slope of CER-BT profile. In addition, early freezing creates ice particles that limit homogeneous freezing by consumption of water vapor by deposition growth and possibly at the cost of small droplets [Heymsfield et al., 2005], which further favors slower decreasing rate of CER with height since numerous small droplets may be evaporated due to lower supersaturation required for larger ice particles and/or accreted by ice particles.

Essentially, our explanation hinges upon the variations of ice water content (IWC) for DCC tops and IWC has systematic latitudinal dependence based on our arguments. A few in-situ measurements reported qualitatively same relationship between IWC and CER-T (Heymsfield and Platt, 1984). In fact, parameterizations based on these in-situ measurements indicate the same relationship between IWC and CER-T (Wyser, 1998). Further investigations are needed to verify or disprove our explanation.

This explanation of slope variation does not seem to apply for conditions over highland areas. For example, examinations of clouds developed over the Rocky Mountains and the Tibet Plateau reveal that slopes for these two areas are more close to maritime conditions. Clearly, other factors need to be taken into account to fully understand the slope variations of CER-BT profiles.

3.5Discussion and Implications

Our analysis on general cloud properties illustrates that seasonally and spatially averaged COD distributions for mature clouds have signature shapes for individual DCC active regions. We may directly compare distributions of cloud optical properties from models with bulk parameterizations of deep convective clouds with our observations to find agreements/disagreements. This serves a reality check for these models and could potentially help to point out directions for future parameterization efforts. The stable statistics for specific regions suggests that organization of cloud ensembles of specific regions may be governed by certain kind

of ‘statistical mechanics of clouds’. Ensemble simulations by cloud resolving models with representative input settings for a region can generate ensemble distributions of cloud properties. These simulated ensemble distributions can be analyzed to evaluate cloud resolving model’s ability to capture the statistical aspect of cloud organization. The so-called super-parameterization for global circulation models (GCMs) embeds a cloud resolving model in each GCM grid utilizing the sounding and other environmental conditions that the GCM provides [Grabowski, 2001; Khairoutdinov and Randall, 2001]. Statistics of cloud properties from simulations of GCMs with super-parameterization could be used to evaluate our observation. In addition, significant geographical variations of statistical properties of DCC observed in our study is useful to investigate the performance of ensemble simulations of the cloud resolving model with different local climates.

Our observations of BT distributions suggest preferential detraining levels of DCC although significant variations exist both temporally and spatially. This characteristic of DCCs is in favor of a relatively stable LW forcing, at least by thick anvils and convective cores. At the same time we reason that SW forcing of the thickest component of DCC systems is also stable averaged over long time period and over large spatial area given the stable organization of DCC as indicated by COD distributions. Thus DCCs defined here shall exert a relatively fixed forcing on our study regions averaged over long time period and large area. These DCCs are only one component of the real deep convective cloud system, which also includes accompanying shallow to middle level cumuli, moderately thick to thin anvil clouds and associated cirrus clouds. Because DCC systems as a whole are almost radiatively

neutral we infer that other components of the DCC systems must also have statistically stable organizations in an ensemble sense to support the observed neutral DCC forcing. We therefore postulate that the DCC systems are made up of a hierarchy of components with each having stable statistics. Different components interact with each other through radiative and dynamical processes. The interaction among these components may be strongly associated with local environmental conditions as suggested by systematic geographical variations in signature distributions of the thickest part of DCC system. Detailed analysis on these other components of DCC system is needed to completely understand interactions among these components and their relation to general environmental conditions. Indeed, this has been done for two regions over the Pacific, East Pacific Warm Pool and West Pacific Warm Pool where systematic differences exist both for local climate conditions and for cloud statistics [Kubar et al., 2007].

Cirrus cloud formations are strongly affected by deep convective cloud systems either by direct detrainment of anvil clouds or are dynamically driven and radiatively maintained by convective core and anvil clouds, respectively [Garrett et al., 2004]. In fact nearly half of the cirrus clouds are connected to DCC systems as observed by satellite [Massie et al., 2002]. Cloud top microphysical properties are especially important in determining cirrus properties and more importantly its lifetime [Mace et al., 2006]. The depression in ice particle size we observe for highland areas has important implications for cirrus cloud characteristics and troposphere-stratosphere exchange. *Sherwood* (2002) demonstrated smaller ice particle size is favorable for troposphere-stratosphere water vapor transport and is vital to explain the

moistening of stratosphere in recent decades. The smaller ice particle size together with lower CTP and high frequency of DCCs over the Tibet Plateau and the Rocky Mountains strongly suggest that conditions over these highland regions are active in exchanging water mass between troposphere and stratosphere in the form of ice particles. In fact, it has been hypothesized that active and strong convection over Tibet Plateau may be one major route for transporting water vapor from troposphere to stratosphere [Fu et al., 2006] and our results certainly support their hypothesis. These conditions are also favorable for generating cirrus clouds off DCC anvils that can last longer given smaller ice particle sizes over the region. We may infer that special conditions associated with the high elevation areas in the summer are the nature's way of regulating cirrus cloud properties and modulating troposphere-stratosphere exchange.

We have also demonstrated that both anthropogenic aerosols like pollution and natural aerosols like smoke can strongly affect mean microphysical properties of a large ensemble of DCCs. Polluted clouds tend to have smaller ice particles and the reduction in size ranges from 1 μm to several μm (not shown here). Smokes have similar ability of reducing cloud top ice particle sizes and part of the smokes over Amazon in the rainy season is man-made. A difference of 1μm is significantly large to affecting cloud processes like cirrus cloud formation and its lifetime [Mace et al., 2006], and troposphere-stratosphere moisture exchange [Sherwood, 2002]. Not only can anthropogenic pollution and smoke modify DCC microphysical properties, but also they can alter the macro properties. We have demonstrated that increased level of pollution or smokes can increase significantly the freezing height of DCC, which may

in turn re-invigorate the convection and help cloud grow higher. The invigoration effect of aerosols on clouds may increase the frequency of overshooting into the tropopause region. This is more effective in sending water mass and also aerosols into lower stratosphere because overshooting clouds directly reach the tropopause region. Extreme events have confirmed this possibility with direct observations of large amount of aerosols smoked out of overshooting clouds [Andreae et al., 2004; Rosenfeld et al., 2007 and references therein]. As a result we think humans may exert significant influence on high clouds and stratosphere-troposphere exchange through aerosol's impact on both DCC microphysics and macro properties. Its magnitude of impact needs to be assessed by taking this effect into consideration of GCMs. On the other hand, before further validating using in-situ observations results observed in our study contain some uncertainties due to retrieving methods and assumptions made on ice properties like ice habits etc.

Dust effects on cloud formation and precipitation have been debated between two schools of thoughts based on observational and modeling evidences. We show evidences from large statistics that local dust particles may increase ice particle sizes by acting as giant CCN or heterogeneous IN. We argue that a key step in investigating dust effects on cloud is to consider the effects of the dry air mass that dust particles reside. Otherwise, mixing effects resulting from dry air mass mixing with the moister cloudy air mass will be entangled with any dust effect on cloud microphysics. In addition, distinct differences in sizes of dust particles may exist between local dust particles and long distance transported ones. Long distance transported dust particles are usually smaller in size and likely stay at a higher level.

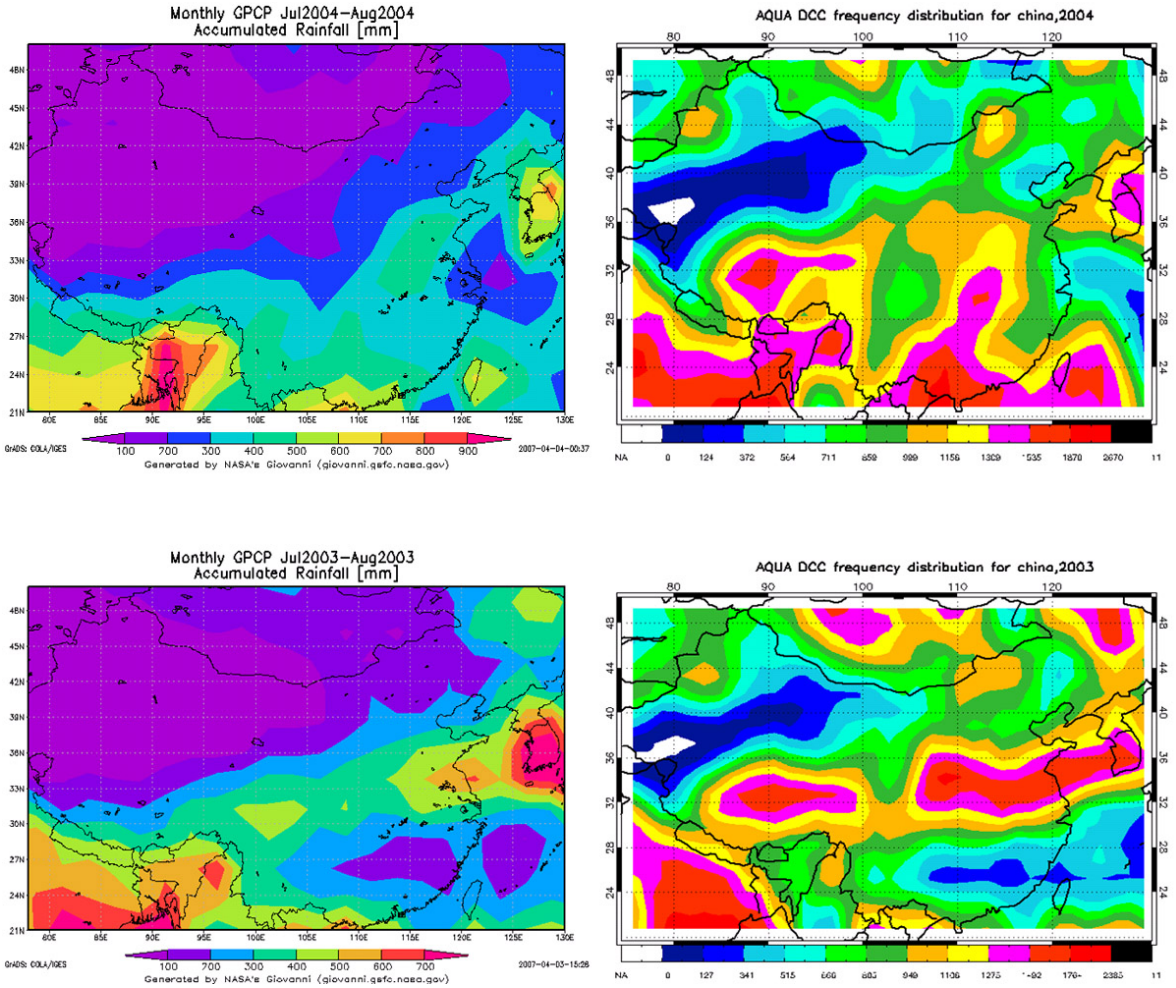

Figure 50: GPCP Precipitation and DCC occurring frequency patterns over China for 2003 and 2004; A good spatial correspondence between these two quantities is notable

The small and numerous dust particles can increase concentrations of CCN and middle troposphere level IN, which leads to reduction in cloud particles sizes and possibly precipitation. As such dust particle sizes also matter in determining their effects on clouds. Taking these two considerations, origin of air mass and dust sizes, many previous contradictory findings may be understood.

DCC are major source of precipitation for monsoon affected areas like India and East Asia in the summer. This connection is clearly noted in Fig 50 that shows patterns of precipitation and DCC occurring frequency from Aqua. Apart from the Tibet Plateau, the South China Sea and the Mongolian Plateau the precipitation pattern correlates extremely well with DCC frequency. Precipitation retrieval using IR satellite data is known to have difficulty over the South China Sea area and the lack of ground measurement and difficulty of retrieving precipitation over mountains by satellite data explain the low precipitation over the Tibet Plateau. The Mongolian plateau may also suffer from lack of data, but we note a combination of unusually high value of COD, low value of CER and high CTP for the Mongolian Plateau. This combination of cloud properties suggests high concentration of small droplets that is detrimental for precipitation formation, which may or may not be related to aerosols. However, suppression of convective precipitation has been reported by previous studies as a result of increase level of fine aerosol particles [Rosenfeld, 1999; Rosenfeld, 2000]. Results of our study show that anthropogenic pollutions and smokes reduce ice particles at the top and delays freezing in clouds. Both results may have important implications for precipitation formation.

The parameterization of high cloud properties is usually a fixed relationship between environmental temperature and ice water content, and ice particle size. Our observations however suggest a different picture of the relationship between temperature and ice particle size. The relationship between BT and CER constructed based on our data show systematic geographical variations. The variation over relatively lowland areas and ocean can be attributed to basic environmental conditions like relative humidity and temperature that determines cloud base and cloud microphysical processes like freezing level. There seems to be an association of intrinsic microphysical relationship for DCC systems with local climate conditions, which leads to the observed variation in BT-CER profiles because of local environmental condition changes. This argues against the fixed relationships used in current climate models. Aqua cloud retrievals are qualitatively validated by in-situ measurements [Gettelman et al., 2004] and therefore variations in BT-CER may contain significant information about the true relationship between these two quantities. It thus warrants further detailed in-situ measurements to validate our observations. If in-situ measurements agree with our results in this study changes in the model parameterization and efforts on understanding reasons behind these variations are needed. These changes have important consequences radiatively as shown by previous studies [Kristjansson, et al., 2000; van Zadelhoff et al., 2007]. In addition, in a scenario of global climate change the relationship is bound to change and may have important feedbacks to climate change itself.

3.6 Summary

We define deep convective clouds as clouds with cloud top brightness temperature no warmer than 243K and cloud optical depth no less than 40. This definition, combined with information from other retrievals, effectively filters out thick cold cirrus and includes mainly thick anvil clouds and convective cores. DCCs formed over the East Asian Monsoon region, the Indian Monsoon region, North America, South America and Africa, during summer time are analyzed. DCC occurrence frequency is strongly influenced by the large scale circulation pattern except for highland areas, where solar heating of land mass in the summer generates enough energy to form DCC frequently. Cloud top pressure shows a latitudinal dependence, decreasing towards lower latitude. No clear correlations are noted between patterns of cloud optical depth and crystal effective radius and those of DCC frequency or CTP. A universally observable relationship between cloud top BT and crystal effective radius is discovered from MODIS retrievals. CER is found to positively correlate with BT, which can be explained by size sorting and limitation of water vapor at temperatures colder than around 240K. We show extremely small CER values are associated with high elevation areas. We outline several factors that contribute to this association. COD distributions for individual regions suggest a stable structure of clouds in an ensemble sense, referred to as signature shape. We demonstrate that the signature shapes have systematic geographic variations, which imply structural variations in cloud organization because of difference in environmental conditions. A relatively narrow zone of detraining height is noted in

BT distributions, which qualitatively agrees with the fixed anvil temperature hypothesis, although we show that significant spatial and temporal variations exist.

Two traditional approaches to studying the aerosol influence on DCCs, time series correlation and spatial pattern correlation, are introduced and improved. We demonstrate that aerosol influences on DCCs using these two methods. At the same time, shortcomings and limitations of these two approaches are discussed. A new approach based on the physical relationship between BT and CER is proposed to study aerosol's influence on DCC statistical properties by investigating an ensemble of data. With proper control of environmental conditions we show for the first time that both anthropogenic pollutions and smokes can decrease CER significantly for a large set of samples, by 1 to 2 μm, at all cloud height. Local dust particles, on the other hand, are shown to increase CER by acting as giant CCN and/or heterogeneous IN. Homogeneous freezing level is identified based on CER-BT profiles. Systematic differences exist between maritime and continental DCC homogeneous freezing levels. For the first time we present direct evidence that supports the hypothesis that increased aerosol concentrations delay cloud droplet freezing. We propose a chain of reactions of cloud microphysics processes to the increased aerosol level and explain the delayed freezing. Slopes of CER-BT profiles are examined and shown to have systematic geographic variations. These slopes are shown to have strong latitudinal dependence, steeper in the tropics and flatter in the mid-latitudes. Only exception is found over highland area where CER-BT slopes are similar to those of the tropics. A simple thermodynamical model is used to explain the slope variation. Temperature

and humidity, and cloud freezing height, related to microphysics, are shown to be major factors that affect the slopes.

Important implications and applications of our results are discussed for studying DCCs and related studies on cirrus, troposphere-stratosphere mass and energy exchange, and precipitation.

Chapter 4: Summary and Future Work

4.1 Summary

Enhanced technology provides unprecedented information from space to study global changes with a truly global view. My study concentrates on using data mostly from NASA's suite of satellites to investigate interactions of aerosols and clouds, especially convective clouds including shallow cumulus and deep convective clouds on a global scale. Recognizing important limitation of Twomey's framework and different characteristics between cumuliform and stratiform clouds this study tries to answer a few unexplored questions.

In Chapter 2, high resolution remote sensing products on aerosol and cloud properties are utilized to formulate a new semi-collocated method to study interaction between fair weather cumuli and local aerosols. We find evidences of variability of aerosol indirect effect on these fair-weather cumuli. For the first time observations show both positive and negative AIE efficiencies, which means aerosols can either increase of decrease cloud top droplet sizes. Analyses show AIE efficiency depends positively on the remote sensed column integrated water vapor amount (PW), an important environmental condition. Quantitative analysis suggests that nearly 70% of variations in AIE efficiency can be explained by the variations in area averaged PW.

This finding could provide another pathway by which aerosol can affect small but ubiquitous clouds. Considerations of this effect in a GCM may alleviate the discrepancy between forward model and backward estimates for aerosol indirect forcing. However, we recognize the necessity of scrutinizing data employed in our

analysis given the uncertain nature of remotely sensed properties. A suite of scenarios in which artificial correlations between aerosol optical depth and cloud effective radius may form, are examined to investigate their respective role in affecting our finding. These scenarios including partially cloudy pixels, cloud 3-D radiation field, aerosol swelling, surface effect and dynamic effect are mostly shown to have limited influence on our observed relationships. In addition, the analysis done over other geographic locations for the same type of clouds further negates the possibility that an artifact correlation is fully responsible for our results while our results agree qualitatively well with past established studies concerning aerosol indirect effect at several locations.

We then explore physical mechanisms that can shed light on the observed results with a state-of-the-art cloud resolving model. One mechanism suggests that aerosol composition plays an important role in determining what portion of aerosols is active as CCNs and thus affects the relationship between aerosol number concentration and CCN concentration that ultimately influences cloud microphysics. The idealized model simulations demonstrate this mechanism is applicable if aerosols are coated with slightly soluble organic matters. Another mechanism involves giant CCNs that can accelerate cloud droplet coalescence growth process and this acceleration effect can out-weight the opposite effect of higher CCN concentrations, which is simulated with our model simulations. Both mechanisms are possible given the nature of aerosol composition in eastern US. With the model we also demonstrate that positive correlation between AOD and DER can only be simulated under moist conditions, qualitatively agreeing with our observational results.

Global analysis of AIE for both continental fair weather cumuli and maritime stratocumuli and trade cumuli indicates a systematic variation. This variation is postulated to depend upon aerosol type, cloud formation dynamics and other environmental conditions. Increased level of aerosol pollution seems to increase cloud average liquid water path for continental cumuli while on the other hand the opposite is true for maritime stratocumuli. This systematic perturbation to cloud development by aerosols calls for a systematic view/approach to study AIE on this cloud type as hypothesized in our introduction. This systematic view suggests that aerosols are not just passive participants of cloud development, meaning that they are essentially partitioning existing cloud water into different amount of cloud droplets, but also are actively involved in the cloud evolution process, meaning that they can also influence the total amount of water a cloud can develop through interactions between aerosol induced microphysics change and cloud dynamic development.

In Chapter 3, deep convective cloud properties and their interaction with aerosols are investigated extensively. Cloud top ice particle sizes are shown to be tightly correlated with cloud vertical reach based on a large ensemble of simultaneous observation of DCCs for the first time. DCC top ice particle sizes also depend systematically on topography and the underlying mechanisms are explored. Brightness temperature statistics of a large ensemble of DCCs suggest significant geographic variations and may provide evidence for the fixed anvil temperature hypothesis. Signature cloud optical depth distributions are found for individual active DCC forming areas. Statistics of these signature distributions are almost time invariant for a fixed location, but change significantly from one place to another.

Differences between signature distributions are thought to be due to different large scale environmental conditions and each distribution provides implications for DCC structures.

Shortcomings of past methods investigating AIE on DCCs are discussed. A new methodology is proposed based on a physical conceptual model of cloud hydrometeor evolution. Using this methodology anthropogenic pollution and smoke aerosols are shown to decrease ice particle sizes because of delayed coalescence growth process and prolonged condensational growth. Major redistribution of latent heat in the vertical is resulted from this interaction between aerosols and clouds with more liquid water content frozen up at higher level and thus possibly providing further boost for cloud development. With CER-BT profiles we find evidence of higher freezing level as the result of aerosols' microphysical effects.

Slopes of CER-BT profiles are shown to have a clear latitudinal dependence. It is observed over the globe that CER-BT slopes are flatter in the Mid-latitude DCCs than those in the tropics, which suggests ice particle sizes decrease with height faster in the mid-latitudes. With a simple thermodynamic model we demonstrate that ice mixing ratio is positively correlated with cloud glaciation height and pressure and is also positively correlated with CER-BT slopes. Both dynamical and microphysical conditions in the tropics are favorable for higher ice mixing ratio and therefore slower decreasing rate of ice particle size.

We suggest that our results regarding both DCC general properties and aerosol-DCC interactions may find important applications in understanding some of the outstanding issues regarding DCC cloud forcing and statistical characteristics.

DCC ice particle sizes are intimately linked to cirrus development which has profound impact on climate due to their ubiquity and important radiative forcing. Close connection between precipitation and DCCs are demonstrated and far reaching effects of aerosol-precipitation warrant further investigation.

4.2 Future Work

4.2.1 Shallow Cumulus

Continuing efforts will be made to study aerosols' interaction with shallow cumulus using in-situ and/or ground data. Fair weather cumulus clouds will be measured in future campaigns of Department of Energy's Atmospheric Radiation Measurements (ARM) program along with aerosol properties. Together with existing ARM data at the Southern Great Plain super site we can validate our results and make further progress on the new framework of studying aerosol's interactions with these clouds as a whole system. A major field campaign utilizing ARM's mobile facility instruments will be carried out this year in China led by my advisor Dr. Li. Data from this campaign will provide data under extremely polluted conditions and can be used to do detailed analysis of aerosol indirect effects.

Stratocumulus morphology is of great interest to understand this cloud type, one of most important elements of our climate system given their large cloud forcing and vast coverage. The so called pockets of open cells (POCs) have been puzzling because of their almost instantaneous triggering and profound impact on stratocumulus cloud evolution [Stevens et al., 2004]. Several studies have hypothesized a connection between aerosols and the

morphology of these clouds [e.g. Rosenfeld et al., 2006]. This issue cannot be understood until a detailed understanding of cloud structure and cloud lifetimes of these clouds are achieved. For this purpose I have made some progress towards constructing necessary tools to tack this problem.

4.2.2 Deep Convective Clouds

Based on our results of DCC cloud statistics on cloud optical depth and cloud brightness temperature the cloud forcing can be calculated using broadband models. Further analysis of temporal change of these statistics may shed light on the large scale control for them. At the same time more direct measurements of these clouds are available from CloudSat products. Statistics of cloud properties from CloudSat can be compared with our passive results to further understand them.

In light of our results on DCC's interaction with aerosols further analysis on how aerosol effects may impact cirrus clouds that are formed as residues of DCC anvils. Products from NASA's Microwave Limb Sounder (MLS) provide information on ice water content of cirrus clouds. Together with measurements from other satellite sensors we can answer the question whether cirrus properties are consequently affected. CloudSat also has detailed microphysics information available that can be analyzed to verify our results.

Aerosol-precipitation interactions are critical not only for their scientific reasons but also for the potential impact on human society. Future efforts will be made to gain further insight of this problem by looking at data

from the Tropical Rain Measurement Mission (TRMM) cloud radar. Preliminary results suggest aerosol can indeed exert significant influence on the precipitation characteristics of DCC clouds. Also with data from TRMM more direct DCC measurements on the cloud structure are available, especially that of separating stratiform and convective clouds. These measurements can be used to independently validate our inference based cloud optical depth distributions.

Modeling is another important tool to understanding idealized processes in the cloud development and cloud-aerosol interactions. With collaboration of modeling experts we will try to investigate individual mechanisms that can be responsible for our observed results. Ensemble simulations of DCCs can also be generated to study the cloud statistics from models.

References

Ackerman, A. S., et al. (2000), Effects of aerosols on cloud albedo: Evaluation of Twomey's parameterization of cloud susceptibility using measurements of ship tracks, *Journal of the Atmospheric Sciences*, *57*, 2684-2695.

Albrecht, B. A.(1989), Aerosols, cloud microphysics, and fractional cloudiness, *Science*, *245*, 1227–1230.

Anderson, T.H., R.J. Charlson, S.E. Schwartz, R. Knutti, O. Boucher, H. Rodhe, and J. Heintzenberg (2003), Climate forcing by aerosols-a hazy picture, *Science*, *300*, 1103.

Andreae, M.O., D. Rosenfeld, P. Artaxo, A. Costa, G. Frank, K. Longo, M. Silva_dias, (2004), Smoking rain clouds over the Amazon, *Science,* 303, 1337-1342.

Baum B. A., D. P. Kratz, P. Yang, S. C. Ou, Y. X. Hu, P. F. Soulen, and S. C. Tsay, 2000: Remote sensing of cloud properties using MODIS airborne simulator imagery during SUCCESS 1. Data and models. *J. Geophys. Res.*, **105**, 11767–11780.

Baum, B. A., et al. (2005), Bulk scattering properties for the remote sensing of ice clouds. Part I: Microphysical data and models, *Journal of Applied Meteorology*, *44*, 1885-1895.

Boucher, O., and U. Lohmann (1995), The sulfate-CCN-cloud albedo effect: A sensitivity study using two general circulation models, *Tellus, Ser. B.*, *47*, 281-300.

Brenguier, J.L., H. Pawlowska, and L. Schuller (2003), Cloud microphysical and radiative properties for parameterization and satellite monitoring of the indirect effect of aerosol on climate, *J. Geophy. Res.,* 108, doi: 10.1029/2002JD002682.

Breon, F.-M., et al. (2002), Aerosol Effect on Cloud Droplet Size Monitored from Satellite, *Science*, *295*, 834-838.

Broekhuizen, K., P. P. Kumar, and J. P. D. Abbatt (2004), Partially soluble organics as cloud condensation nuclei: Role of trace soluble and surface active species, *Geophys. Res. Lett.*, *31*, L01107, doi:10.1029/2003GL018203.

Chang, F.L., Z. Li, 2005, A new method for detection of cirrus overlapping water clouds and determination of their optical properties, J. Atmos. Sci., 62, 3993-4009.

Chen, B., and X. Liu (2005), Seasonal migration of cirrus clouds over the Asian Monsoon regions and the Tibetan Plateau measured from MODIS/Terra, *Geophys. Res. Lett.*, 32, L01804, doi:10.1029/2004GL020868.

Chylek, P., et al. (2006), Aerosol indirect effect over the Indian Ocean, *Geophysical Research Letters*, *33*.

Coakley, J., R. Bernstein, P. Durkee (1987) Effect of ship-stack effluents on cloud reflectivity, *Science, 237*, 1020-1022

Conover, J. H., 1966: Anomalous cloud lines. *J. Atmos. Sci.,* **23,** 778–785

DeMott, P. J., et al. (2003), Measurements of the concentration and composition of nuclei for cirrus formation, *Proceedings of the National Academy of Sciences of the United States of America*, *100*, 14655-14660.

Desalmand F., 1987: Observations of CCN concentrations south of the Sahara during a dust haze. *Atmos. Res.*, **21**, 13–28

Donovan, D. P. (2003), Ice-cloud effective particle size parameterization based on combined lidar, radar reflectivity, and mean Doppler velocity measurements, *Journal of Geophysical Research-Atmospheres*, *108*.

Dubovik, O., et al. (2006), Application of spheroid models to account for aerosol particle nonsphericity in remote sensing of desert dust, *Journal of Geophysical Research-Atmospheres*, *111*.

Dusek, U., et al. (2006), Size matters more than chemistry for cloud-nucleating ability of aerosol particles, *Science*, 312, 1375-1377.

Eagan, R. C., P. V. Hobbs, and L. F. Radke, 1974: Particle emissions from a large Kraft paper mill and their effects on the microstructure of warm clouds. *J. Appl. Meteor.,* **13,** 535–552.

Facchini, M.C., M. Mircea, S. Fuzzi and R.J. Charlson (1999), Cloud albedo enhancement by surface-active organic solutes in growing droplets, *Nature*, 401, 257-259.

Fan, J., R. Zhang, G. Li, J. Nielsen-Gammon, and Z. Li (2005), Simulations of fine particulate matter ($PM_{2.5}$) in Houston, Texas, *J. Geophys. Res.*, *110*, D16203, doi:10.1029/2005JD005805.

Fan, J., R. Zhang, D. Collins, and G. Li (2006), Contribution of Secondary Condensable Organics to New Particle Formation: A Case Study in Houston, Texas, *Geophys. Res. Lett., 33*, doi:10.1029/2006GL026295.

Fan, J., R. Zhang, G. Li, W.-K. Tao, and X. Li (2007), Simulations of cumulus clouds using a spectral microphysics cloud-resolving model, *J. Geophys. Res.*, 112, D0420110.1029/2006JD007688.

Feingold, G., W.R. Cotton, S.M. Kreidenweis, and J.T. Davis (1999), The impact of giant cloud condensation nuclei on drizzle formation in stratocumulus: implications for cloud radiative properties, *J. Atmos. Sci.,* 56, 4100-4117.

Feingold, G., L.A. Remer, J. Ramaprasad and Y. J. Kaufman (2001), Analysis of smoke impact on clouds in Brazilian biomass burning regions: An extension of Twomey's approach. *J. Geophys. Res.*,*106*, 22,907-22,922.

Feingold, G., W.L. Eberhard, D.E. Veron, and M. Previdi (2003), First measurements of the Twomey effect using ground-based remote sensors, *Geophy. Res. Lett*., 30(6), 1287, doi: 10.1029/2002/GL016633.

Ferek, R. J., Hegg, D. A., Hobbs, P. V., Durkee, P., and Nielsen, K.: Measurements of shipinduced tracks in clouds off the Washington coast, J. Geophys. Res., 103, 23 199–23 206, 1998.

Fitzgerald, J. W.: Dependence of supersaturation spectrum of CCN on aerosol size distribution and composition, J. Atmos. Sci., 30, 628–634, 1973.

French J.R., Vali, G. and Kelly, R.D. (2000), Observations of microphysics pertaining to the development of drizzle in warm, shallow cumulus clouds, *Quart. J. Roy. Meteor. Soc.*, vol. 126, 415-443.

Fridlind, A. M., et al. (2004), Evidence for the predominance of mid-tropospheric aerosols as subtropical anvil cloud nuclei, *Science*, *304*, 718-722.

Fu, R., et al. (2006), Short circuit of water vapor and polluted air to the global stratosphere by convective transport over the Tibetan Plateau, *Proceedings of the National Academy of Sciences of the United States of America*, *103*, 5664-5669.

Futyan, J. M. and J. E. Russell,and J. E. Harries, 2004: Cloud radiative forcing in Pacific, African, and Atlantic tropical convective regions. *J. Climate,* **17,** 3192–3202.

Ganguly, D., et al. (2006), Physical and optical properties of aerosols over an urban location in western India: Seasonal variabilities, *Journal of Geophysical Research-Atmospheres*, *111*.

Gao, B. C., P. Yang, W. Han, R. R. Li, and W. J. Wiscombe (2002), An algorithm using visible 1.38 channels to retrieve cirrus cloud reflectances from aircraft and satellite data, *IEEE-Trans. Geosci. Remote Sensing*, 40, 1659-1668.

Gao, B. C., and Y. J. Kaufman (2003), Water vapor retrievals using Moderate Resolution Imaging Spectroradiometer (MODIS) near-infrared channels. J. Geophys. Res., *108, D13, 4389, doi:10.1029/2002JD003023.*

Garrett, T. J., et al. (2004), Convective generation of cirrus near the tropopause, *Journal of Geophysical Research-Atmospheres*, *109*.

Gettelman, A., and P. M. D. Forster (2002), A climatology of the tropical tropopause layer, *J. Meteorol. Soc. Jpn.*, *80*, 911-924.

Gettelman, A., et al. (2004), Impact of monsoon circulations on the upper troposphere and lower stratosphere, *Journal of Geophysical Research-Atmospheres*, *109*, 14.

Grabowski, W. W. (2003), Impact of Cloud Microphysics on Convective–Radiative Quasi Equilibrium Revealed by Cloud-Resolving Convection Parameterization, *Journal of Climate*, *16*, 3463-3475.

Guttikunda, S. K., et al. (2003), The contribution of megacities to regional sulfur pollution in Asia, *Atmospheric Environment*, *37*, 11-22.

Han, Q., W. B. Rossow, and A. A. Lacis (1994), Near-global survey of effective droplet radii in liquid water clouds using ISCCP data. *J. Clim*., 7, 465–497.

Han, Q., W.B. Rossow, J. Chou, and R.M. Welch (1998), Global variations of column droplet concentration in low-level clouds. *Geophys. Res. Lett.* 25, 1419-1422

Hanel, G.(1976), The properties of atmospheric aerosol particles as function of the relative humidity at thermodynamic equilibrium with the surrounding moist air, *Adv. Geophys.*, 19, 73–188.

Hansen, J., Mki. Sato, R. Ruedy, A. Lacis, K. Asamoah, K. Beckford, S. Borenstein, E. Brown, B. Cairns, B. Carlson, B. Curran, S. de Castro, L. Druyan, P. Etwarrow, T. Ferede, M. Fox, D. Gaffen, J. Glascoe, H. Gordon, S. Hollandsworth, X. Jiang, C. Johnson, N. Lawrence, J. Lean, J. Lerner, K. Lo, J. Logan, A. Luckett, M.P. McCormick, R. McPeters, R.L. Miller, P. Minnis, I. Ramberran, G. Russell, P. Russell, P. Stone, I. Tegen, S. Thomas, L. Thomason, A. Thompson, J. Wilder, R. Willson, and J. Zawodny (1997), Forcings and chaos in interannual to decadal climate change, *J. Geophys. Res.*, *102*, 25679-25720, doi:10.1029/97JD01495.

Harrison, E. F., et al. (1990), SEASONAL-VARIATION OF CLOUD RADIATIVE FORCING DERIVED FROM THE EARTH RADIATION BUDGET

EXPERIMENT, *Journal of Geophysical Research-Atmospheres*, *95*, 18687-18703.

Hartmann, D. L., et al. (1992), THE EFFECT OF CLOUD TYPE ON EARTHS ENERGY-BALANCE - GLOBAL ANALYSIS, *Journal of Climate*, *5*, 1281-1304.

Hartmann, D. L., (1994), Global Physical Climatology, Academic Press, ISBN 0-12-328530-5

Hartmann, D. L., et al. (2001), Tropical convection and the energy balance at the top of the atmosphere, *Journal of Climate*, *14*, 4495-4511.

Hartmann, D. L. and K. Larson, An Important Constraint on Tropical Cloud Climate Feedback. *Geophys. Res. Lett.*, **29(**20), 19514, 2002.

Haywood, J. and Boucher, O., 2000: Estimates of the direct and indirect radiative forcing due to tropospheric aerosols: A review. Rev Geophys, 38 (4), 513-543, 10.1029/1999RG000078.

Hegg, D. A. and Y. J. Kaufman (1998), Measurements of the relationship between submicron aerosol number and volume concentration. *J. Geophys. Res.*, 103, 5671-5678.

Herman, J. R., et al. (1997), Global distribution of UV-absorbing aerosols from Nimbus 7/TOMS data, *Journal of Geophysical Research-Atmospheres*, *102*, 16911-16922.

Heymsfield, A. (1975), Cirrus Uncinus Generating Cells and Evolution of Cirriform Clouds .1. Aircraft Observations of Growth of Ice Phase, *Journal of the Atmospheric Sciences*, *32*, 799-808.

Heymsfield, A. J., and C. M. R. Platt (1984), A Parameterization of the Particle-Size Spectrum of Ice Clouds in Terms of the Ambient-Temperature and the Ice Water-Content, *Journal of the Atmospheric Sciences*, *41*, 846-855.

Heymsfield, A. J., et al. (2005), Homogeneous ice nucleation in subtropical and tropical convection and its influence on cirrus anvil microphysics, *Journal of the Atmospheric Sciences*, *62*, 41-64.

Hindman, E.E., Hobbs, P.V. and Radke, L.F. (1977), Cloud condensation Nuclei from a Paper Mill, Part I: Measured Effects on Clouds, *J. Atmos. Sci.,*16, 745-752.

Hobbs, P. V., L. F. Radke and S. E. Shumway, 1970a: Cloud condensation nuclei from Industrial sources and their apparent influence on precipitation in Washington State. *J. Atmos. Sci.* , 27,81-89.

Holben, B. N., et al. (1998), AERONET - A federated instrument network and data archive for aerosol characterization, *Remote Sensing of Environment*, *66*, 1-16.

Hoppel, W.A., G.M. Frick, J.W. Fitzgerald, and B.J. Wattle (1994), A cloud chamber study of the effect that nonprecipitating water clouds have on the aerosol size distribution, *Aerosol Sci. Technol., 20,* 1—30.

Houze, R. A., Jr., 1989: Observed structure of mesoscale convective systems and implications for large-scale heating. *Quart. J. Roy. Meteor. Soc.,* 115, 425-461.

Houze, R. A., Jr., 1993: *Cloud Dynamics*. Academic Press, San Diego, 573 pp.

IPCC, 2001: Climate Change 2001: The Scientific Basis. Contribution of Working Group I to the Third Assessment Report of the Intergovernmental Panel on Climate Change, Cambridge University Press, United Kingdom and New York, NY, USA, 881pp.

Jayaraman, A., et al. (2006), Spatial variations in aerosol characteristics and regional radiative forcing over India: Measurements and modeling of 2004 road campaign experiment, *Atmospheric Environment*, *40*, 6504-6515.

Jensen, E. J., et al. (1996), On the formation and persistence of subvisible cirrus clouds near the tropical tropopause, *Journal of Geophysical Research-Atmospheres*, *101*, 21361-21375.

Jeong, M.-J., Z. Li, D. A. Chu, and S.-C. Tsay (2005), Quality and compatibility analyses of global aerosol products derived from the advanced very high resolution radiometer and Moderate Resolution Imaging Spectroradiometer, J. Geophys. Res., 110, D10S09, doi:10.1029/2004JD004648.

Jeong, M.-J., Z. Li, E. Andrews, and S.-C. Tsay, 2007, Effect of aerosol humidification on the column aerosol optical thickness over the Atmospheric Radiation Measurement Southern Great Plains site, J. Geophys. Res., 112, D10202, doi:10.1029/2006JD007176.

Jethwa H. et al., Aerosol Properties and regional distribution over Indo-Gangetic plains, *J.Geophys. Res*. , 2005

Johnson, D.B., 1980: The Influence of Cloud-Base Temperature and Pressure on Droplet Concentration. *J. Atmos. Sci.*, **37**, 2079–2085.

Kahn, R., B. Gaitley, J. Martonchik, D. Diner, K. Crean, and B. Holben (2005), Multiangle Imaging SpectroRadiometer (MISR) global aerosol optical depth validation based on two years of coincident AERONET observations, *J. Geophys. Res.,* **110**, doi:jd004706R.

Kaufman, Y. J., P. V. Hobbs, V. Kirchoff, P. Artaxo, L. Remer, B. Holben, M.D. King, D. Ward, E. Prins, K. Longo, L. Mattos, C. Nobre, J. Spinhirne, Q. Ji, A. Thompson, J. Gleason, S. Christopher, S.C. Tsay (1998), Smoke, Clouds, and Radiation-Brazil (SCAR-B) ,experiement, *J. Geophys. Res.,* 103, 31,783-31,808.

Kaufman, Y. J., D. Tanré, L. Remer, E. F. Vermote, A. Chu and B. N. Holben (1997), Operational remote sensing of tropospheric aerosol over the land from EOS-MODIS, *J. Geophys. Res.,* **102(14)**, 17051-17068.

Kaufman, Y. J., A. Seltzer, D. Ward, D. Tanre, B. Holben, P. Menzel, M. Pereira, R. Rasmussen (1992), Biomass burning aireborne and spaceborne experiment in the Amazonas (Base-A), *J. Geophys. Res.,* 97, 14,581-14,599.

Kaufman, Y. J. and R. S. Fraser (1997), The effect of smoke particles on clouds and climate forcing. *Science*,277,1636-1639.

Kaufman, Y. J., D. Tanré and O. Boucher (2002), A satellite view of aerosols in the climate system, *Nature*, 419, 215-223.

Kaufman, Y. J. N. Gobron, B. Pinty, J.L. Widlowski and M.M. Verstraete (2002), Relationship between surface reflectance in the visible and mid-IR used in MODIS aerosol algorithm – theory, *Geophy. Res. Lett., 29,* doi: 10.1029/2001GL014492.

Kaufman, Y. J., et al. (2005), The effect of smoke, dust, and pollution aerosol on shallow cloud development over the Atlantic Ocean, *Proceedings of the National Academy of Sciences of the United States of America*, *102*, 11207-11212.

Khain , A.P. , D. Rosenfeld, and A. Pokrovsky, 2001: Simulation of deep convective clouds with sustained supercooled liquid water down to –37.5 C using a spectral microphysics model. *Geophys. Rev. Lett.*, 3887-3890.

Khain, A., and A. Pokrovsky (2004), Simulation of effects of atmospheric aerosols on deep turbulent convective clouds using a spectral microphysics mixed-phase cumulus cloud model. Part II: Sensitivity study, *Journal of the Atmospheric Sciences*, *61*, 2983-3001.

Khvorostyanov, V. I., and J. A. Curry (2007), Refinements to the Kohler's theory of aerosol equilibrium radii, size spectra, and droplet activation: Effects of humidity and insoluble fraction, *Journal of Geophysical Research-Atmospheres*, *112*.

Kiehl, J. T. (1994), On the Observed near Cancellation between Longwave and Shortwave Cloud Forcing in Tropical Regions, *Journal of Climate*, *7*, 559-565.

Kim, B.-G., S. E. Schwartz, M. A. Miller, and Q. Min (2003), Effective radius of cloud droplets by ground-based remote sensing: Relationship to aerosol, *J. Geophys. Res.*, 108(D23), 4740, doi:10.1029/2003JD003721.

King, M. D. and D. M. Byrne, (1976): A method for inferring total ozone content from the spectral variation of total optical depth obtained with a solar radiometer, *J. Atmos. Sci.*, 33, 2242-2251.

King, M. D., Y. J. Kaufman, W. P. Menzel and D. Tanré (1992), Remote sensing of cloud, aerosol and water vapor properties from the Moderate Resolution Imaging Spectrometer (MODIS). *IEEE Trans. Geosci. Remote Sens.*, 30, 2–27

King, M. D., et al. (2004), Remote sensing of liquid water and ice cloud optical thickness and effective radius in the Arctic: Application of airborne multispectral MAS data, *Journal of Atmospheric and Oceanic Technology*, *21*, 857-875.

Knopf, D. A., and T. Koop (2006), Heterogeneous nucleation of ice on surrogates of mineral dust, *Journal of Geophysical Research-Atmospheres*, *111*.

Koren, I., Y. J. Kaufman, L. A. Remer, and J. V. Martins, 2004: Measurement of the effect of Amazon smoke on inhibition of cloud formation. Science, 303, 1342-1345.

Koren, I., et al. (2005), Aerosol invigoration and restructuring of Atlantic convective clouds, *Geophysical Research Letters*, *32*.

Kristjansson, J. E., et al. (2000), Impact of a new scheme for optical properties of ice crystals on climates of two GCMs, *Journal of Geophysical Research-Atmospheres*, *105*, 10063-10079.

Kubar, T. L., et al. (2007), Radiative and convective driving of tropical high clouds, *Journal of Climate*, *20*, 5510-5526.

Laaksonen, A., P. Korhonen, M. Kulmala, R. J. Charlson (1998), Modification of the Köhler Equation to include soluble trace gases and slightly soluble substances, *J. Atmos. Sci.*, *55*, 853-862.

Lau, K. M. and J. M. Kim (2007), How nature foiled the 2006 hurricane forecasts, *EOS Trans.*, 88, No. 9, pp. 105–107.

Leaitch, W. R., C. M. Banic, G. A. Isaac, M. D. Couture, P. S. K. Liu, I. Gultepe, L. Kleinman, P. H. Daum and J. I. MacPherson (1996), Physical and chemical observations in marine stratus during the 1993 North Atlantic Regional

Experiment: Factors controlling cloud droplet number concentration. *J. Geophys. Res.*,101,29123-29135.

Levin, Z., E. Ganor and V. Gladstein, The effects of desert particles coated with sulfate on rain formation in the eastern Mediterranean. J. Appl. Meteor., 35, 1511-1523, 1996.

Levin, Z., et al. (2005), On the interactions of mineral dust, sea-salt particles, and clouds: A measurement and modeling study from the Mediterranean Israeli Dust Experiment campaign, *Journal of Geophysical Research-Atmospheres*, *110*.

Levy, R. C., Remer, L. A., and Dubovik, O. (2007). Global aerosol optical properties and application to Moderate Resolution Imaging Spectroradiometer aerosol retrieval over land. *Journal of Geophysical Research*, 112(D13210), doi: 10.102.

Liou, K.-N. (1986), Influence of Cirrus Clouds on Weather and Climate Processes: A Global Perspective, *Monthly Weather Review*, *114*, 1167-1199.

Liu, C. T., et al. (2007), Global distribution of tropical deep convection: Different perspectives from TRMM infrared and radar data, *Journal of Climate*, *20*, 489-503.

Liu, G., H. Shao, J. A. Coakley Jr., J. A. Curry, J. A. Haggerty, and M. A. Tschudi (2003), Retrieval of cloud droplet size from visible and microwave radiometric measurements during INDOEX: Implication to aerosols' indirect radioactive effect, *J. Geophys. Res.*, 108(D1), 4006, doi:10.1029/2001JD001395.

Liu, Y and P. H. Daum (2002), Indirect warming effect from dispersion forcing, *Nature* 419, 580.

Liu, C. T., et al. (2007), Global distribution of tropical deep convection: Different perspectives from TRMM infrared and radar data, *Journal of Climate*, *20*, 489-503.

Lohmann, U., and G. Lesins (2002), Stronger constraints on the anthropogenic indirect aerosol effect. *Science*., 298, 1012–1015.

Lohmann U., Feichter J. (2005): Global indirect aerosol effects: A Review, Atmospheric Chemistry and Physics; 5 (2005), 715-737 - SRef-ID: 1680-7324/acp/2005-5-715.

Lu, M., and J. H. Seinfeld (2006), Study of the aerosol indirect effect by large-eddy simulation of marine stratocumulus, *J. Atmos. Sci.*, 62, 3909-3932.

Miller, M.A., B. A. Albrecht, and E.E. Clothiaux (1998), Diurnal cloud and thermodynamic variations in the stratocumulus transition regime: A case study using in situ and remote sensors, *J. Atmos. Sci.*, 55, 2294-2310.

Mace, G. G., et al. (2006), Association of tropical cirrus in the 10-15-km layer with deep convective sources: An observational study combining millimeter radar data and satellite-derived trajectories, *Journal of the Atmospheric Sciences*, *63*, 480-503.

Martins, J. V., D. Tanre, L. Remer, Y.J. Kaufman, S. Mattoo, and R. Levy (2002), MODIS cloud screening for remote sensing of aerosols over oceans using spatial variability, *Geophys.Res.Lett.*, 29, doi: 10.1029/2001GL013252

Martins, J.V., Marshak, A., Remer, L. A., Rosenfeld, D., Kaufman, Y. J., Fernandez-Borda, R., Koren, I., Zubko, V., and Artaxo, P.: Remote sensing the vertical

profile of cloud droplet effective radius, thermodynamic phase, and temperature, Atmos. Chem. Phys. Discuss., 7, 4481-4519

Massie, S., et al. (2002), Distribution of tropical cirrus in relation to convection, *Journal of Geophysical Research-Atmospheres*, *107*.

Massie, S. T., A. Heymsfield, C. Schmitt, D. Müller, and P. Seifert (2007), Aerosol indirect effects as a function of cloud top pressure, *J. Geophys. Res.*, 112, D06202, doi:10.1029/2006JD007383.

McFarquhar, G. M., and A. J. Heymsfield (1997), Parameterization of tropical cirrus ice crystal size distributions and implications for radiative transfer: Results from CEPEX, *Journal of the Atmospheric Sciences*, *54*, 2187-2200.

Nakajima T. and M.D. King (1990), Determination of theoretical thickness and effective particle radius of clouds from reflected solar radiation measurements, part I: theory. *J. Atmos. Sci.*, 47, 1878-1893.

Nakajima,T.,and A.Higurashi (1998), A use of two-channel radiances for an aerosol characterization from space, *Geophys.Res.Lett.*,25,3815-3818

Nakajima, T., A. Higurashi, K. Kawamoto and J. E. Penner (2001), A possible correlation between satellite-derived cloud and aerosol microphysical parameters. *Geophys. Res. Lett.*,28,1171-1174.

O'Dowd, C.D., J. Lowe, M.H. Smith and A.D. Kaye, The relative importance of sea-salt and nss-sulphate aerosol to the marine CCN population: An improved multi-component aerosol-droplet parameterisation. *Q. J. Roy. Met. Soc.,* 125, 1295-1313. 1999.

Ou, S. C., and K. N. Lieu (1995), ICE MICROPHYSICS AND CLIMATIC TEMPERATURE FEEDBACK, *Atmospheric Research*, *35*, 127-138.

Peng, Y., U. Lohmann, R. Leaitch, C. Banie, and M. Couture (2002), The cloud albedo-cloud droplet effective radius relationship for clean and polluted clouds from RACE and FIRE.ACE, *J. Geophys. Res., 107(*D11), 4106, doi:10.1029/2000JD000281,

Penner, J.E., R. E. Dickinson, C.A. O'Neill: Effects of aerosol from biomass burning on the global radiation budget, *Science,* 256, 1432-1434, 1992.

Penner, J.E., X. Dong, and Y. Chen (2004), Observational evidence of a change in radiative forcing due to the indirect aerosol effect, *Nature*, **427**, 231-234.

Phillips, V. T. J., Choularton, T. W., Blyth, A. M., and Latham,J. : The influence of aerosol concentrations on the glaciation and precipitation of a cumulus cloud, Q. J. Roy. Met. Soc., 128, 951– 971, 2002.

Platnick, S., and S. Twomey (1994), Determining the Susceptibility of Cloud Albedo to Changes in Droplet Concentration with the Advanced Very High Resolution Radiometer. *J. Appl. Meteor.*, 33, 334-347

Platnick, S., M. D. King, S. A. Ackerman, W. P. Menzel, B. A. Baum, J. C. Riedi, and R. A. Frey (2003), The MODIS cloud products: Algorithms and examples from Terra, *IEEE Trans. Geosci. Remote Sens.*, **41**, 459-473.

Platt, C. M. R., and A. C. Dilley (1981), Remote Sounding of High Clouds .4. Observed Temperature-Variations in Cirrus Optical-Properties, *Journal of the Atmospheric Sciences*, *38*, 1069-1082.

Platt, C. M. R. (1989), The Role of Cloud Microphysics in High-Cloud Feedback Effects on Climate Change, *Nature*, *341*, 428-429.

Pruppacher, H. R. and J. D. Klett (1997), Microphysics of clouds and precipitation, Springer, Inc.

Ramanathan, V., et al. (1989), Cloud-Radiative Forcing and Climate: Results from the Earth Radiation Budget Experiment, *Science*, *243*, 57-63.

Ramanathan, V., P. J. Crutzen, J. Lelieveld, A. P. Mitra, D. Althausen, J. Anderson, M. O. Andreae, W. Cantrell, G. R. Cass, C. E. Chung, A. D. Clarke, J. A. Coakley, W. D. Collins, W. C. Conant, F. Dulac, J. Heintzenberg, A. J. Heymsfield, B. Holben, S. Howell, J. Hudson, A. Jayaraman, J. T. Kiehl, T. N. Krishnamurti, D. Lubin, G. McFarquhar, T. Novakov, J. A. Ogren, I. A. Podgorny, K. Prather, K. Priestley, J. M. Prospero, P. K. Quinn, K. Rajeev, P. Rasch, S. Rupert, R. Sadourny, S. K. Satheesh, G. E. Shaw, P. Sheridan, and F. P. J. Valero, (2001): Indian Ocean Experiment: An integrated analysis of the climate forcing and effects of the great Indo-Asian haze. *J. Geophys. Res.*, 106**,** 28371-28398.

Remer, L. A., Y. J. Kaufman, D. Tanré S. Mattoo, D. A. Chu, J. V. Martins, R-R. Li, C. Ichoku, R. C. Levy, R. G. Kleidman, T. F. Eck, E. Vermote, and B. N. Holben (2005), The MODIS Aerosol Algorithm, Products and Validation**,** *J. Atmos. Sci.*, Special Section, *l 62, 947-973.*

Remer, L.A, and Y. J. Kaufman (1998), Dynamical Aerosol Model: Urban/industrial Aerosol. *J. Geophys. Res.,* **103**, 13859-13871.

Roca, R., and V. Ramanathan (2000), Scale dependence of monsoonal convective systems over the Indian Ocean, *Journal of Climate*, *13*, 1286-1298.

Rosenfeld, D. and I. M. Lensky (1998), Satellite based insights into precipitation formation processes in continental and maritime convective clouds, *Bull. Am. Meteorol. Soc.,* 79, 2457-2476.

Rosenfeld, D., and W. L. Woodley (2000), Deep convective clouds with sustained supercooled liquid water down to -37.5[thinsp][deg]C, *Nature*, *405*, 440-442.

Rosenfeld, D., et al. (2001), Desert dust suppressing precipitation: A possible desertification feedback loop, *Proceedings of the National Academy of Sciences of the United States of America*, *98*, 5975-5980.

Rosenfeld, D. and G. Feingold (2003), Explanation of discrepancies among satellite observation of aerosol indirect effects, *Geophy. Res. Lett*., **30**(14), 1776, doi: 10.1029/2003GL017684.

Rosenfeld, D., et al. (2006), Switching cloud cover and dynamical regimes from open to closed Benard cells in response to the suppression of precipitation by aerosols, *Atmospheric Chemistry and Physics*, *6*, 2503-2511.

Rotstayn, L. D. and Y. G. Liu (2003), Sensitivity of the first aerosol indirect effect to an increase of cloud droplet spectral dispersion with droplet number concentration, *J. Climate*, **16**, 3476 –3481.

Russell, M., D. T. Allen, D. R. Collins, and M. P. Fraser **(**2004**),** Daily, seasonal and spatial trends in $PM_{2.5}$ mass and composition in southeast Texas, *Aerosol Sci. Technol.*, *38*, 14–26.

Sekiguchi, M., T. Nakajima, K. Suzuki, K. Kawamoto, A. Higurashi, D. Rosenfeld, I. Sano, S. Mukai (2003), A study of the direct and indirect effects of aerosols using

global satellite data sets of aerosol and cloud parameters, *J. Geophys. Res.*, **108**(D22), 4699, doi: 10.1029/2002JD003359.

Schwartz S. E., Charlson R. J. and Rodhe H. Quantifying climate change -- Too rosy a picture? *Nature Reports -- Climate Change* **1**, 23-24, (2007); doi: 10.1038/climate.2007.22.

Shantz, N. C., W. R. Leaitch, and P. F. Caffrey (2003), Effect of organics of low solubility on the growth rate of cloud droplets, *J. Geophys. Res.*, *108*(D5), 4168, doi:10.1029/2002JD002540.

Sheridan, P. J., D. J. Delene, and J. A. Ogren (2001), Four years of continuous surface aerosol measurements from the Department of Energy's Atmospheric Radiation Measurement Program Southern Great Plains Cloud and Radiation Testbed site. *J. Geophys. Res*., **106**, 20735–20747.

Sherwood, S. (2002), A microphysical connection among biomass burning, cumulus clouds, and stratospheric moisture, *Science*, *295*, 1272-1275.

Stephens, G. L., S-C Tsay, P. W. Stackhouse, Jr., and P. J. Flatau, 1990: The relevance of the microphysical and radiative properties of cirrus clouds to climate and climate feedback. J. Atmos. Sci., 47, 1742--1753.

Stephens, G. L. (2005), Cloud feedbacks in the climate system: A critical review, *Journal of Climate*, *18*, 237-273.

Stevens, B., et al. (2005), Pockets of open cells and drizzle in marine stratocumulus, *Bulletin of the American Meteorological Society*, *86*, 51

Strorelvmo, T., J. E. Kristjansson, G., Myhre, M. Johnsrud, and F. Stordal (2006), Combined observational and modeling based study of the aerosol indirect effect, *Atmos. Chem. Phys.,* 6, 3583-3601.

Tao, W.-K., J. Simpson, D. Baker, S. Braun, M.-D. Chou, B. Ferrier, D. Johnson, A. Khain, S. Lang, B. Lynn, C.-L. Shie, D. Starr, C.-H. Sui, Y. Wang, and P. Wetzel (2003), Microphysics, radiation and surface processes in the Goddard Cumulus Ensemble (GCE) model, *Meteorol. Atmos. Phys., 82*, 97-137.

Tao, W.-K., X. Li, A. Khain, T. Matsui, S. Lang, and J. Simpson (2007), Role of atmospheric aerosol concentration on deep convective precipitation: Cloud-resolving model simulations, *J. Geophys. Res.*, 112, D24S18, doi:10.1029/2007JD008728.

Twohy, C. H., M. D. Petters, J. R. Snider, B. Stevens, W. Tahnk, M. Wetzel, L. Russell, and F. Burnet (2005), Evaluation of the aerosol indirect effect in marine stratocumulus clouds: Droplet number, size, liquid water path, and radiative impact, *J. Geophys. Res.*, 110, D08203, doi:10.1029/2004JD005116.

Twomey, S. A. (1954), The composition of hygroscopic particles in the atmosphere, *J. Meteor.* ,11, 334-338.

Twomey, S. A. (1977), The influence of pollution on the shortwave albedo of clouds. *J. Atmos. Sci.*,34,1149-1152.

van den Heever, S. C., et al. (2006), Impacts of nucleating aerosol on Florida storms. Part I: Mesoscale simulations, *Journal of the Atmospheric Sciences*, *63*, 1752-1775.

Vant-Hull, B., A. Marshak, L. Remer, and Z. Li (2007), The effects of scattering angle and cumulus cloud geometry on satellite retrievals of cloud drop effective radius, *IEEE TGRS.,* accepted.

van Zadelhoff, G. J., et al. (2007), Sensitivity of the shortwave radiative budget to the parameterization of ice crystal effective radius, *Journal of Geophysical Research-Atmospheres*, *112*.

Varnai, T., and A. Marshak (2002), Observations of three-dimensional radiative effects that influence MODIS cloud optical thickness retrievals. *J. Atmos. Sci.*, **59**, 1607-1618.

Verma, S., O. Boucher, C. Venkataraman, M. S. Reddy, D. Müller, P. Chazette, and B. Crouzille (2006), Aerosol lofting from sea breeze during the Indian Ocean Experiment, *J. Geophys. Res.*, 111, D07208, doi:10.1029/2005JD005953.

Wen, G., A. Marshak, and R. F. Cahalan, (2006), Impact of 3D clouds on clear sky reflectance and aerosol retrieval in a biomass burning region of Brazil, *IEEE Geo. Rem. Sens. Lett.,* 3, 169-172.

Wetzel, M.A., and L.L. Stowe, (1999), Satellite-observed patterns in stratus cloud microphysics, aerosol optical thickness and shortwave radiative forcing. *J. Geophys. Res.*, **104,** 31286-31299.

Wielicki, B. A., et al. (2002), Evidence for Large Decadal Variability in the Tropical Mean Radiative Energy Budget, *Science*, *295*, 841-844.

Wyser, K., 1998: The Effective Radius in Ice Clouds. *J. Climate*, **11**, 1793–1802.

Yang, P., L. Zhang, G. Hong, S. L. Nasiri, B. A. Baum, H. L. Huang, M. D. King, and S. Platnick, 2007: Differences between collection 4 and 5 MODIS ice cloud

optical/microphysical products and their impact on radiative forcing simulations. *IEEE Trans. Geosci. Remote Sens*, **45**, 2886-2899.

Yang, S and E.A. Smith, 2006: Mechanisms for Diurnal Variability of Global Tropical Rainfall Observed from TRMM *Journal of Climate Volume 19, Issue 20 (October 2006)* pp. 5190-5226

Yin, Y., Z. Levin, T. G. Reisin and S. Tzivion: The effects of giant cloud condensation nuclei on the development of precipitation in convective clouds - A numerical study. Atmos. Res. 1999.

Young, K.C. (1993), Microphysics processes in clouds, Oxford University Press, Inc., New York, New York.

Yuan, T., Z. Li, R. Zhang, J. Fan, 2008, Increase of cloud droplet size with aerosol optical depth: An observation and modeling study, *J. Geophy. Res.*, 113, D04201, doi: 10.1029/2007JD008632.

Yuan, T., Z. Li and Vant-Hull, B., A global survey of aerosol indirect effect for shallow cumulus clouds, to be submitted.

Zhang, R., I. Suh, J. Zhao, D. Zhang, E.C. Fortner, X. Tie, L.T. Molina, and M.J. Molina (2004), Atmospheric new particle formation enhanced by organic acids, *Science* **304**, 1487-1490.

Zipser, E. J., et al. (2006), Where are the most intense thunderstorms on earth?, *Bulletin of the American Meteorological Society*, *87*, 1057